

8-2018

Improved Target Coverage of Spinal Metastases Through the Use of Flattening Filter Free Beams

Laura Bennett

Follow this and additional works at: https://digitalcommons.library.tmc.edu/utgsbs_dissertations



Part of the [Other Medical Sciences Commons](#), and the [Other Physics Commons](#)

Recommended Citation

Bennett, Laura, "Improved Target Coverage of Spinal Metastases Through the Use of Flattening Filter Free Beams" (2018). *The University of Texas MD Anderson Cancer Center UTHealth Graduate School of Biomedical Sciences Dissertations and Theses (Open Access)*. 896.
https://digitalcommons.library.tmc.edu/utgsbs_dissertations/896

This Thesis (MS) is brought to you for free and open access by the The University of Texas MD Anderson Cancer Center UTHealth Graduate School of Biomedical Sciences at DigitalCommons@TMC. It has been accepted for inclusion in The University of Texas MD Anderson Cancer Center UTHealth Graduate School of Biomedical Sciences Dissertations and Theses (Open Access) by an authorized administrator of DigitalCommons@TMC. For more information, please contact digitalcommons@library.tmc.edu.

STEREOTACTIC RADIOTHERAPY FOR SPINAL METASTASES USING
FLATTENING FILTER FREE BEAMS

A

THESIS

Presented to the Faculty of

The University of Texas

MD Anderson Cancer Center UTHealth

Graduate School of Biomedical Sciences

in Partial Fulfillment

of the Requirements

for the Degree of

MASTER OF SCIENCE

by

Laura Christine Bennett, B.S.
Houston, Texas

August 2018

Acknowledgements

I would like to thank my advisor Dr. Oleg Vassiliev for his guidance during the course of this project and his patience when things did not always go well. I would also like to thank my advisory committee – Dr. Stephen Kry, Dr. Dershan Luo, Dr. Shouhao Zhou, and Dr. Mary Frances McAleer for their input and understanding.

An incredible amount of gratitude should be allotted to Neal Rebueno, Medical Dosimetrist, who taught me the fundamentals of treatment planning and without whom this project would likely not have seen the light of day. Thank you for putting up with my endless barrage of questions and your support when I didn't have a clue what I was doing.

I would also like to thank Dr. Wendt for all of his advice during my time at MD Anderson, all of which I value and will forever be grateful for.

Lastly, I would like to thank my family and friends for their support during this project. For my parents, Malia and Steve, for having faith in me, my godfather Jan Lovell for encouraging scholastics throughout my life, my good friend Constance Owens for providing either a couch to mope on or a push when needed, and my partner Dao Thong Lim for everything else.

Dedication

Dedicated to my mother, Malia Katherine Bennett. I know it's the wrong cancer.

And

To the memory of Jan Wantland and Dao Xian Lim

IMPROVED TARGET COVERAGE OF SPINAL METASTASES THROUGH THE USE OF FLATTENING FILTER FREE BEAMS

Laura Christine Bennett, B.S.

Advisory Professor: Oleg Vassiliev, Ph.D.

Of the patients that are diagnosed with metastatic disease, up to 40% will develop vertebral osseous metastases. These metastases tend to be located in close proximity to the spinal cord itself, making it difficult to achieve the recommended minimum dose of 14 Gy for single fraction SBRT or 21 Gy¹ for three fraction SBRT while maintaining acceptable doses to the cord and cauda equina. This proximity of the target to critical structures has the potential to compromise the efficacy of the radiation treatment plan in favor of reducing normal tissue dose, resulting in poor local control and tumor recurrence at follow-up. Flattening Filter Free (FFF) photon beams have been shown to have lower out-of-field dose and sharper dose gradients when compared with conventionally flattened (FF) photon beams of similar energy; this sharp dose fall-off could potentially prove beneficial in cases where greater precision is required, such as for high-dose hypofractionated radiation treatments of vertebral metastases. The purpose of this project was to compare the physical properties, namely penumbral width and penumbral and out-of-field dose of FFF and FF photon beams as well as determine the clinical effects of these beams on vertebral osseous tumors. It was hypothesized that FFF beams would show a definitive improvement in target coverage while maintaining acceptable normal tissue doses when compared with FF beams. To test this hypothesis, penumbral width and dose were measured for FF and FFF beam profiles at various

depths and field sizes using the Varian Standard Beam Data by examining the treatment plans for twelve patients with spine metastases using both FF and FFF beams. There was a statistically significant reduction in penumbral width for FFF plans when compared to FF plans; however, this difference was in effect quite small and may not translate into better treatment plans. There was no demonstrable difference between treatment plans developed using FF or FFF beams in terms of minimum dose to the GTV. However, there was significant reduction in treatment delivery time for FFF plans, which may lead to reduced intrafractional variation from patient motion and a more positive patient experience.

TABLE OF CONTENTS

1	INTRODUCTION	1
1.1	– Spine Metastases.....	1
1.1.1	– Prevalence of Spine Metastases	1
1.1.2	– Standard Treatments and Typical Patient Outcomes	1
1.2	– Flattening Filter Free Beams	3
1.2.1	– Characteristics of Flattening Filter Free Beams.....	3
1.2.2	– Biology and Physics of Flattening Filter Free Beams	5
1.2.3	– Prior Studies.....	6
1.3	– Hypothesis and Specific Aims	8
2	MATERIALS AND METHODS.....	10
2.1	– Analysis of Dose Profiles.....	10
2.1.1	– Varian Standard Beam Data.....	10
2.1.2	– Normalization of Profiles.....	11
2.2	– Treatment Planning	12
2.2.1	– Patient Population	12
2.2.2	– Treatment Planning Parameters	15
2.3	– Statistical Analysis.....	18
3	RESULTS	19
3.1	– Analysis of Dose Profiles.....	19
3.1.1	– Penumbral Dose	19
3.1.2	– Penumbral Width	22
3.2	– Comparison of Treatment Plans.....	23
4	DISCUSSION	34
4.1	– General Discussion	34
4.2	– Conclusions.....	36
4.3	– Future Work	37
5	APPENDIX.....	38

5.1 – Individual Patient Plans	38
5.2 – Dose to Water vs. Dose to Medium	86
References	87
Vita	93

List of Figures

Figure 1-1: Profiles for FFF (red) and FF (blue) beams; FFF profile is noticeably more "peaked"	4
Figure 2-1: Dose profiles before and after normalizing. On the left is the raw beam data (normalized to 100% max dose on the central axis); on the right is the renormalized data (FF normalized to 110% dose, FFF normalized to FFF dose at location of 100% dose on FF profile).....	12
Table 2-1: Summary of patient population by site, prescription dose, and number of fractions.....	13
Table 2-2: ESCC/Bilsky Grading Scale.....	14
Table 2-3: GTV Volume (cm ³)	14
Figure 2-2: Standard beam arrangement for spinal SBRT patients	15
Table 2-4: Institutional Guidelines for Normal Tissue Tolerances	17
Figure 3-1: FF (solid lines) and FFF (dashed lines) penumbral dose at 5 cm depth	19
Figure 3-2: FF (solid lines) and FFF (dashed lines) penumbral dose at 10 cm depth	20
Figure 3-3: FF (solid lines) and FFF (dashed lines) penumbral dose at 20 cm depth	20
Figure 3-4: FF (solid lines) and FFF (dashed lines) penumbral dose at 30 cm depth	21
Figure 3-5: Close up of penumbral doses of FFF and FF beams at 5 cm depth.	21
Table 3-1: Difference (mm) in penumbral width of FFF beams relative to FF beams in water at various depths (cm)	22
Figure 3-6: Median DVHs for single-and three-fraction GTV	24
Figure 3-7: Cauda and Cord Median DVH.....	26
Table 3-2: GTV Dmin for FF and FFF Plans	27
Table 3-3: OAR _{0.03cc}	28
Table 3-4: Beam-on time per fraction.....	29
Table 3-5: Total MUs for each patient plan.....	30
Table 3-6: Dose grid size (pixels).....	31
Table 3-7: Heterogeneity Index for all plans	32
Table 3-8: Average field sizes (cm).....	33
Figure 5-1: Patient 1 axial isodose images. Top: FF Plan, Bottom: FFF Plan	38
Figure 5-2: Patient 1 coronal isodose images. Top: FF Plan, Bottom: FFF Plan	39
Figure 5-3: Patient 1 sagittal isodose images. Top: FF Plan, Bottom: FFF Plan.....	40
Figure 5-4: Patient 1 DVH.....	41
Figure 5-5: Patient 2 axial isodose images. Top: FF Plan, Bottom: FFF Plan	42
Figure 5-6: Patient 2 coronal isodose images. Top: FF Plan, Bottom: FFF Plan	43
Figure 5-7: Patient 2 sagittal isodose images. Top: FF Plan, Bottom: FFF Plan.....	44
Figure 5-8: Patient 2 DVH.....	45
Figure 5-9: Patient 3 axial isodose images. Top: FF Plan, Bottom: FFF Plan	46
Figure 5-10: Patient 3 coronal isodose images. Top: FF Plan, Bottom: FFF Plan	47
Figure 5-11: Patient 3 sagittal isodose images. Top: FF Plan, Bottom: FFF Plan.....	48
Figure 5-12: Patient 3 DVH.....	49

Figure 5-13: Patient 4 axial isodose images. Top: FF Plan, Bottom: FFF Plan, Bottom:	
Plan	50
Figure 5-14: Patient 4 coronal isodose images. Top: FF Plan, Bottom: FFF Plan, Bottom:	
Plan	51
Figure 5-15: Patient 4 sagittal isodose images. Top: FF Plan, Bottom: FFF Plan.....	52
Figure 5-16: Patient 4 DVH.....	53
Figure 5-17: Patient 5 axial isodose images. Top: FF Plan, Bottom: FFF Plan	54
Figure 5-18: Patient 5 coronal isodose images. Top: FF Plan, Bottom: FFF Plan	55
Figure 5-19: Patient 5 sagittal isodose images. Top: FF Plan, Bottom: FFF Plan.....	56
Figure 5-20: Patient 5 DVH.....	57
Figure 5-21: Patient 6 axial isodose images. Top: FF Plan, Bottom: FFF Plan	58
Figure 5-22: Patient 6 coronal isodose images. Top: FF Plan, Bottom: FFF Plan	59
Figure 5-23: Patient 6 sagittal isodose images. Top: FF Plan, Bottom: FFF Plan.....	60
Figure 5-24: Patient 6 DVH.....	61
Figure 5-25: Patient 7 axial isodose images. Top: FF Plan, Bottom: FFF Plan	62
Figure 5-26: Patient 7 coronal isodose images. Top: FF Plan, Bottom: FFF Plan	63
Figure 5-27: Patient 7 sagittal isodose images. Top: FF Plan, Bottom: FFF Plan.....	64
Figure 5-28: Patient 7 DVH.....	65
Figure 5-29: Patient 8 axial isodose images. Top: FF Plan, Bottom: FFF Plan	66
Figure 5-30: Patient 8 coronal isodose images. Top: FF Plan, Bottom: FFF Plan	67
Figure 5-31: Patient 8 sagittal isodose images. Top: FF Plan, Bottom: FFF Plan.....	68
Figure 5-32: Patient 8 DVH.....	69
Figure 5-33: Patient 9 axial isodose images. Top: FF Plan, Bottom: FFF Plan, Bottom:	
Plan	70
Figure 5-34: Patient 9 coronal isodose images. Top: FF Plan, Bottom: FFF Plan, Bottom:	
Plan	71
Figure 5-35: Patient 9 sagittal isodose images. Top: FF Plan, Bottom: FFF Plan, Bottom:	
Plan	72
.....	73
Figure 5-36: Patient 9 DVH.....	73
Figure 5-37: Patient 10 axial isodose images. Top: FF Plan, Bottom: FFF Plan	74
Figure 5-38: Patient 10 coronal isodose images. Top: FF Plan, Bottom: FFF Plan	75
Figure 5-39: Patient 10 sagittal isodose images. Top: FF Plan, Bottom: FFF Plan.....	76
Figure 5-40: Patient 10 DVH.....	77
Figure 5-41: Patient 11 axial isodose images. Top: FF Plan, Bottom: FFF Plan	78
Figure 5-42: Patient 11 coronal isodose images. Top: FF Plan, Bottom: FFF Plan	79
Figure 5-43: Patient 11 sagittal isodose images. Top: FF Plan, Bottom: FFF Plan.....	80
Figure 5-44: Patient 11 DVH.....	81
Figure 5-45: Patient 12 axial isodose images. Top: FF Plan, Bottom: FFF Plan, Bottom:	
Plan	82
Figure 5-46: Patient 12 coronal isodose images. Top: FF Plan, Bottom: FFF Plan	83
Figure 5-47: Patient 12 sagittal isodose images. Top: FF Plan, Bottom: FFF Plan.....	84
.....	85
Figure 5-48: Patient 12 DVH.....	85

Figure 5-49: DVH for Dose to Medium vs. Dose to Water. Dose to Water is indicated with triangles; dose to medium with squares. Magenta, yellow, and red represent cauda equina, CTV, and GTV, respectively..... 86

1 INTRODUCTION

1.1 – Spine Metastases

1.1.1 – Prevalence of Spine Metastases

Of all patients that are diagnosed with metastatic cancer each year, it is estimated that 40% will develop metastases in the spinal column, and of those who eventually die due to cancer, up to 70% will have spinal metastases at the time of death²⁻⁵. Often, these patients may experience pain, incontinence, or loss of ambulatory function due to compression of the spine – a complication that occurs in up to 20% of patients with spine metastases⁶. The recommended treatment in these cases is often a combination of therapies including surgical resection of the tumor and radiation therapy⁷.

1.1.2 – Standard Treatments and Typical Patient Outcomes

Patients undergoing radiotherapy for spinal cord lesions either adjuvant with surgery or as a stand-alone treatment often receive stereotactic body radiation therapy (SBRT). Standard fractionation external-beam radiotherapy (EBRT) is typically scheduled as 1.8-2.0 Gy delivered 5 days per week for up to 8 weeks⁸. In comparison, SBRT treatments typically include prescriptions doses of 24-30 Gy over a course of 1-5 fractions⁹. This is most often the preferred method of radiation therapy due to the sensitivity of the spinal cord to radiation and the proximity of the tumor to the cord itself; in such cases, hypofractionated, high dose radiation is favored in order to limit

normal tissue dose while delivering adequate radiation to the target. In order to minimize dose to healthy tissue (spine, lungs, kidney, etc.) while maintaining target coverage and prescription dose constraints, a large number of convergent beams are directed at the target to maximize dose around the gross tumor volume (GTV)¹⁰. In most cases, some sort of immobilization device such as a vac-loc bag or thermoplastic cast is used to limit intrafractional motion during treatment¹¹. Additionally, image-guided tracking in the form of a combination of CT and MRI is used in almost all cases to limit intrafractional motion during treatment^{11,12}.

Outcomes for patients undergoing SBRT for spinal metastases are typically positive. A study by Zelefsky et al¹³ in 1992 examining patients undergoing radiation treatment of the spine reported that 92% who completed treatment experienced pain relief; another study by Yamada et al¹⁴ examining high-dose hypofractionated IMRT for spinal metastasis in 93 patients showed 90% local control at 15 months post therapy. Ahmed et al¹⁵ treated eighty-five spinal lesions using SBRT; local control at 12 months was 83.3% and 91.2% for patients with and without prior radiotherapy respectively.

Local control is more likely for these patients when a minimum “threshold dose” is met in the GTV; an investigation of 285 patients with spinal metastases treated with SBRT by Bishop et al found that local control was more likely with higher GTV minimum dose (Dmin) and recommended that patients undergoing a single fraction course receive at least 14 Gy to the GTV Dmin while those undergoing a three fraction course should receive at least 21 Gy to the GTV Dmin¹. Unfortunately, spine metastases are often located close to the cord itself –often within a millimeter or less - making it difficult to meet the thresholds necessary to establish tumor local control without

imparting excessive dose to the cord or cauda equina^{16,17}. Due to the risk of permanent radiation myelopathy, many physicians may be forced to limit dose to the GTV in order to maintain clinically acceptable doses to the cord, reducing the overall efficacy of treatment¹⁸.

1.2 – Flattening Filter Free Beams

1.2.1 – Characteristics of Flattening Filter Free Beams

In recent years, manufacturers of medical linear accelerators (linacs) have begun to produce machines capable of producing beams in Flattening Filter Free (FFF) mode. Traditionally, photon beams use a metal flattening filter (FF) in order to produce dose profiles with uniform photon intensity across the field; FFF beams are the result of removing the flattening filter, creating a more “peaked” dose distribution^{19,20}. FFF beams were originally conceived for use with fluence-modifying devices such as multi-leaf collimators for IMRT, where smaller average field sizes make a large, uniform dose distribution unnecessary²¹.

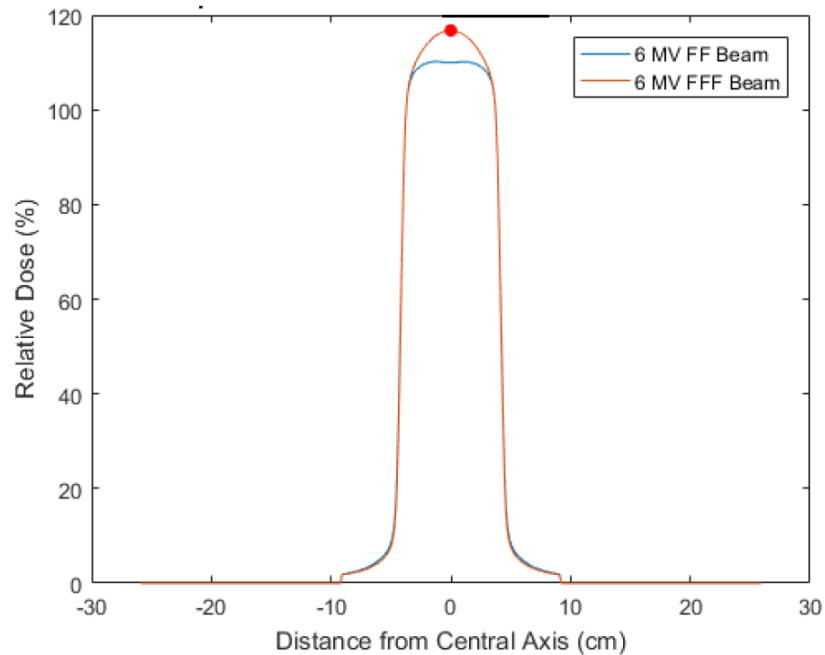


Figure 1-1: Profiles for FFF (red) and FF (blue) beams; FFF profile is noticeably more "peaked"

Compared to traditionally flattened beams, FFF beams have a number of unique characteristics, the first and most obvious being the singular shape of their dose distributions: unlike FF beams, FFF beams are marked by high fluence in the center of the field with steep fall-off at the field edges²². The sharper dose gradient is likely a function of the demonstrated reduction in head scatter, electron contamination, and overall out-of-field dose common to FFF beams due to elimination of the filter^{23–25}. An additional benefit of FFF beams is their ability to deliver the same prescription as FF beams at a significantly higher dose rate, allowing beam-on time to be greatly reduced^{26,27} while reducing the amount of scatter generated. The resultant reduction in treatment time is highly beneficial for treatments wherein high precision is essential, as it limits the potential for intrafractional motion to create unacceptable errors^{28,29}.

1.2.2 – Biology and Physics of Flattening Filter Free Beams

There is a reasonable biological component as to why FFF should be considered over FF beams: to begin with, the softer energy spectrum of FFF may result in a higher relative biological effectiveness (RBE). A traditional FF beam has a much harder spectra due to the selective removal of lower energy photons by the flattening filter. This results in a beam that is more penetrating, but has a lower linear energy transfer (LET). A softer beam produces lower energy electrons in the medium, resulting in a higher LET and therefore a higher RBE³⁰. Additionally, the increased dose rate of FFF beams may have an effect on tumor cell survival. Radiosensitivity is reduced at low dose rates, as intracellular repair may begin to take place for longer treatment times, as the half-time for repair may be less than one hour³¹.

For vertebral osseous tumors, energy deposition varies with respect to other types of tissue (muscle, fat). Bone has a higher average atomic number than normal tissues at 12.31 kg/m³ versus 7.64 kg/m³ for muscle, 6.46 kg/m³ for fat, or 7.51 kg/m³ for water³². At lower energies, this results in a higher probability for interaction via the photoelectric effect which has a high Z dependence, resulting in greater dose deposition in bone. However, this is more of a concern at diagnostic energies (30-150 keV) than therapeutic energies (6-18 MeV), as the cross section of the photoelectric effect is inversely proportional to photon energy. Instead, the Compton effect predominates at therapeutic energy levels and effectively determines dose in this range. Unlike the photoelectric effect, which has a strong dependence on the Z of the material, the Compton effect is primarily dependent on electron density. Bone, having a lower electron density than water (3.192×10^{26} elect/kg versus 3.343×10^{26}

elect/kg), is subject to fewer Compton interactions and thus has slightly lower energy deposition than other tissues³².

Physically, the removal of the flattening filter is associated with a reduction in out-of-field dose. This is primarily a function of the elimination of the flattening filter as a source of scatter²³ as well as the improvement in delivery efficiency resulting in reduced head leakage²².

1.2.3 – Prior Studies

There are a number of extant studies that have investigated the physical properties of FFF beams as well as their clinical implications. A research group at MD Anderson Cancer Center published three studies in 2006 examining the dosimetric properties of FFF beams; backscatter, depth dose profiles, lateral dose profiles, MLC leakage, total scatter factor, and dose rate were investigated and compared with conventional FF beams^{33–35}. In later studies by Kry et al at MD Anderson Cancer Center²³ and Almberg et al at the Norwegian University of Science and Technology²⁵, out-of-field dose produced by FFF beams was examined using Monte Carlo simulations; both groups determined that FFF showed clinically relevant reductions in out-of-field dose when compared with FF beams of similar energy.

Treatment planning studies examining FFF beams in a clinical setting have been carried out cancers in a variety of sites, including prostate^{36–38}, lung^{39–41}, liver^{42,43}, and brain^{44,45}. Studies on the effect of FFF-based treatments on spinal column – where the potential for increased precision from reduction in out-of-field dose, treatment time,

and head scatter would prove to be of great benefit due to the proximity of tumors to the spinal cord – are somewhat limited in number and scope. A study by Ong et al conducted in 2012 investigated the impact of FFF beams compared with FF beams using RapidArc delivery of SBRT treatments of vertebral bodies in order to determine the effect of the reduction in treatment time demonstrated by FFF beams on intrafractional shifts⁴⁶. The results of the study indicated that dosimetric variations were greater for FFF plans due to the significantly higher dose rate; however, these results may be complicated by the fact that the energies examined for each beam – 6 MV for FF and 10 MV for FFF – introduced differences in the dosimetric properties of each beam such that direct comparison of the two would be difficult. Additionally, the probability of an intrafractional shift occurring during a given treatment is lower for FFF beams due to the much shorter beam-on time, a factor that was not considered by this study. Another study investigating the effect of FFF beams in IMRT and VMAT treatments of spinal column metastases where prior radiotherapy had been performed was undertaken by Dobler et al in 2016 compared target coverage and spinal cord dose between FF and FFF plans. This study demonstrated significant improvement for FFF beams in normal tissue sparing and dose homogeneity⁴⁷. No studies have been found to examine the effect of FFF beams on minimum dose (Dmin) to the GTV in spine metastases. Due to the limited number of fractions in SBRT treatments of spine tumors, ensuring that a threshold dose is met is necessary to ensure that local control is maintained; Bishop et al have found that Dmin should be at least 14 Gy for single-fraction, 24 Gy plans or at least 21 Gy for three-fraction, 27 Gy plans to limit the risk of recurrence at follow-up¹. The current study was undertaken to evaluate the effects of FFF beams on GTV Dmin and determine

the feasibility of using FFF beams in stereotactic radiotherapy for spinal column metastases.

1.3 – Hypothesis and Specific Aims

We hypothesize that a clinically significant reduction in out-of-field and penumbral dose such that improved tumor coverage is achieved may be accomplished through the use of Flattening Filter Free (FFF) photon beams given their unique dosimetric profile and that FFF beams will generate treatment plans that are clinically equivalent to those plans developed using FF beams. The hypothesis was tested with the following specific aims:

1. Examine and characterize the difference in penumbral and peripheral dose between Flattening Filter Free beams and conventionally flattened beams of similar depth-dose distributions. This aim shall be done by examining beam profile data for both FFF and FF beams provided by Varian (Varian Representative Data) as well as Monte Carlo generated data. The FF beams will be normalized by central axis dose (or some nominal percentage thereof); the FFF beams will be normalized to 110% at the central axis for FF profiles and the dose of the FFF profile at the point of 100% dose on the FF profile in order to account for the different shapes of the two profiles and make a more fair comparison of peripheral dose. After normalization, we intend to calculate and compare penumbral widths (the distance between 80%-20% maximum dose) and the relative dose at varying distances from the field edge (0.5-20 mm from 50% central axis dose).

2. Develop and compare treatment plans using FFF and FF beams. This shall be done using the ECLIPSE treatment planning system and the Varian Representative Data. We intend to pre-existing plans generated in Pinnacle for 12 unique patients with spinal metastases, and compare them to plans generated using the Varian Representative Data for FFF beams. We will be using the Acuros XB Advanced Dose Calculation algorithm in the ECLIPSE treatment planning system in order to achieve maximum accuracy, as this project aims to examine high dose gradients, heterogeneities, and out-of-field doses, all of which are best modeled using Acuros XB. The same dosimetric constraints will be used to normalize the plans in order to make a fair comparison of the plans. Parameters to be investigated will include minimum dose to the GTV, $D_{0.03cc}$ to the spinal cord and cauda equina, beam-on time, and total machine units.

2 MATERIALS AND METHODS

2.1 – Analysis of Dose Profiles

2.1.1 – Varian Standard Beam Data

Prior to developing treatment plans, we first analyzed the dose profiles for FF and FFF beams provided in the Varian Standard Beam Data (Varian Medical Systems Inc, Palo Alto, CA) - previously the Varian Golden Beam Data - from which we would be developing beam models for the treatment planning system. The Varian Standard Beam Data contains Percent Depth Dose (PDD) and dose profile measurements of a standard Varian TrueBeam for a number of different field sizes and beam energies. These measurements were taken using an IBA Dosimetry CC13 ionization chamber in a 3D water phantom in step sizes of 1 mm. We compared dose profiles of 6 MV FF and 6 MV FFF beams at depths of 5 cm, 10 cm, 20 cm, and 30 cm and at field sizes of 3x3 cm², 4x4 cm², 8x8 cm², and 10x10 cm². Penumbra width – defined here as the distance between the 80% maximum dose point and the 20% maximum dose point – and relative dose at 2 mm, 5 mm, 10 mm, 30 mm, and 50 mm from the field edge were reviewed. For this study, absolute difference between penumbra width and penumbra and out-of-field dose for FF and FFF beam profiles were assessed and evaluated by Wilcoxon Signed Rank test.

2.1.2 – Normalization of Profiles

Due to the difference in shapes between FF and FFF dose profiles, it is necessary to renormalize each beams in order to make comparison of the penumbral width more objective. As of this study, there is no standard for this normalization, though a number of techniques have been used. Pönisch et al. suggested using the inflection point at the field edge³⁴. This method, though intuitive, has the disadvantage of introducing a large degree of uncertainty due to the need for incredibly granular measurements in a high gradient region; often, measurements are taken with no less than 1 mm separation for quality assurance, limiting precision and imposing a minimum degree of uncertainty into dose profile measurements⁴⁸. Fogliata et al. favored using a separate “renormalization point” to determine the normalization factor. A shoulder point could be found by calculating the third derivative of the FF beam in the penumbra region and using the second maximum to normalize the FFF beam to the same point⁴⁸. Since this study was primarily focused on the effects of the different beams on SBRT treatments, we elected to normalize FF and FFF beams as described here: FF beams were normalized such that central axis dose was 110% maximum dose. The location of 100% maximum dose on the FF profiles was then marked; FFF beams were normalized according to the relative dose of the FFF beams at that location. This method of normalization controlled the profile shapes effectively while keeping the dose distribution within the treatment field within clinically acceptable limits. Figure 2-1 below depicts the two beam profiles before and after normalization.

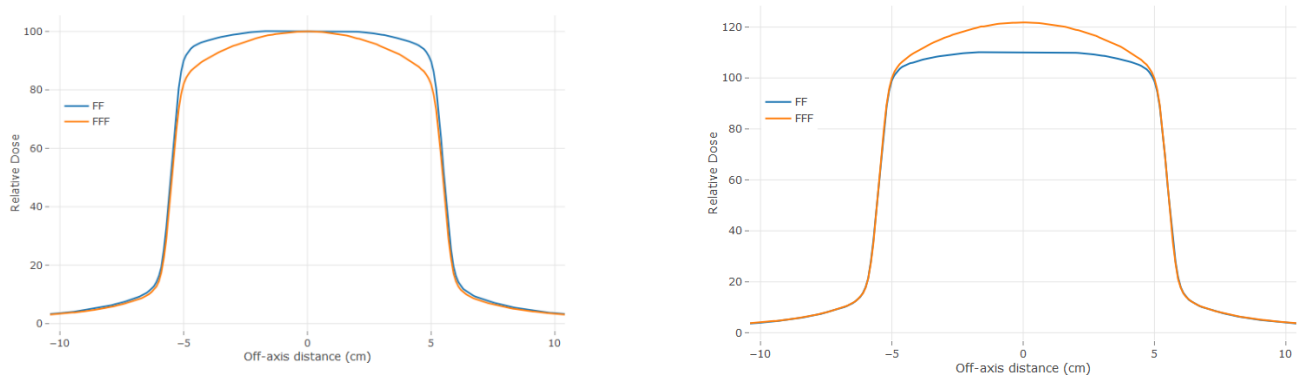


Figure 2-1: Dose profiles before and after normalizing. On the left is the raw beam data (normalized to 100% max dose on the central axis); on the right is the renormalized data (FF normalized to 110% dose, FFF normalized to FFF dose at location of 100% dose on FF profile).

2.2 – Treatment Planning

2.2.1 – Patient Population

A cohort of 12 patients previously treated for spinal metastases at MDACC were selected for this study. Of these, four had tumors in the cervical region of the spinal cord, three in the thoracic region, and five in the lumbar region. Half of these patients were prescribed 24 Gy in a single fraction by a radiation oncologist; the other half were prescribed 27 Gy in three fractions. The entire patient population is summarized in Table 2-1 below.

Table 2-1: Summary of patient population by site, prescription dose, and number of fractions.

Patient #	Site	Prescription, Gy	# of fractions
1	L1-L2	24	1
2	T1	24	1
3	L2	24	1
4	T10	24	1
5	L2	24	1
6	L4	24	1
7	C2	27	3
8	C7	27	3
9	C4	27	3
10	T2-T4	27	3
11	C5-C6	27	3
12	L5-S1	27	3

Epidural spinal cord compression grading (ESCC), also known as the Bilsky score, was used to determine suitability of patients for SBRT treatment and prescription dose and normal tissue dose constraints. The Bilsky system defines 6 stages of cord compression, with Grade 0 defining bone-only disease, Grade 1 defining epidural impingement (with three stages describing degree of impingement), Grade 2 cord compression with visible cerebrospinal fluid (CSF) still visible, and Grade 3 cord compression without visible CSF⁴⁹. Complete definitions are summarized in Table 2-2 below.

Spine SBRT is recommended for cases with a Bilsky grade of 0-1; higher Bilsky grades (2-3) are indicative of a need for high caution or unsuitability of SBRT due to the proximity of the tumor to cord⁵⁰. Grades 2-3 often require surgical decompression before SBRT may be considered. Cases where the tumor volume is quite large or has been previously irradiated are more typically prescribed a higher number of fractions (27 Gy in 3 fractions versus 24 Gy in a single fraction)⁵⁰.

Table 2-2: ESCC/Bilsky Grading Scale

Bilsky Score	Definition
Grade 0	<ul style="list-style-type: none"> • Bone only
Grade 1a	<ul style="list-style-type: none"> • Epidural impingement, no deformation of thecal sac
Grade 1b	<ul style="list-style-type: none"> • Epidural impingement, deformation of thecal sac, no spinal cord abutment
Grade 1 c	<ul style="list-style-type: none"> • Epidural impingement, deformation of thecal sac, spinal cord abutment, no cord compression
Grade 2	<ul style="list-style-type: none"> • Cord compression with visible cerebrospinal fluid (CSF) around cord
Grade 3	<ul style="list-style-type: none"> • Cord compression without visible CSF around spinal cord

GTV volume for each patient is summarized below; average volume for all twelve patients was 21.10 cm³ and ranged from 10.3 cc (Patient 8) to 100.7 cc (Patient 6).

Table 2-3: GTV Volume (cm³)

Patient ID	GTV Volume (cc)
24 Gy Single-Fraction	
1	53.2
2	11.1
3	50.1
4	19.7
5	42.5
6	100.7
27 Gy Three-Fraction	
7	22.5
8	10.3
9	14.6
10	62.7
11	11.1
12	10.5

2.2.2 – Treatment Planning Parameters

For each patient, two treatment plans were developed: one using 6 MV FF beam data and the other using 6 MV FFF beam data. The dose rate was set to 600 MU/min for FF plans; for FFF plans, the dose rate was 1400 MU/min. The maximum dose rate was chosen for FFF plans in order to take advantage of the potential reduction of beam-on time and resultant lowered integral dose²⁰. For each plan, identical beam arrangements were used: for the majority of plans, nine coplanar beams spaced 20° apart from 100° to 260° were defined in the treatment planning system (TPS). Figure 2-2 shows a representative plan. Three patients (Patient 1, Patient 8, and Patient 11) did not have this arrangement due to the location of the gross tumor volume relative to the respective organs at risk. Multiple Static Segments using 10 segments per field were used for plan delivery.

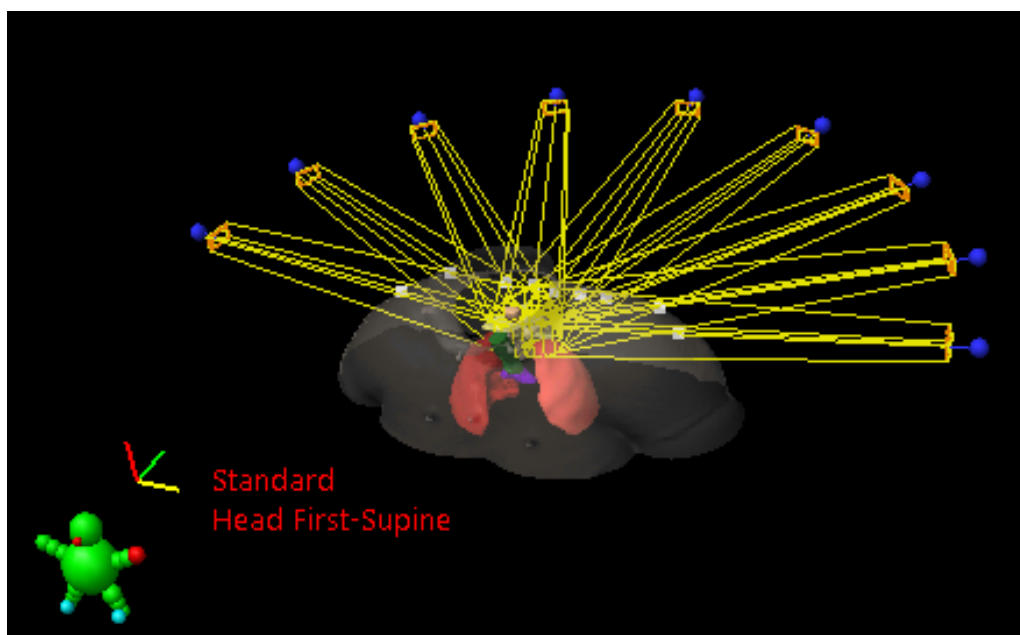


Figure 2-2: Standard beam arrangement for spinal SBRT patients

All treatment plans were generated using the Eclipse TPS and the Acuros XB dose calculation algorithm (Varian Medical Systems, Palo Alto, CA). Eclipse was chosen as the TPS for this study due to the demonstrated ability for Acuros XB – a dose calculation algorithm exclusive to Eclipse that utilizes the Linear Boltzmann Transport Equation - to accurately account for tissue heterogeneities including FFF beams as well as FF beams^{51,52}.

For all patients, plans were developed with the goal of increasing minimum dose to the GTV Dmin up to and beyond the recommended threshold for the prescription without pushing dose to normal tissue and primary organs at risk (OAR) above acceptable levels. For patients receiving 24 Gy in a single fraction, a Dmin of at least 14 Gy was attempted; for patients receiving 27 Gy in three fractions, the goal was a Dmin of at least 21 Gy. These planning directives were used to maintain efficacy of the plans, as doses lower than 14 Gy (single fraction) or 21 Gy (three fraction) were found to be associated with decreased local control¹. To improve comparison between the two sets of plans, dose to the cauda equina (lumbar patients) or spinal cord (cervical and thoracic patients) was kept within 5% between FF and FFF plans.

All patients were originally treated at MD Anderson using plans developed in the Pinnacle TPS. Plans created for this study utilized the plans, physician planning directives, and institutional guidelines (Table 2-2 below) to determine normal tissue tolerance and field arrangement. Dmax to the spinal cord was kept below 10 Gy for all plans regardless of prescription; Dmax to the cauda equina was kept below 16 Gy

or 14 Gy for single- and three-fraction courses, respectively. As most patients had received prior irradiation, more conservative dose guidelines were utilized; this limited how much dose could be delivered to the target volume, but was necessary to limit late effects of radiation on normal tissue volumes had the patients been treated with these plans.

Table 2-4: Institutional Guidelines for Normal Tissue Tolerances

Organ	Single Fraction		Three Fraction	
	Volume Dose	Maximum Dose	Volume Dose	Maximum Dose
Spinal Cord	$V(8\text{Gy}) \leq 1\text{cc}$	10 Gy	$V(9\text{Gy}) \leq 0.01\text{cc}$	10 Gy
Cauda Equina	$V(10\text{Gy}) \leq 1\text{cc}$	16 Gy	$V(12\text{Gy}) \leq 0.1\text{cc}$	14 Gy
Esophagus	$V(12\text{Gy}) \leq 5\text{cc}$	16 Gy	$V(12\text{Gy}) \leq 5\text{cc}$	16 Gy
Brachial Plexus	$V(11.9\text{Gy}) \leq 3\text{cc}$	16 Gy	$V(15\text{Gy}) \leq 0.01\text{cc}$	17 Gy
Heart	$V(16\text{Gy}) \leq 15\text{cc}$	22 Gy	$V(15\text{Gy}) \leq 15\text{cc}$	21 Gy
Trachea	$V(8.8\text{Gy}) \leq 4\text{cc}$	20.2 Gy	$V(8.8\text{Gy}) \leq 4\text{cc}$	18 Gy
Skin	$V(14\text{Gy}) \leq 10\text{cc}$	16 Gy	$V(16\text{Gy}) \leq 10\text{cc}$	21 Gy
Small Bowel	$V(9\text{Gy}) \leq 5\text{cc}$	15.4 Gy	$V(9\text{Gy}) \leq 0.01\text{cc}$	10 Gy
Colon	$V(11\text{Gy}) \leq 20\text{cc}$	18.4 Gy	$V(11\text{Gy}) \leq 20\text{cc}$	18 Gy
Rectum	$V(11\text{Gy}) \leq 20\text{cc}$	18.4 Gy	$V(11\text{Gy}) \leq 20\text{cc}$	18 Gy
Each Kidney	$V(8\text{Gy}) \leq 2/3 \text{ Volume}$	N/A	$V(10\text{Gy}) \leq 4/5 \text{ Volume}$	N/A
Total Kidney	$V(8.4\text{Gy}) \leq 200\text{cc}$, $V(7.4\text{Gy}) \leq 1000\text{cc}$	N/A	$V(10\text{Gy}) \leq 1/5 \text{ Volume}$	N/A
Total Lung	$V(7\text{Gy}) \leq 1000\text{cc}$	N/A	$V(10\text{Gy}) \leq 600\text{cc}$	N/A
Other	Volume outside PTV($\geq 100\%$ - 110% Prescription) $\leq 1\text{cc}$	N/A	Volume outside PTV($\geq 100\%$ - 110% Prescription) $\leq 8\text{cc}$	N/A

Order of plan creation was alternated for each patient such that biases by the primary planner were limited – for example, if Patient 1’s planning order was FF followed by FFF, then Patient 2’s planning order was FFF followed by FF.

2.3 – Statistical Analysis

We applied Wilcoxon signed rank test to compare the dose profiles for FF and FFF beams and GTV Dmin between the treatment plans. A two-sided p-value of less than 0.05 was considered statistically significant. All analyses were performed with statistical software R v3.4.3 (Vienna, Austria 2016).

3 RESULTS

3.1 – Analysis of Dose Profiles

3.1.1 – Penumbral Dose

Relative dose in the penumbra was compared between FF and FFF plans at distances of 2 mm, 5 mm, 10 mm, 30 mm, and 50 mm from the field edge at depths of 5 cm, 10 cm, 20 cm, and 30 cm at four depths and for five different field sizes. The percent difference between FFF and FF was calculated and plotted at 5 cm, 10 cm, 20 cm, and 30 cm depths, shown respectively in Figures 3-1 thru 3-4.

The ratio of FFF dose to FF dose ranged from 0.72 to 1.06 with a mean of 0.971 and a standard deviation of 0.05. The reduction in penumbral dose was found to be significant by Wilcoxon Signed Rank Test ($p < 0.05$).

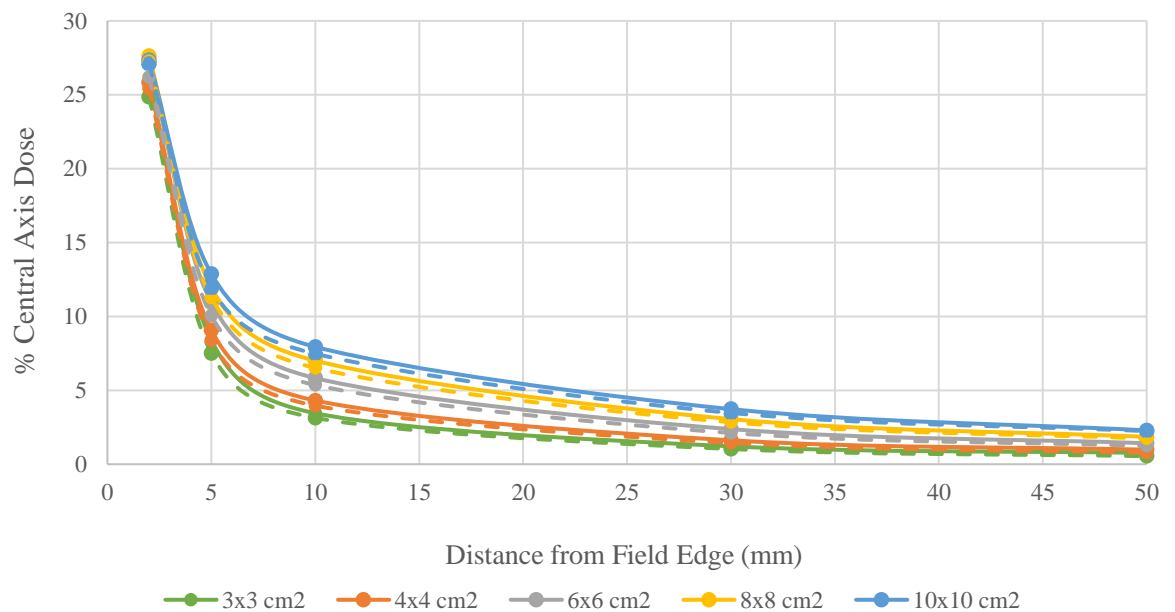


Figure 3-1: FF (solid lines) and FFF (dashed lines) penumbral dose at 5 cm depth

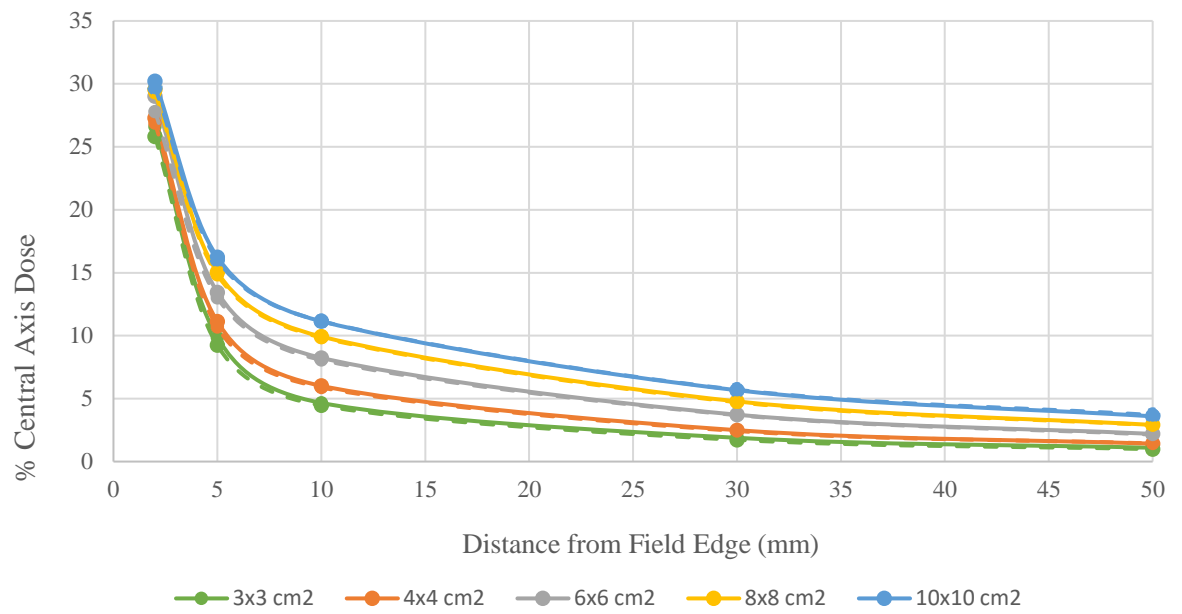


Figure 3-2: FF (solid lines) and FFF (dashed lines) penumbral dose at 10 cm depth

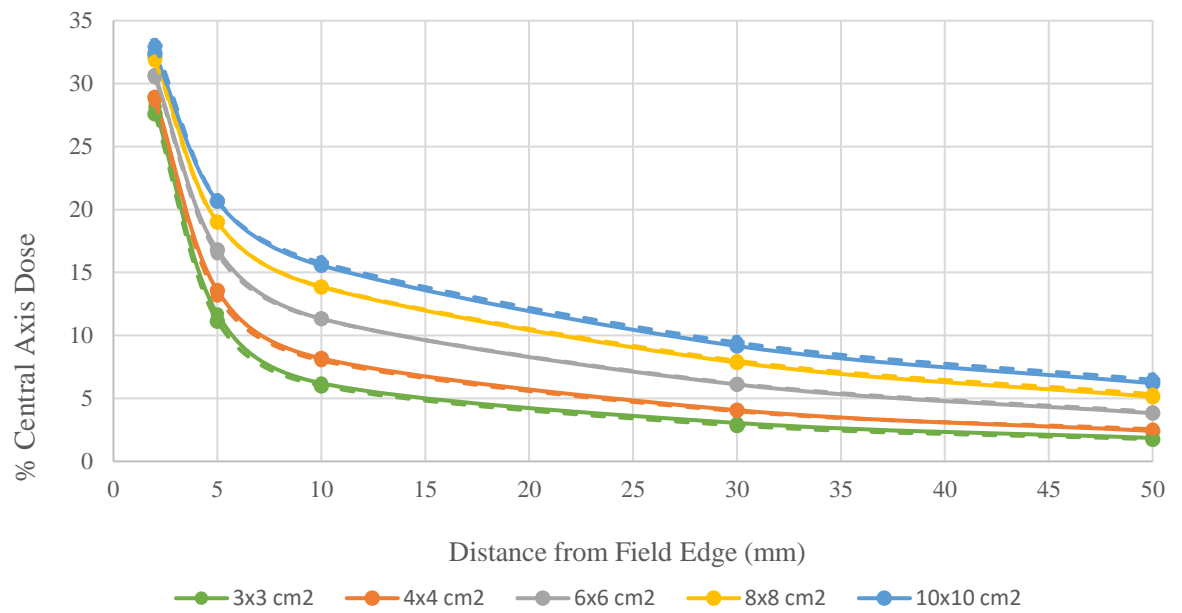


Figure 3-3: FF (solid lines) and FFF (dashed lines) penumbral dose at 20 cm depth

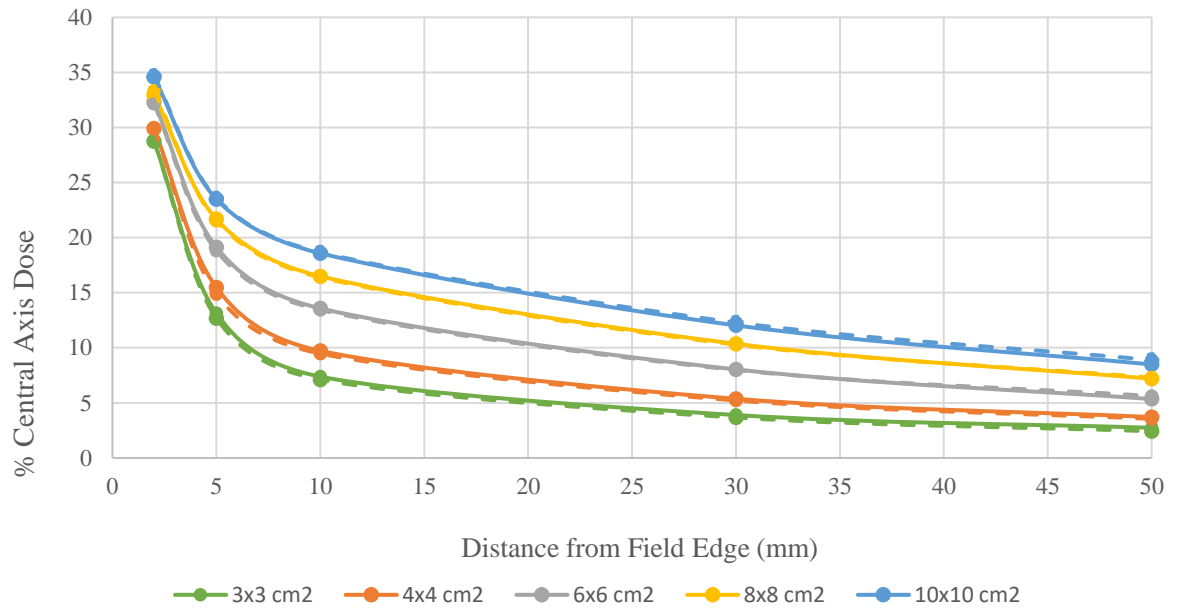


Figure 3-4: FF (solid lines) and FFF (dashed lines) penumbral dose at 30 cm depth

FFF profiles tended to have lower relative penumbral dose compared to FF profiles. This finding was particularly pronounced with smaller field sizes, as the reduction tended to be reduced (and, at greater depths, reversed) as field size increased.

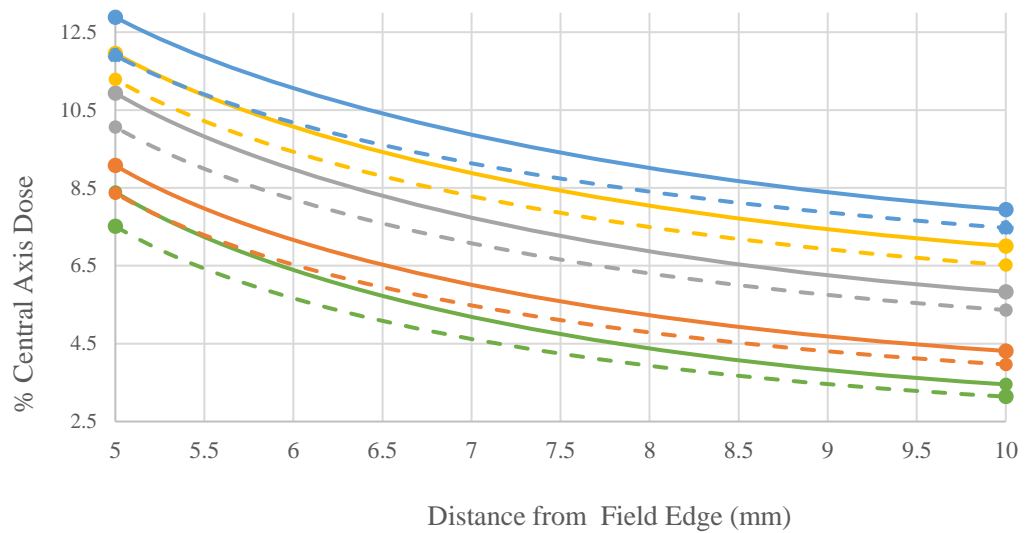


Figure 3-5: Close up of penumbral doses of FFF and FF beams at 5 cm depth.

Figure 3-5 (above) shows the region where the difference between FF and FFF was largest for all field sizes at 5 cm depth; this difference was greatest between 5-10 mm from the field edge.

3.1.2 – Penumbral Width

There was an overall decrease in width for FFF beams when compared with FF beams for all depths and field sizes with the exception of the 10x10 cm² field for both 20 cm depth and 30 cm depth. Reduction in penumbral width ranged from 0.77% to 5.02%. Although there was no significant difference in penumbral width within each individual field size, the overall reduction in width for all field sizes and depths was significant by Wilcoxon signed rank test ($p < 0.05$). The reduced dose and sharpened penumbra associated with FFF beams for fields relevant to spine SBRT treatments motivated continuation with the treatment planning to determine the practical effect of reduced penumbral width on our patient population.

Table 3-1: Difference (mm) in penumbral width of FFF beams relative to FF beams in water at various depths (cm)

Field Size (cm ²)	Depth in Water Phantom				p-value
	5	10	20	30	
3x3	-0.16	-0.11	-0.27	-0.19	0.0625
4x4	-0.10	-0.22	-0.14	-0.13	0.0625
6x6	-0.16	-0.21	-0.15	-0.23	0.0625
8x8	-0.20	-0.12	-0.10	-0.07	0.0625
10x10	-0.23	-0.04	0.04	0.22	0.563

3.2 – Comparison of Treatment Plans

Dmin for the GTV for each treatment plan was compared between FF and FFF plans. The DVH median and interquartile range were calculated and plotted for single- and three-fraction plans (Figure 3-6 A, B). Median dose was higher for FFF plans in the single-fraction set (Figure 3-6A) and lower for FFF plans in the three-fraction set (Figure 3-6B); however, overall differences were not statistically significant.

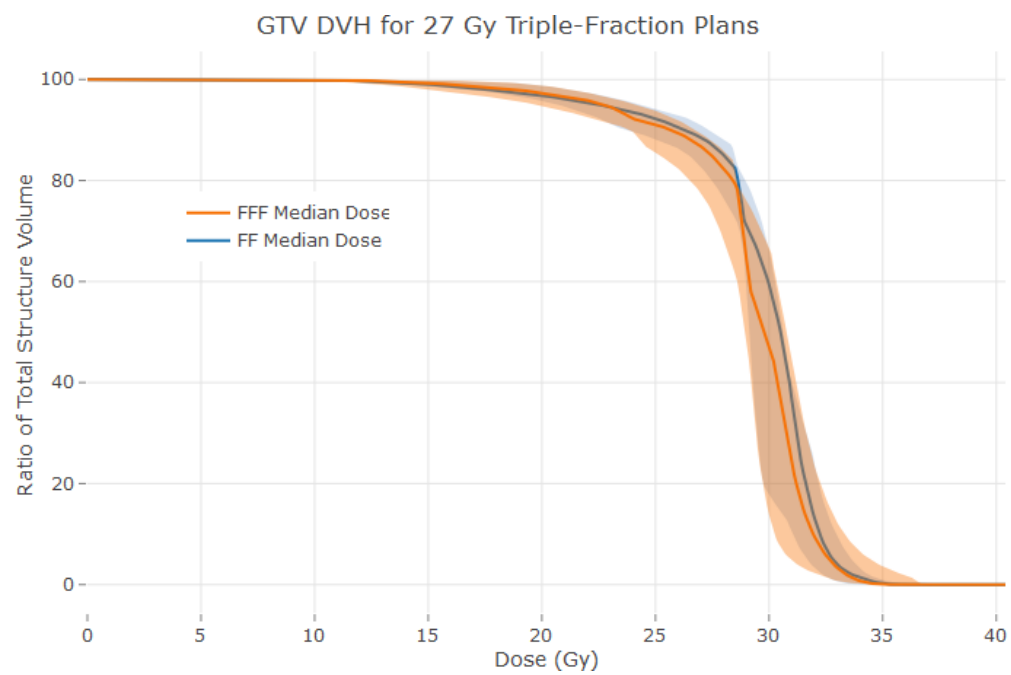
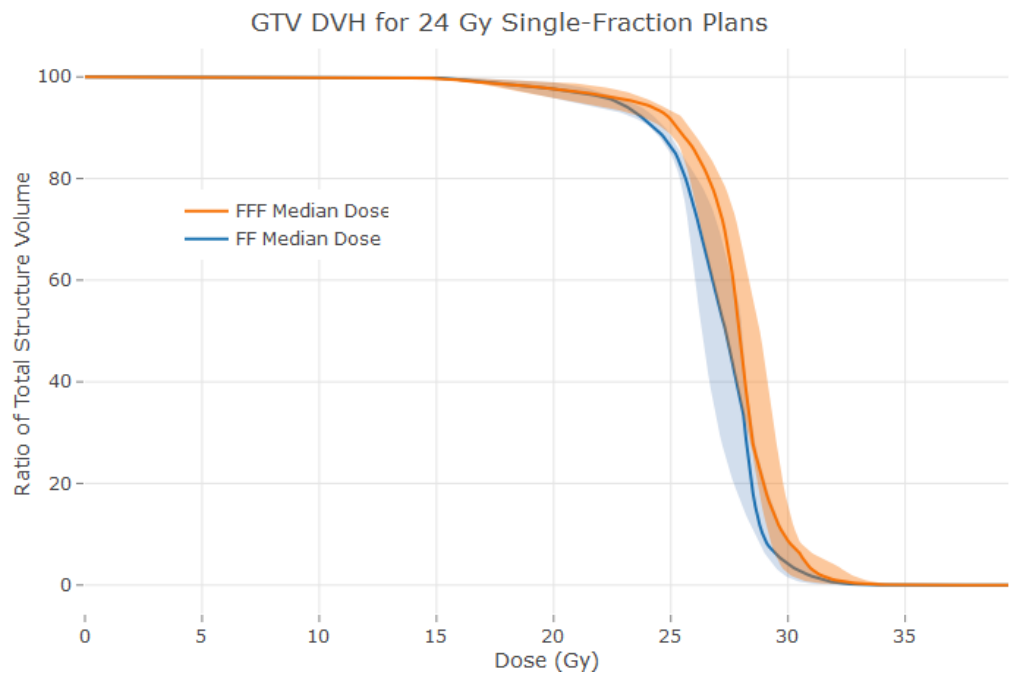


Figure 3-6: Median DVHs for single-and three-fraction GTV

Median DVHs were also calculated and plotted for spinal cord (Figure 3-7A) and cauda equina (Figure 3-7B). This analysis was performed to ensure that there was no significant difference in OAR dose in order to better compare GTV Dmin for each plan. The median dose was nearly identical at all points of the DVH for both cauda equina and spinal cord. Interquartile spread was quite wide for the cauda equina DVH; however, this finding is attributed to the fact that the cauda equina was the primary OAR for both single- and three-fraction plans, for which the max dose limit differed by 2 Gy (16 Gy and 14 Gy for single- and three-fraction plans, respectively). The spinal cord DVH interquartile spread was tighter, as maximum cord dose was the same regardless of fraction number.

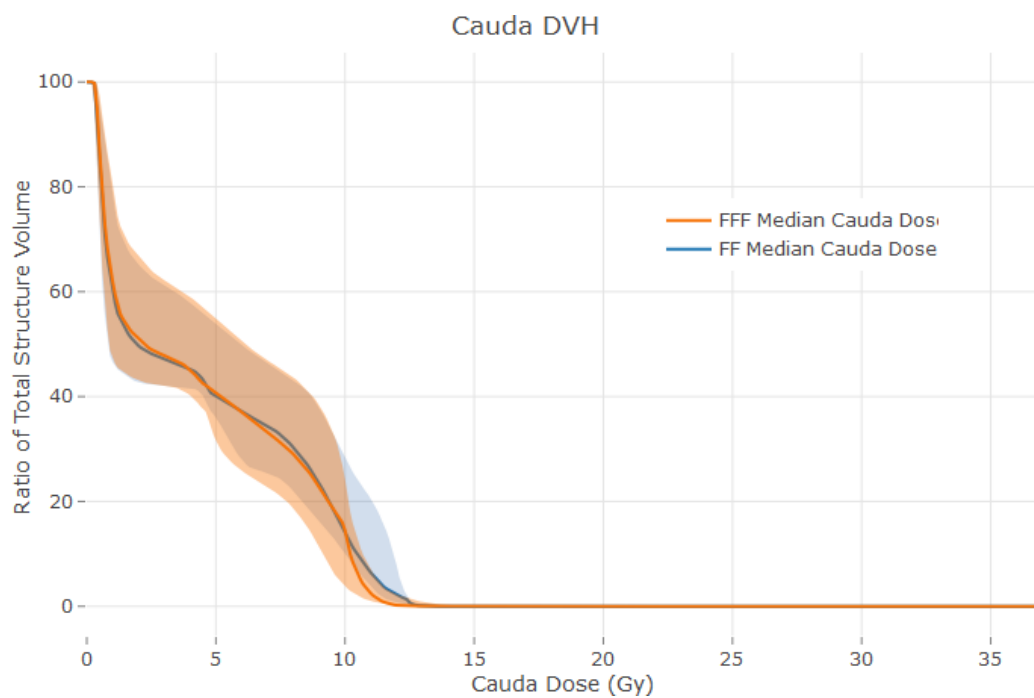
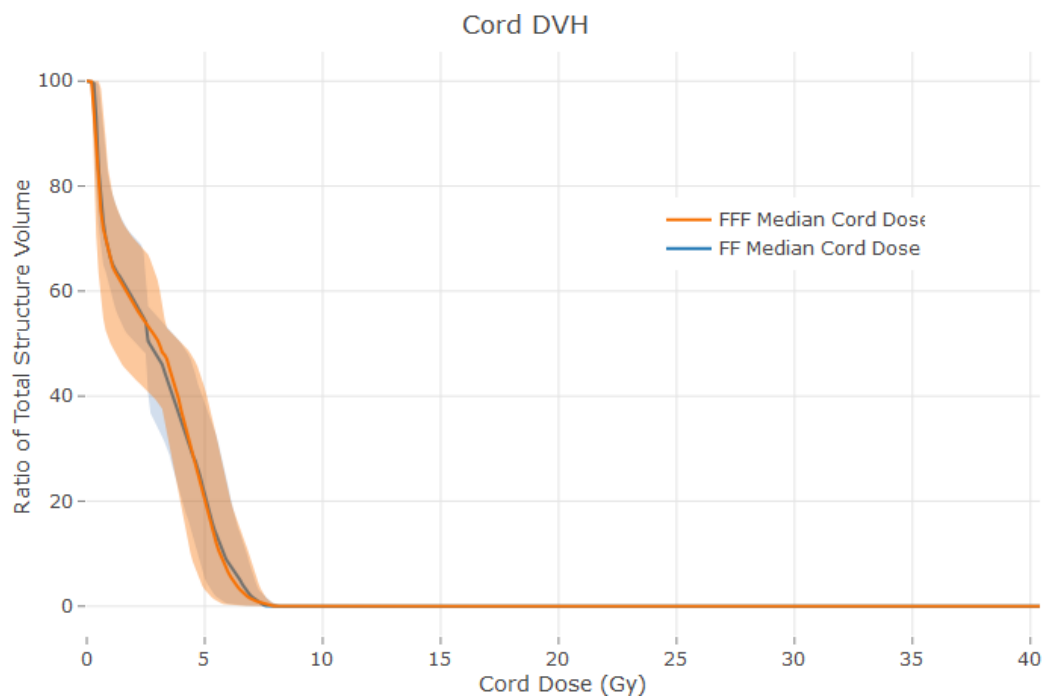


Figure 3-7: Cauda and Cord Median DVH

GTV Dmin was calculated and compared for both FF and FFF plans. Six of the twelve plans demonstrated an increase in Dmin for FFF plans. The increase in Dmin dose was not found to be significant by Wilcoxon Signed Rank Test ($p = 0.17$). The results are summarized below in Table 3-2.

Table 3-2: GTV Dmin for FF and FFF Plans

Minimum GTV Dose			
	FF	FFF	% Difference
24 Gy Single-Fraction			
Patient 1	11.98	10.81	10.21%
Patient 2	10.34	10.63	2.73%
Patient 3	15.78	15.81	0.21%
Patient 4	10.73	10.31	3.91%
Patient 5	22.45	21.07	6.35%
Patient 6	13.82	14.15	2.34%
27 Gy Three-Fraction			
Patient 7	7.30	8.43	14.46%
Patient 8	16.49	15.73	4.73%
Patient 9	9.05	8.93	1.33%
Patient 10	9.73	9.28	4.75%
Patient 11	8.16	8.19	0.35%
Patient 12	20.84	21.89	4.90%

OAR_{0.03cc} was also calculated for each plan to ensure that dose for the spinal cord or cauda was within 5% for FF and FFF plans. The results are listed below in Table 3-4. It is worth noting that although these were the primary OAR, the cord and/or cauda equina did not define the end-point of planning. All normal tissue limits were observed. As such, planning was often considered complete not when maximum primary OAR dose was met, but when other normal tissue began to exceed dose constraints, leading to a lower than expected GTV dose.

Table 3-3: OAR_{0.03cc}

OAR _{0.03cc}				
	Primary OAR	FF	FFF	% Difference
24 Gy Single-Fraction				
Patient 1	Cauda	12.6	12.1	4.05%
Patient 2	Cord	7.4	7.6	2.67%
Patient 3	Cauda	12.6	12	4.88%
Patient 4	Cord	7.7	7.6	1.31%
Patient 5	Cauda	15.2	15.1	0.66%
Patient 6	Cauda	13.7	14.2	3.58%
27 Gy Three-Fraction				
Patient 7	Cord	5.95	5.7	4.29%
Patient 8	Cord	5.6	5.8	0.00%
Patient 9	Cord	7.95	8	0.63%
Patient 10	Cord	8.8	8.6	2.30%
Patient 11	Cord	7.4	7.45	0.67%
Patient 12	Cauda	6.4	6.45	0.00%

Beam-on time was also evaluated for each plan, as the duration of treatment may have an effect on integral dose. Namely, shorter treatment times limit the potential for intrafractional error due to patient motion. Beam on-time per fraction was calculated as the dividend of total MU divided by the dose rate (600 MU/minute for FF, 1400 MU/minute for FFF). Treatment duration was definitively lower for FFF plans compared with FF plans (p -value < 0.05). The average reduction in beam-on time was 12.5

minutes, with the largest difference being a reduction of 27.8 minutes (Patient 6) and the smallest being a reduction of 1.73 minutes (Patient 11). The beam-on time per fraction is summarized below in Table 3-5.

Table 3-4: Beam-on time per fraction		
Beam-on Time		
	FF	FFF
24 Gy Single-Fraction		
Patient 1	23.16	15.39
Patient 2	23.26	9.48
Patient 3	47.29	19.58
Patient 4	44.47	19.85
Patient 5	21.49	9.84
Patient 6	42.52	14.74
27 Gy Three-Fraction		
Patient 7	9.54	3.8
Patient 8	10.78	5.12
Patient 9	5.52	2.57
Patient 10	22.64	12.08
Patient 11	8.84	7.11
Patient 12	11.64	1.98

Total MUs for each patient plan were calculated and have been recorded below in Table 3-6.

Table 3-5: Total MUs for each patient plan		
Total MUs		
Patient ID	FF	FFF
24 Gy Single-Fraction		
1	13896	21543
2	13958	13278
3	28372	27418
4	26682	27789
5	12893	13782
6	25512	20638
27 Gy Three-Fraction		
7	17175	15945
8	19398	21507
9	9939	28788
10	40746	50733
11	15909	29841
12	20943	8328

Grid size for each patient was the same for both FF and FFF plans and was scaled such that the dose calculated included the entire scanned patient volume. Grid resolution was 2.5 mm for all patients and plans. Grid sizes for each patient is listed below in Table 3-6.

Table 3-6: Dose grid size (pixels)

Patient ID	Size (Pixel)	
	Width	Height
1	149	100
2	220	113
3	143	108
4	146	98
5	147	97
6	138	103
7	167	96
8	181	111
9	199	113
10	217	111
11	210	107
12	138	96

Heterogeneity index (HI) was calculated for each plan as the ratio of highest dose received by 5% of the PTV to lowest dose received by 95% of the PTV⁵³ and is shown below in Table 3-7.

Table 3-7: Heterogeneity Index for all plans

Heterogeneity Index		
Patient ID	FF	FFF
1	1.57	1.96
2	1.65	1.63
3	2.03	1.83
4	2.01	1.85
5	1.51	1.78
6	1.59	1.63
7	1.74	1.71
8	1.58	1.53
9	2.13	2.18
10	1.92	2.07
11	1.91	1.93
12	1.41	1.39

Field size varied and was dependent on the size of the CTV. Jaws were collimated such that there was a 5 mm margin around the CTV on all sides. Average field size for each plan is summarized below.

Table 3-8: Average field sizes (cm)				
Average Field Size				
Patient ID	FF		FFF	
	X	Y	X	Y
1	10.1	9.9	10.2	10.0
2	8.6	4.6	8.0	4.5
3	6.6	6.2	6.4	6.2
4	6.4	3.6	6.2	8.0
5	10.0	13.0	6.4	4.6
6	10.5	5.0	10.4	5.1
7	7.3	4.4	7.1	4.5
8	4.4	3.9	4.4	3.9
9	8.3	3.8	8.3	3.8
10	8.3	8.8	7.9	8.9
11	5.7	5.5	5.4	4.9
12	9.2	6.8	9.1	6.8

4 DISCUSSION

4.1 – General Discussion

We compared penumbral width as well as penumbral and out-of-field dose for FF and FFF beams using dose profiles obtained in a 3D water phantom from the Varian Standard Beam Data. Our results indicate that there is a statistically significant ($p < 0.05$) difference between FF and FFF beams in penumbral width and dose. This reduction tended to be more exaggerated at smaller field sizes and at shallower depths with larger field sizes tending towards increased penumbral dose and width for FFF beams compared with FF beams. That smaller field sizes tend to show more benefit from FFF beams is notable, as the trend towards highly-modulated treatment techniques (IMRT and SBRT) translates to field sizes overall growing smaller. This potential for reduction in normal tissue dose is an important factor to be considered in treatment planning, particularly for targets in close proximity to critical OAR.

It is important to note, however, that the absolute difference in penumbral width was quite small. At no field size or depth did the difference exceed 0.3 mm. This observation suggests that the clinical benefits of FFF over FF, with respect to dose fall off, may in fact be quite minimal. Additionally, the difference in penumbral dose determined here represents only the difference in dose relative to the central axis at five points (2 mm, 5 mm, 10 mm, 30 mm, and 50 mm from the field edge). As such, the actual reduction in penumbral dose may be even smaller.

Treatment plans utilizing both FF and FFF beams were developed for 12 patients with spinal metastases in the cervical, thoracic, and lumbar regions. For each patient GTV Dmin was extracted and compared between the FF and FFF plans. Improvement in GTV Dmin was seen in approximately half of the patients while the other half saw either no improvement or a reduction in Dmin. The overall difference in GTV Dmin was deemed to be statistically insignificant by Wilcoxon Signed Rank Test.

The differences in treatment delivery time are pronounced in that FFF plans had overall shorter beam on times compared with FF plans in all but a single case (Patient 12). The potential benefit of this outcome for patients cannot be overstated, as patients with spinal metastases often present with pain and motor dysfunction and find it difficult to lie still on the treatment couch during delivery, introducing a greater potential for intrafractional variation. Shorter treatment times limit that potential and improve patient experience and throughput

One should note that the results of a treatment planning study may be confounded by several factors. Experience and ability of the planner, planning system and dose algorithm used, beam model, optimization parameters, beam configuration, planning objectives, patient positioning, segment number, time spent planning, number of iterations, and gross anatomy may all contribute to the quality of the plan. These factors make achieving a completely objective plan comparison quite difficult, as a different planner may create entirely different plans with the same patient population and achieve different results.

A potential limiting factor of this study is the method in which the beam models were generated and the dose calculation algorithm that was used. The Varian Standard

Beam Data, from which the beam models were generated in Eclipse, were obtained using an ionization chamber – the poor spatial resolution inherent to this measurement in addition to the high dose gradient of the primary region of interest (i.e., the penumbra) may have a negative effect on the beam model, making accurate dose calculation difficult. Additionally, Acuros XB dose calculation algorithm used for this study, while generally quite accurate, is not as precise or accurate as a dose calculation made using Monte Carlo methods would be. As such, it is possible that any demonstrable differences between FF and FFF plans may have been confounded by these factors.

4.2 – Conclusions

In conclusion, the hypothesis that the use of FFF beams in SBRT treatments of spinal cord metastases would improve target coverage was not entirely supported. Half of the patients saw some benefit from FFF in terms of increased GTV Dmin, but half did not. Although there was a statistically significant reduction in penumbral width and dose for FFF beams when compared with FF beams, this difference was in absolute terms quite minute. All but one patient had shorter beam-on times with FFF beams compared to FF beams. Treatment plans developed for patients with spinal metastases using FFF beams were equivalent to those developed using traditional FF beams when dose to the spinal cord or cauda equina was kept within 5% between FF and FFF plans.

4.3 – Future Work

As half of the patients had improved GTV Dmin and all but one had reduced delivery times with plans generated using FFF beams, it is possible that certain specific patients derive more benefits from FFF over others. Future work on this project will likely include multivariate analysis on a much larger patient population in order to determine what factors would indicate that a patient would be better served with a plan generated using FFF. Factors that would be investigated may include tumor size, shape, location, pathology, patient anatomy, treatment history, etc.

5 APPENDIX

5.1 – Individual Patient Plans

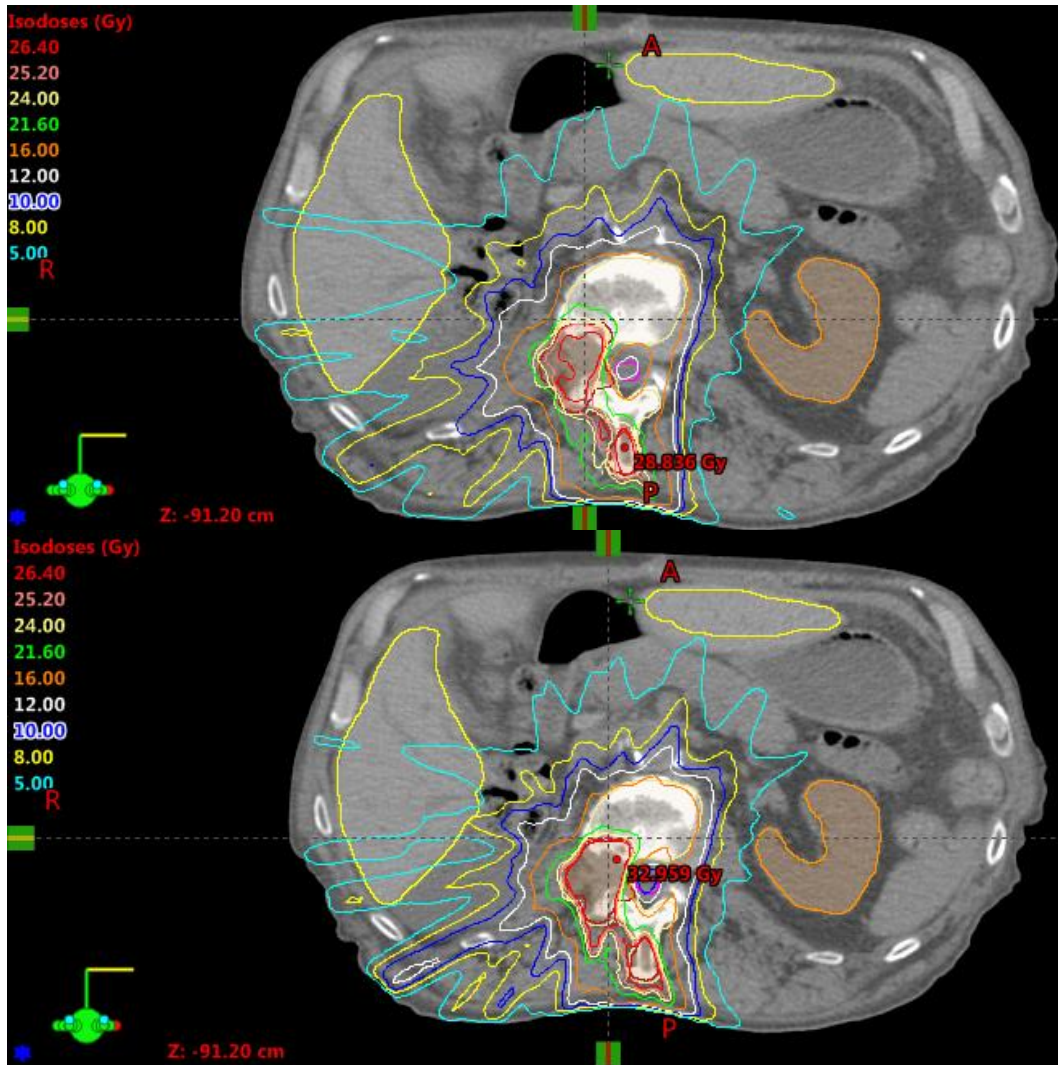


Figure 5-1: Patient 1 axial isodose images. Top: FF Plan, Bottom: FFF Plan

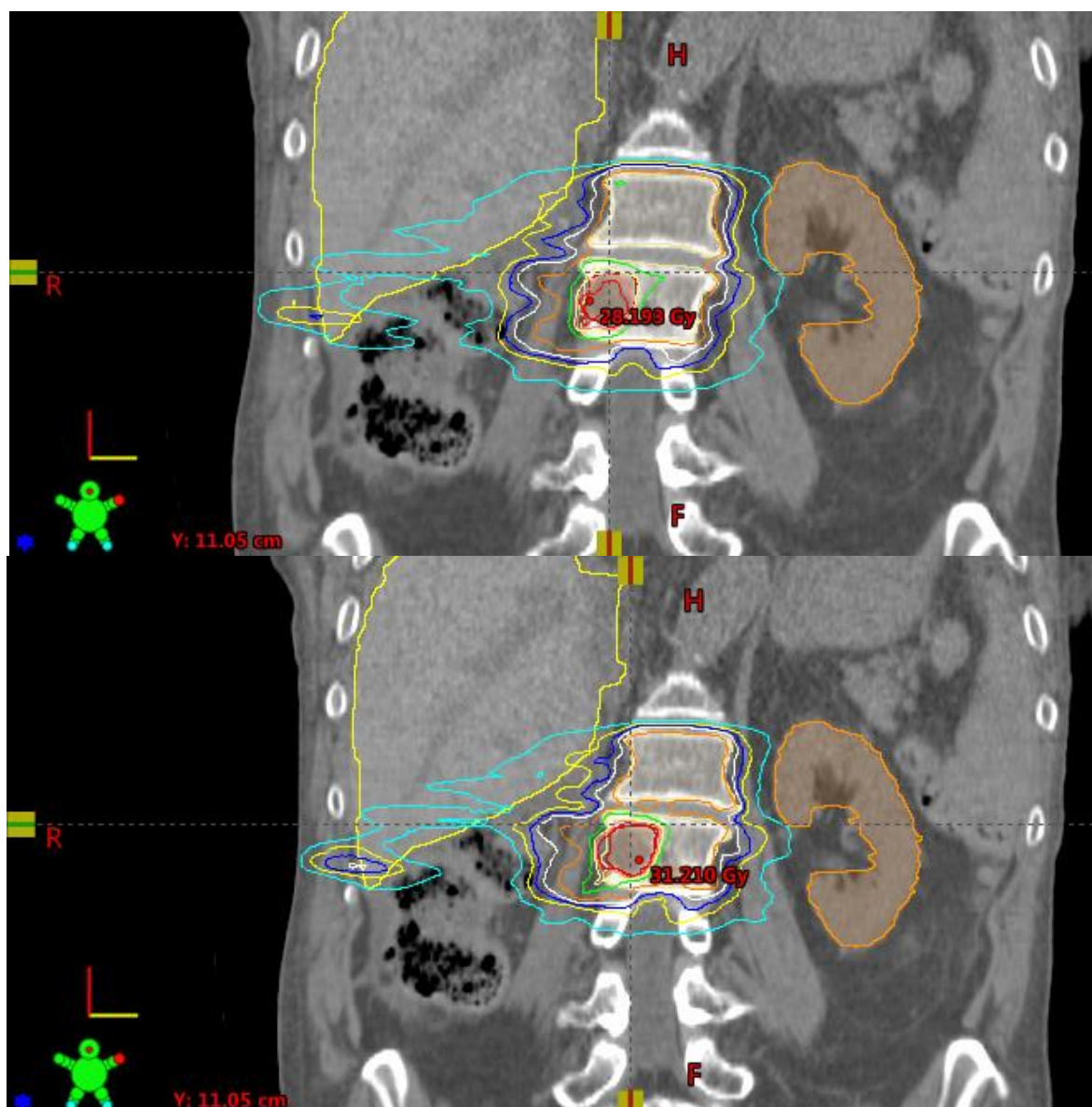


Figure 5-2: Patient 1 coronal isodose images. Top: FF Plan, Bottom: FFF Plan

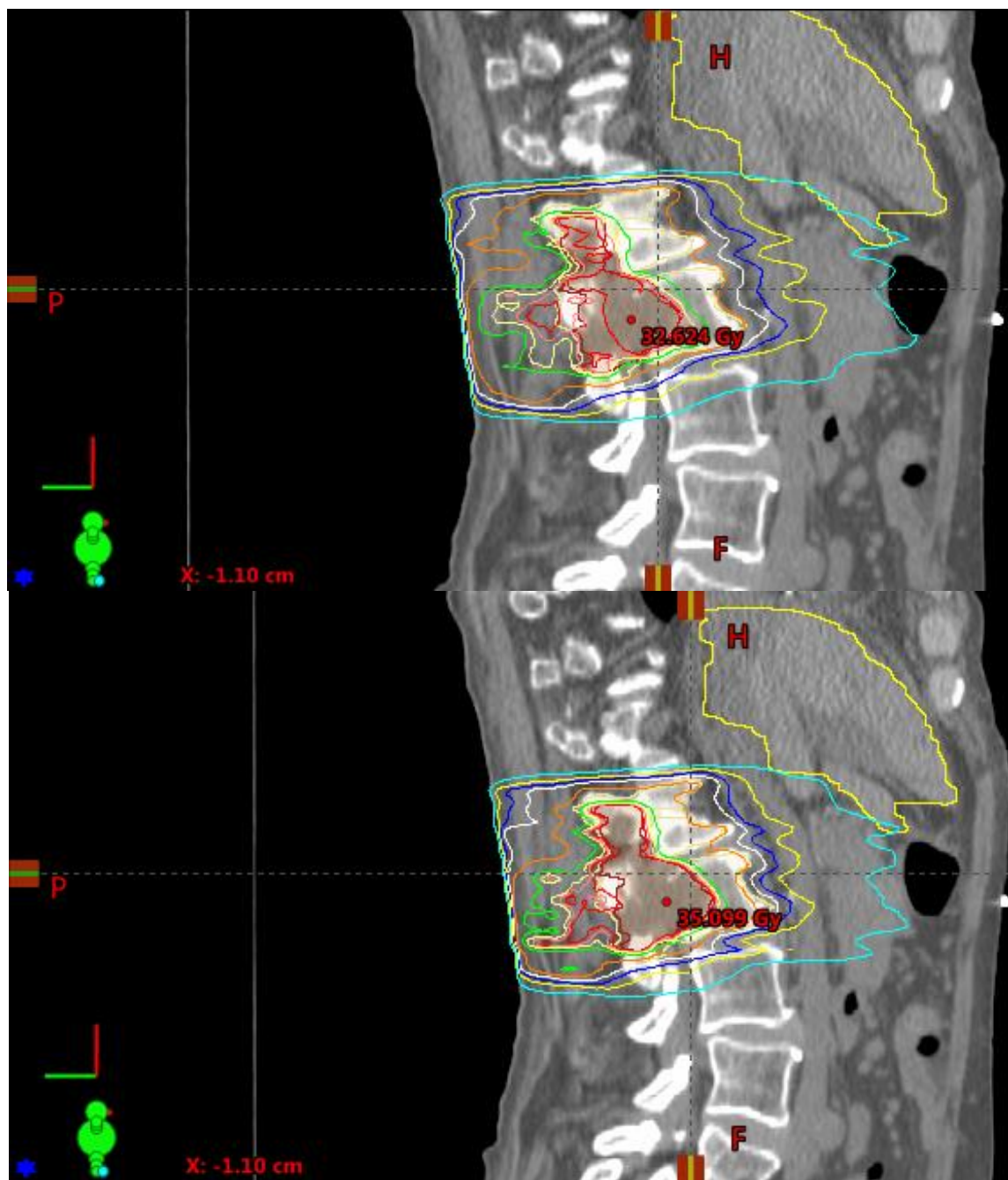


Figure 5-3: Patient 1 sagittal isodose images. Top: FF Plan, Bottom: FFF Plan

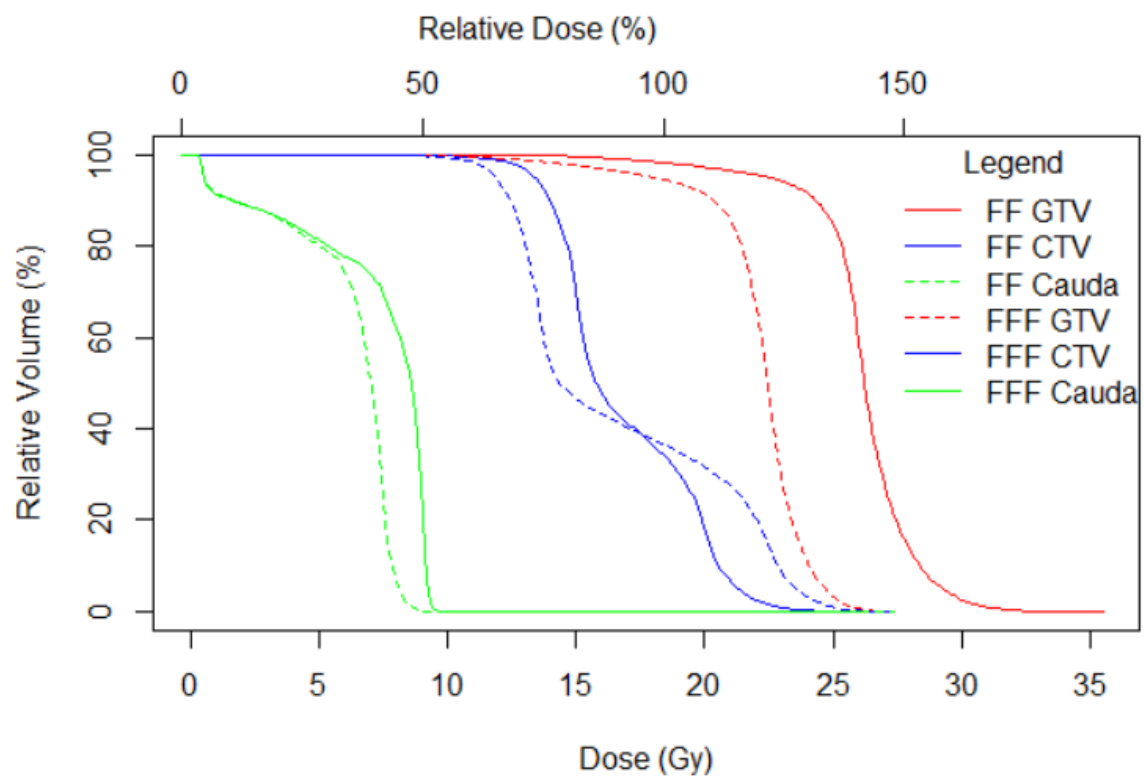


Figure 5-4: Patient 1 DVH

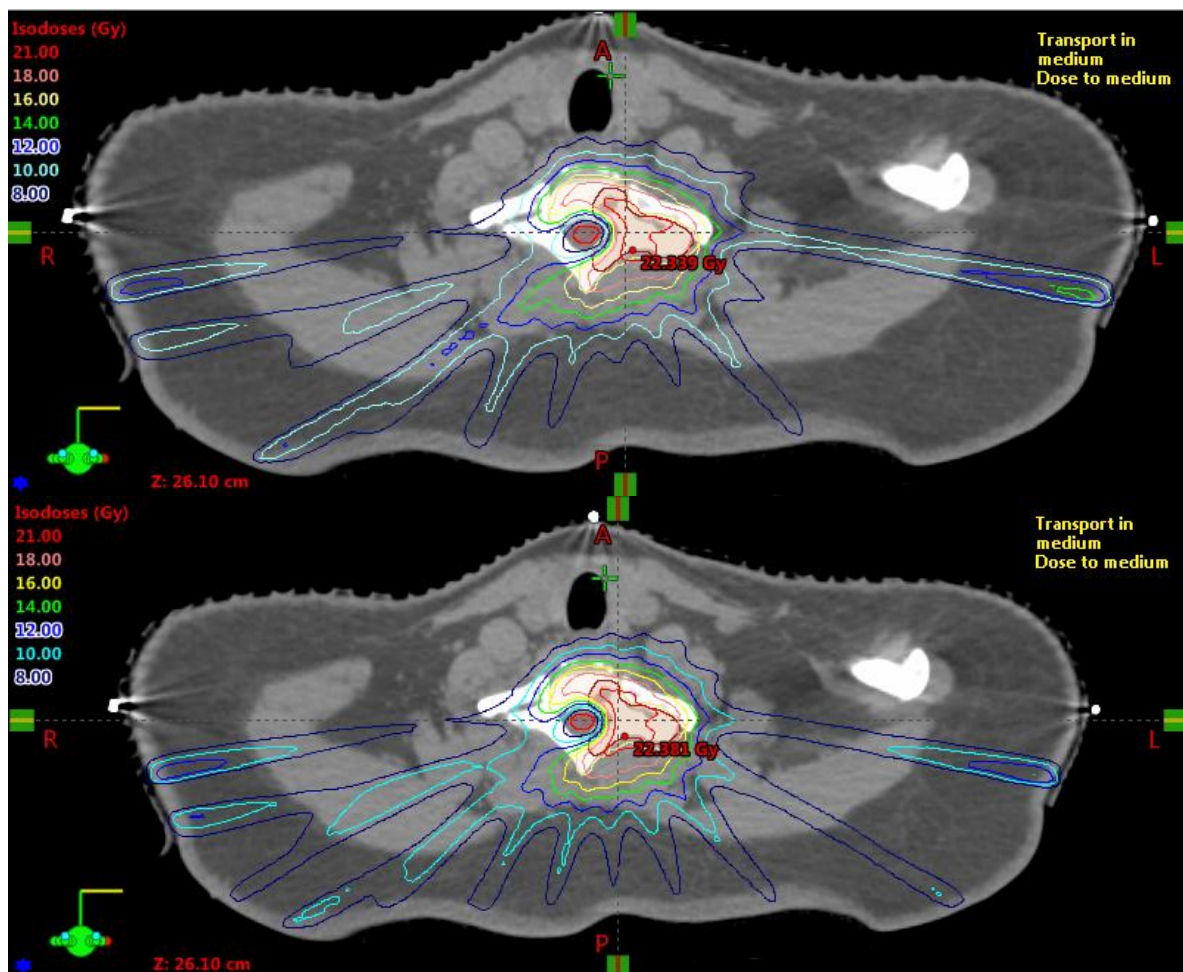


Figure 5-5: Patient 2 axial isodose images. Top: FF Plan, Bottom: FFF Plan

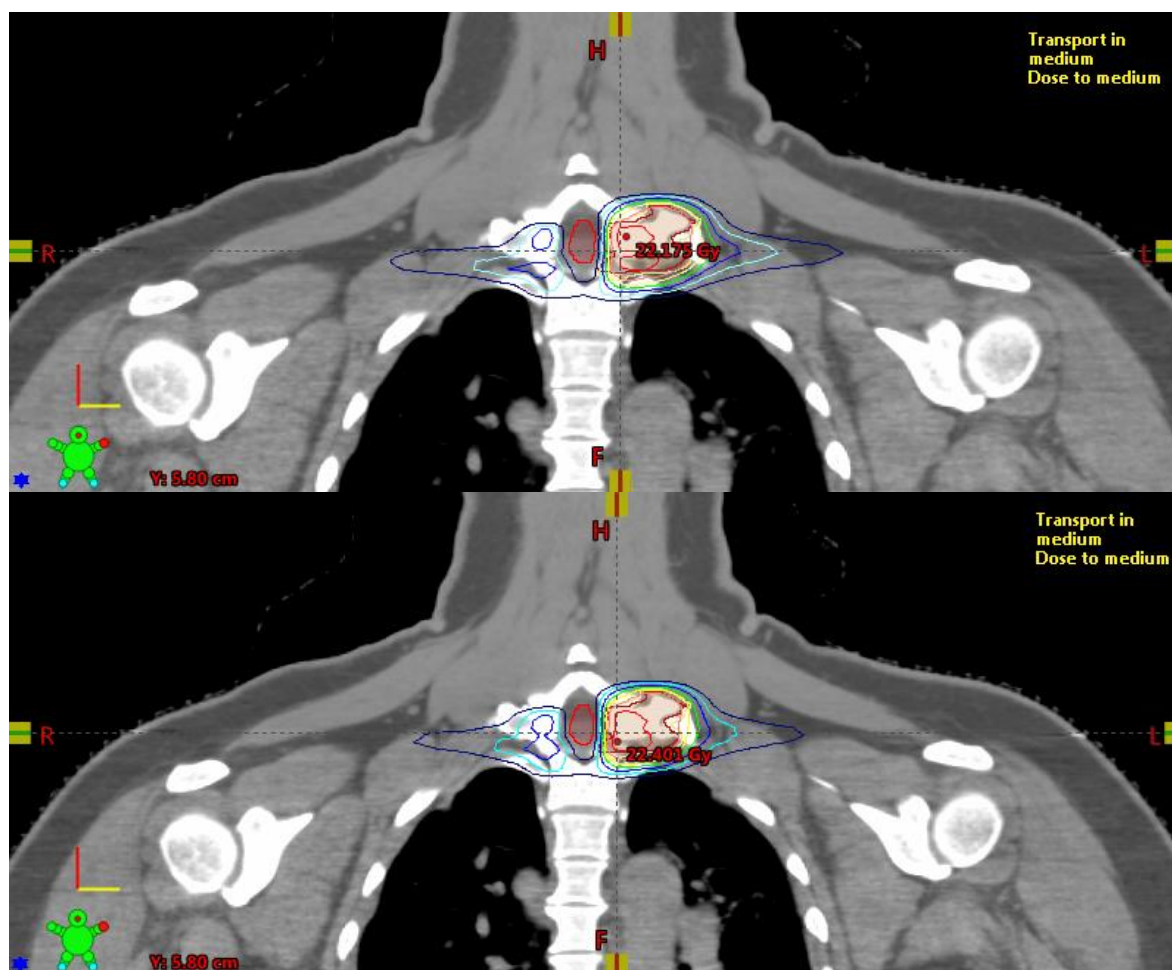


Figure 5-6: Patient 2 coronal isodose images. Top: FF Plan, Bottom: FFF Plan

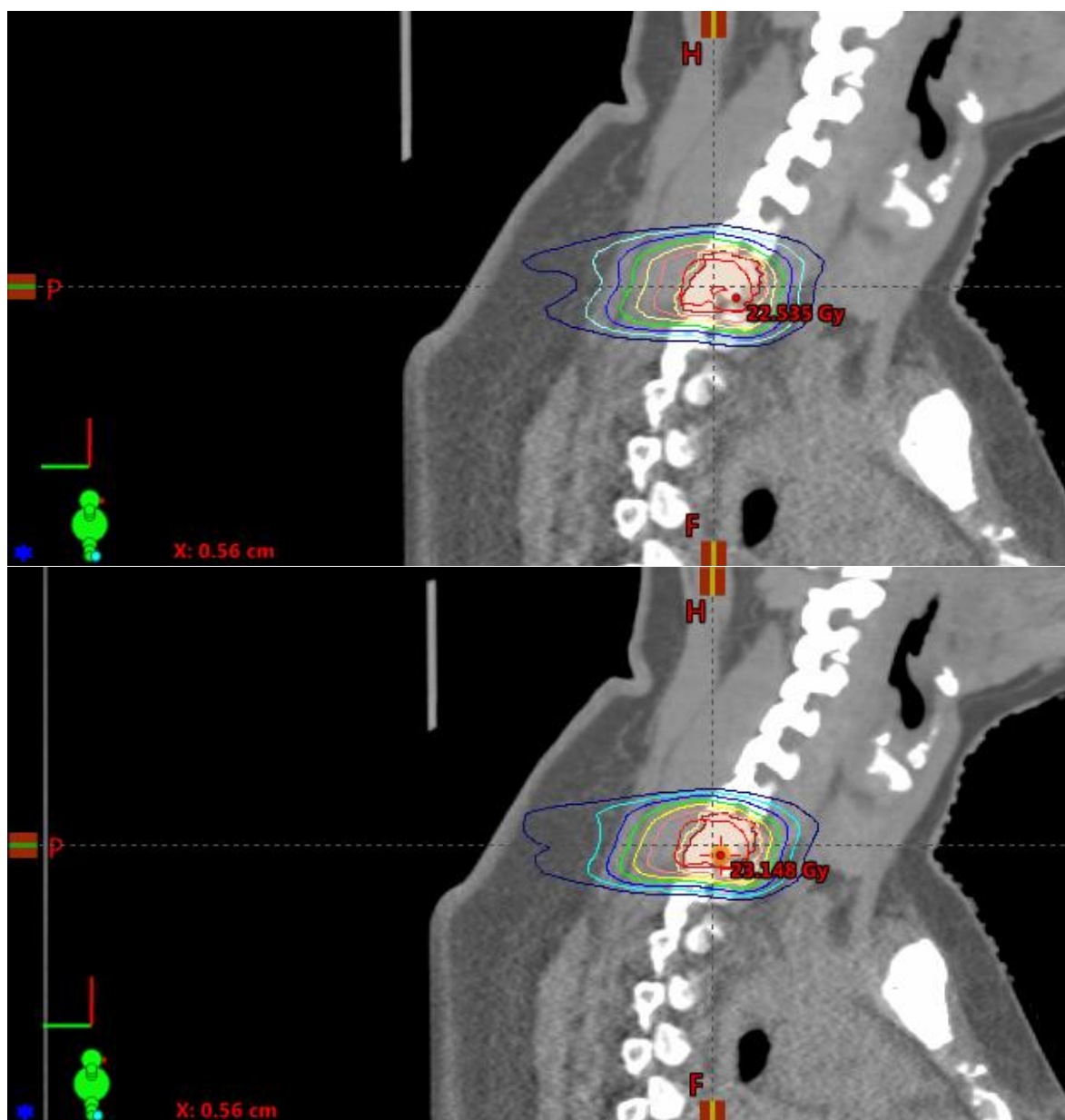


Figure 5-7: Patient 2 sagittal isodose images. Top: FF Plan, Bottom: FFF Plan

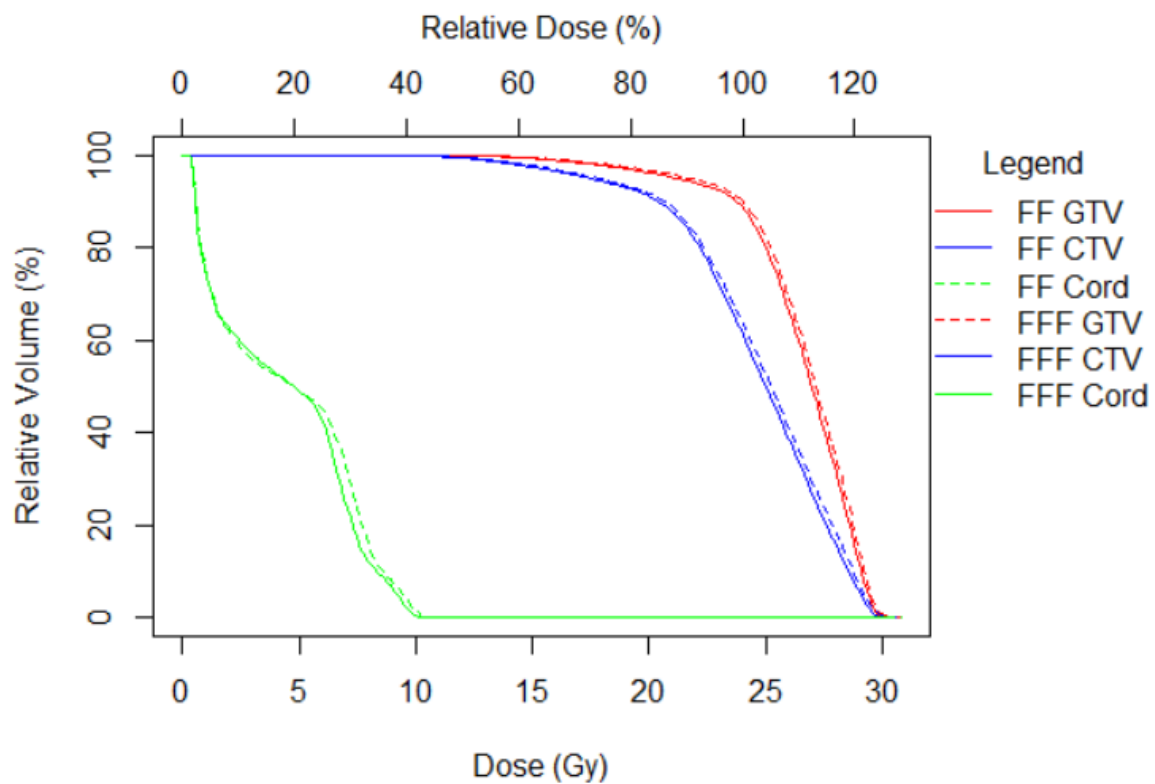


Figure 5-8: Patient 2 DVH

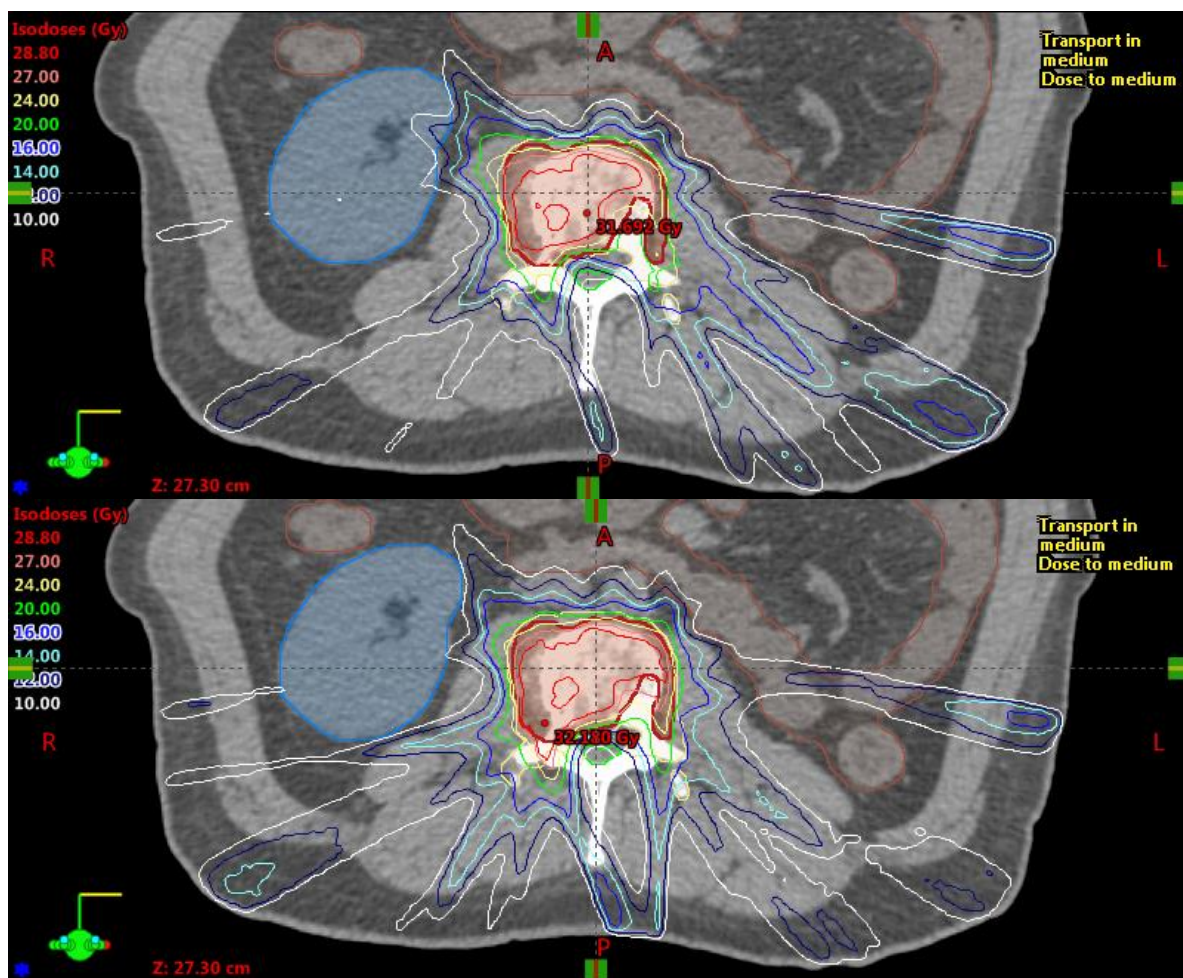


Figure 5-9: Patient 3 axial isodose images. Top: FF Plan, Bottom: FFF Plan

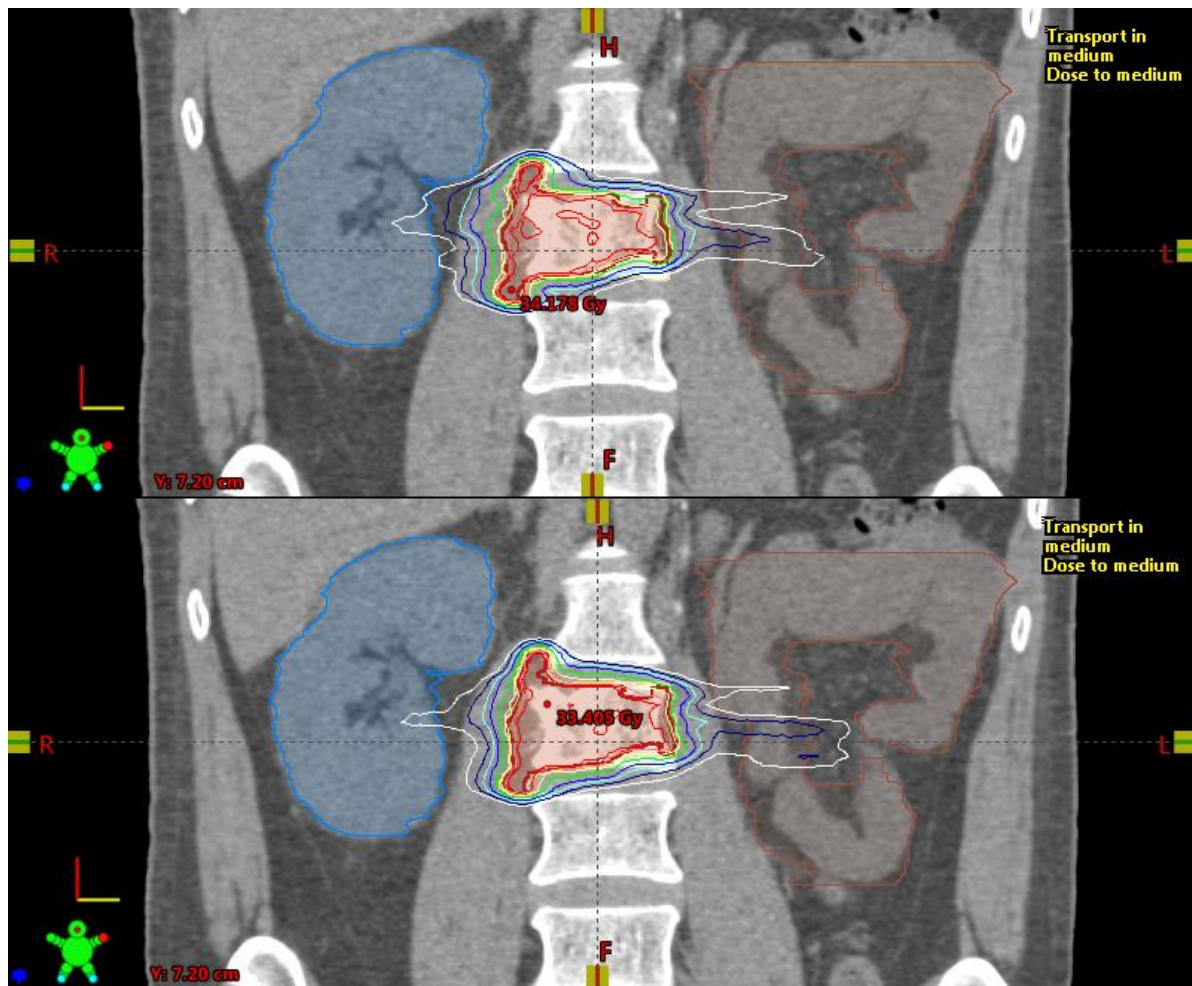


Figure 5-10: Patient 3 coronal isodose images. Top: FF Plan, Bottom: FFF Plan

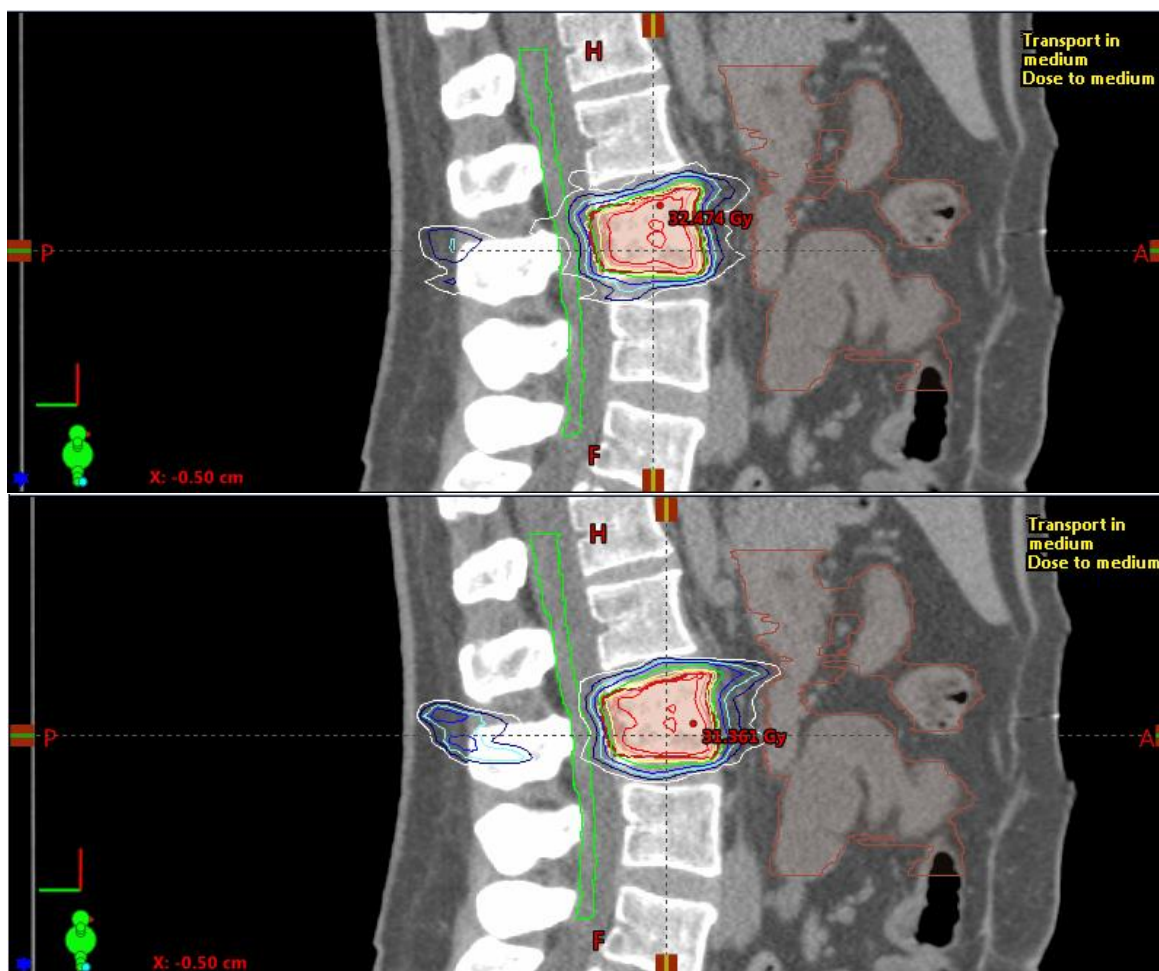


Figure 5-11: Patient 3 sagittal isodose images. Top: FF Plan, Bottom: FFF Plan

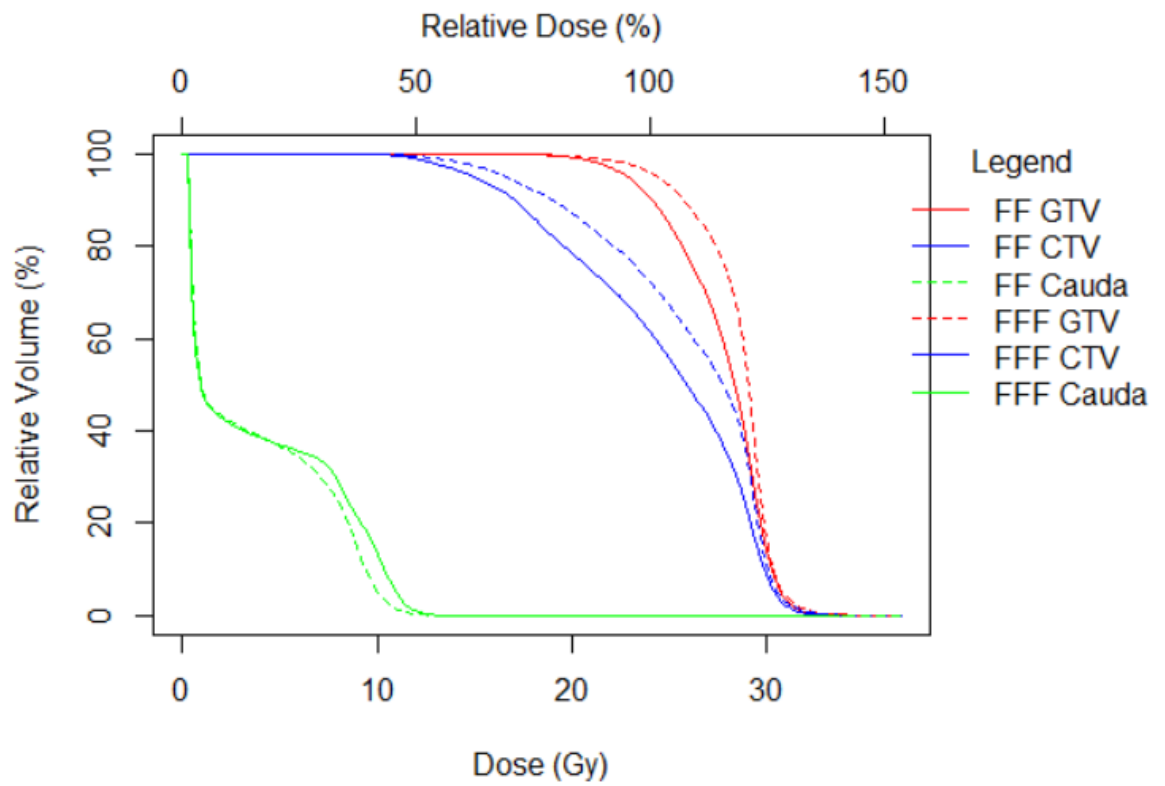


Figure 5-12: Patient 3 DVH

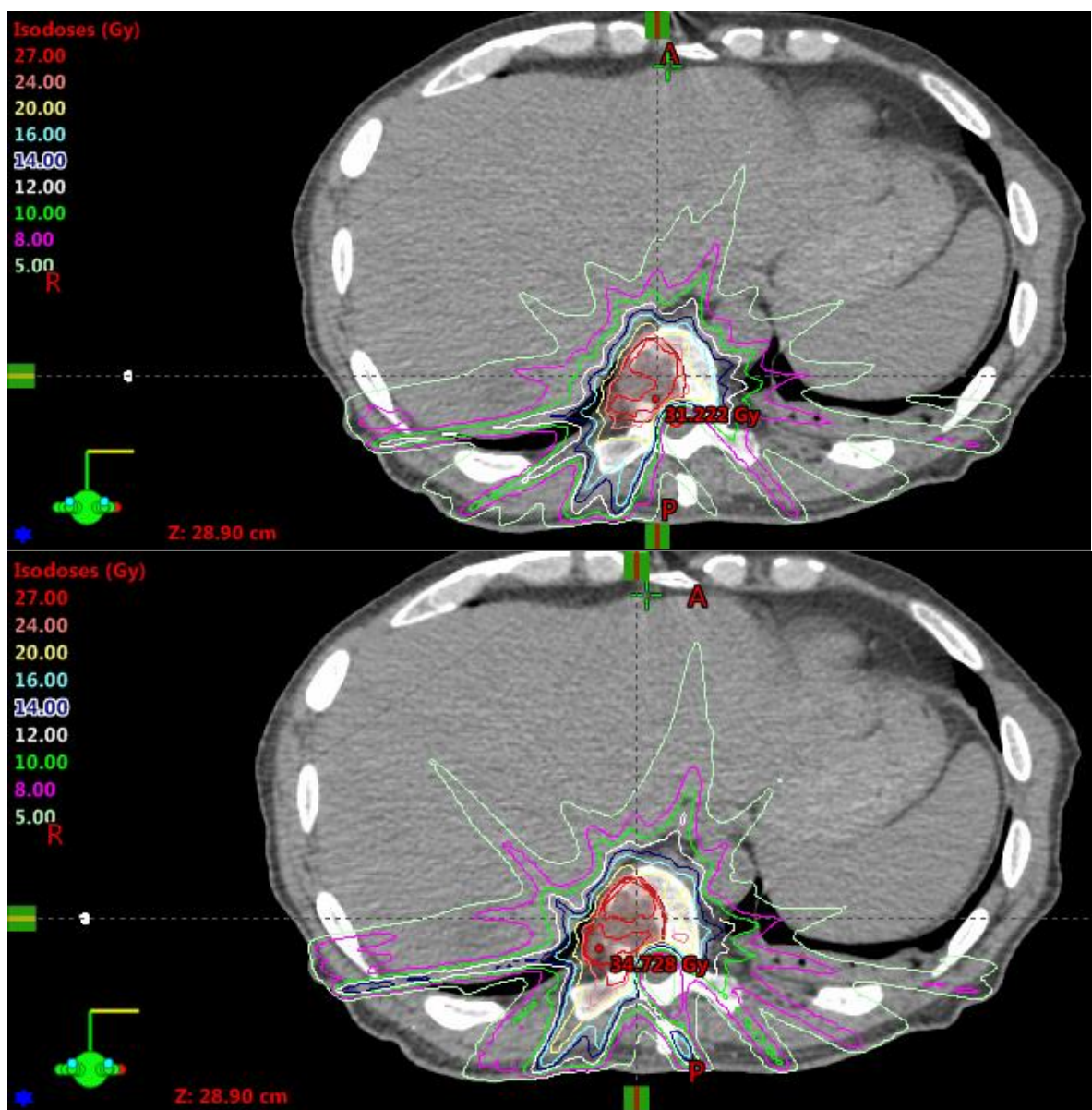


Figure 5-13: Patient 4 axial isodose images. Top: FF Plan, Bottom: FFF Plan, Bottom: Plan

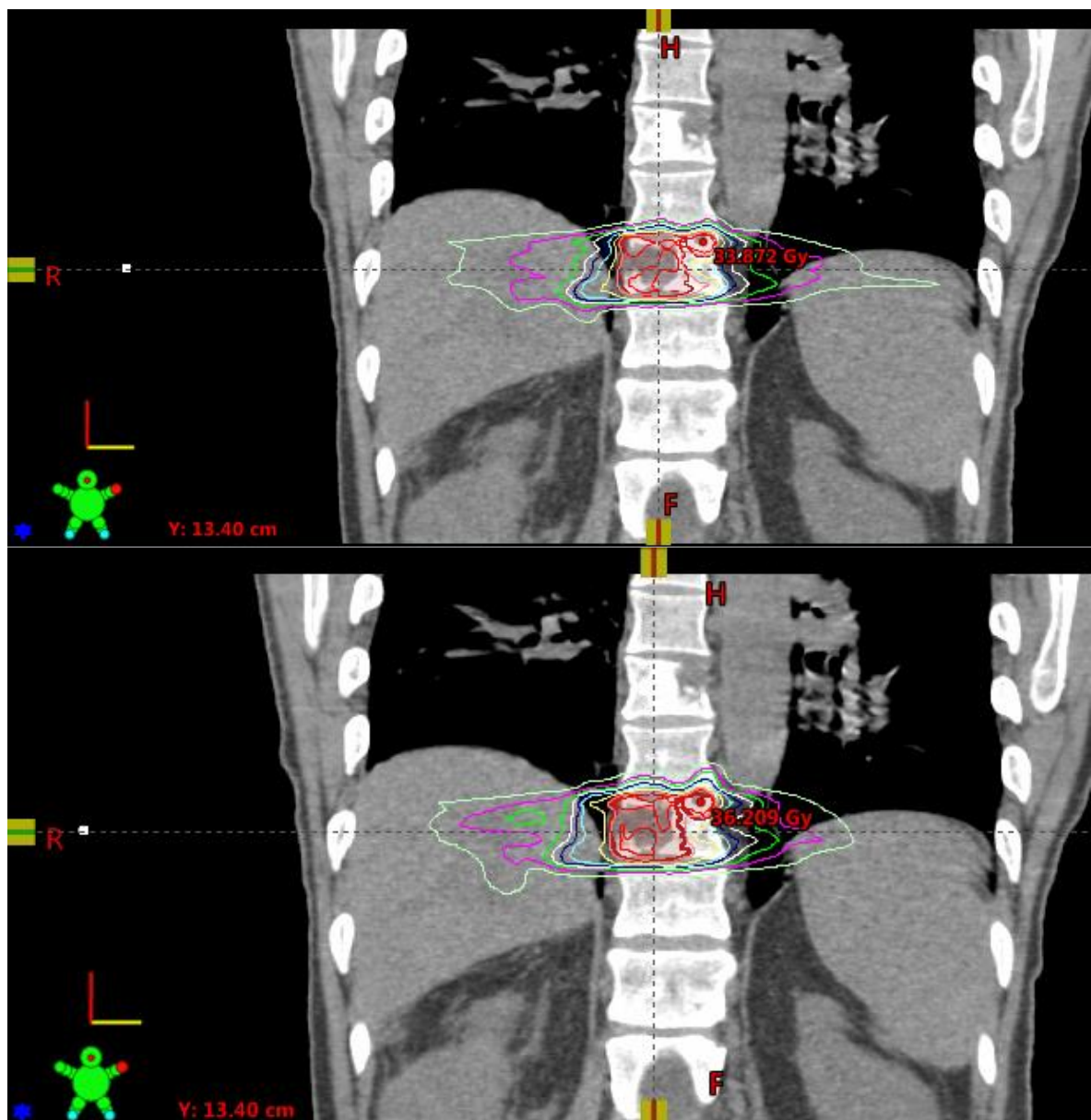


Figure 5-14: Patient 4 coronal isodose images. Top: FF Plan, Bottom: FFF Plan, Bottom: Plan

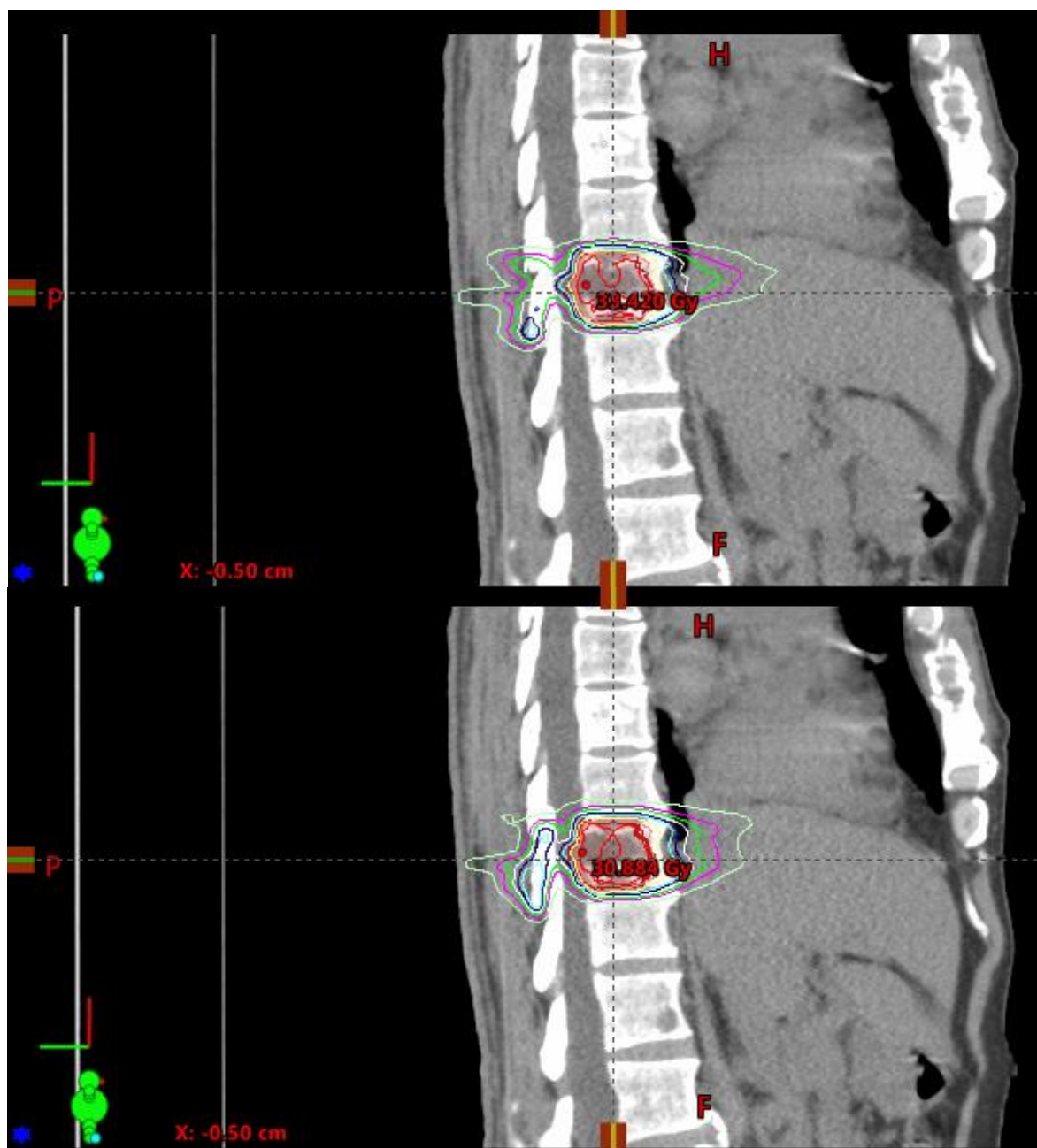


Figure 5-15: Patient 4 sagittal isodose images. Top: FF Plan, Bottom: FFF Plan

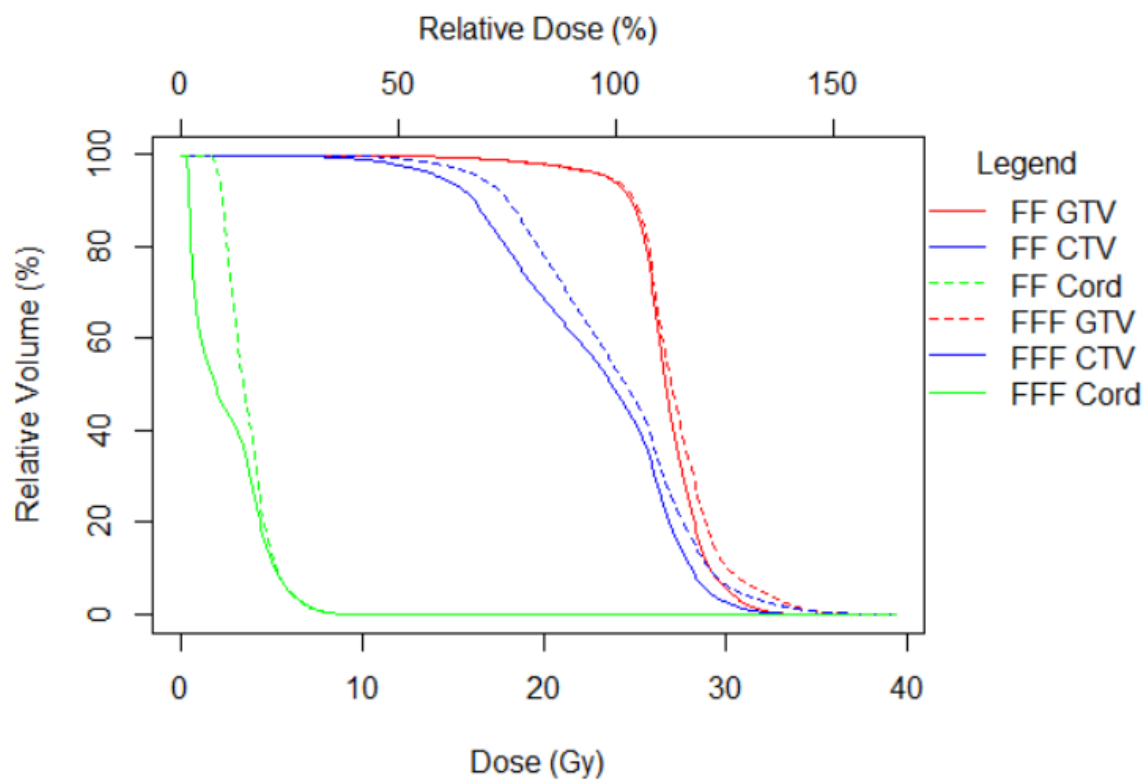


Figure 5-16: Patient 4 DVH

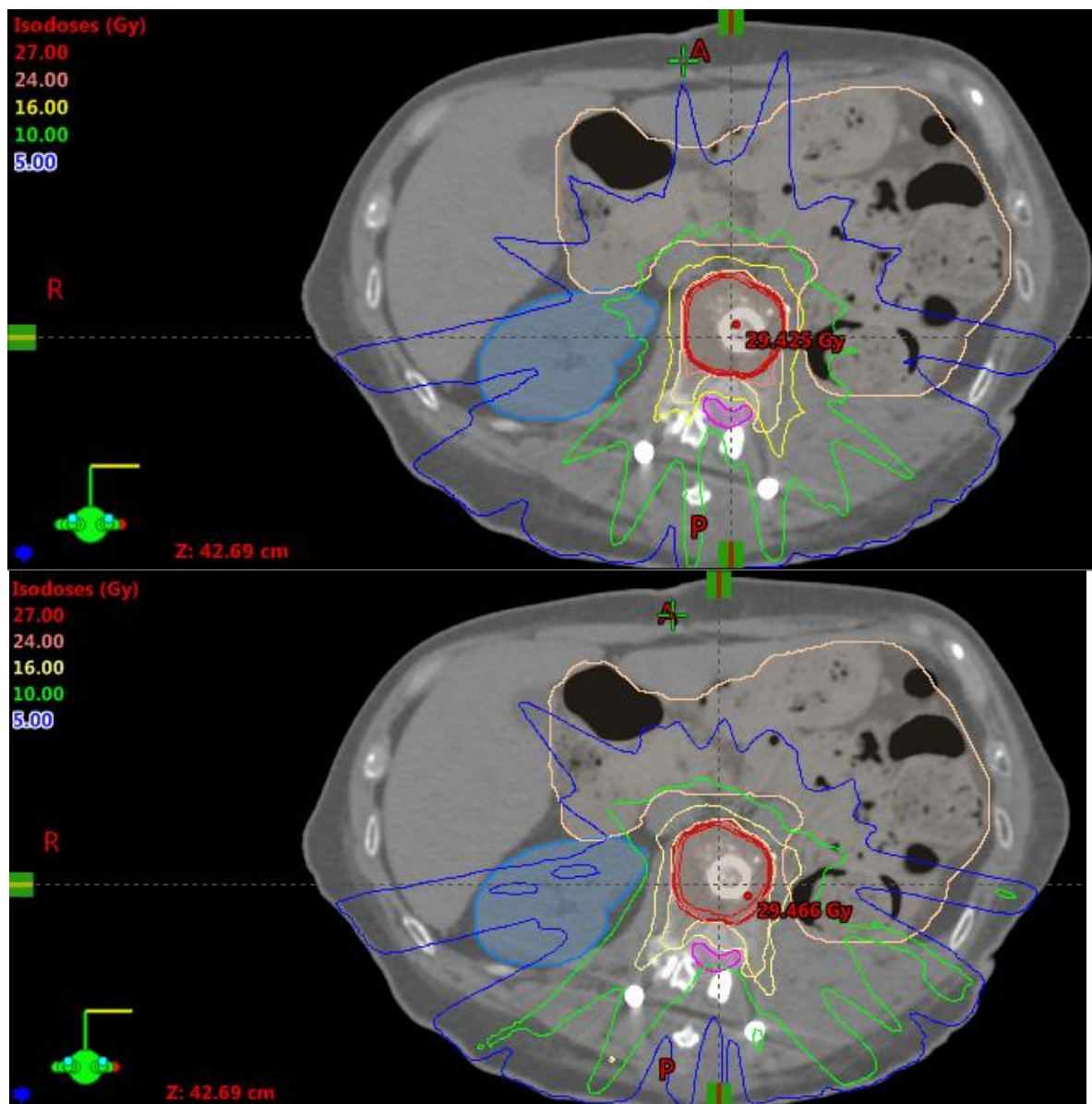


Figure 5-17: Patient 5 axial isodose images. Top: FF Plan, Bottom: FFF Plan

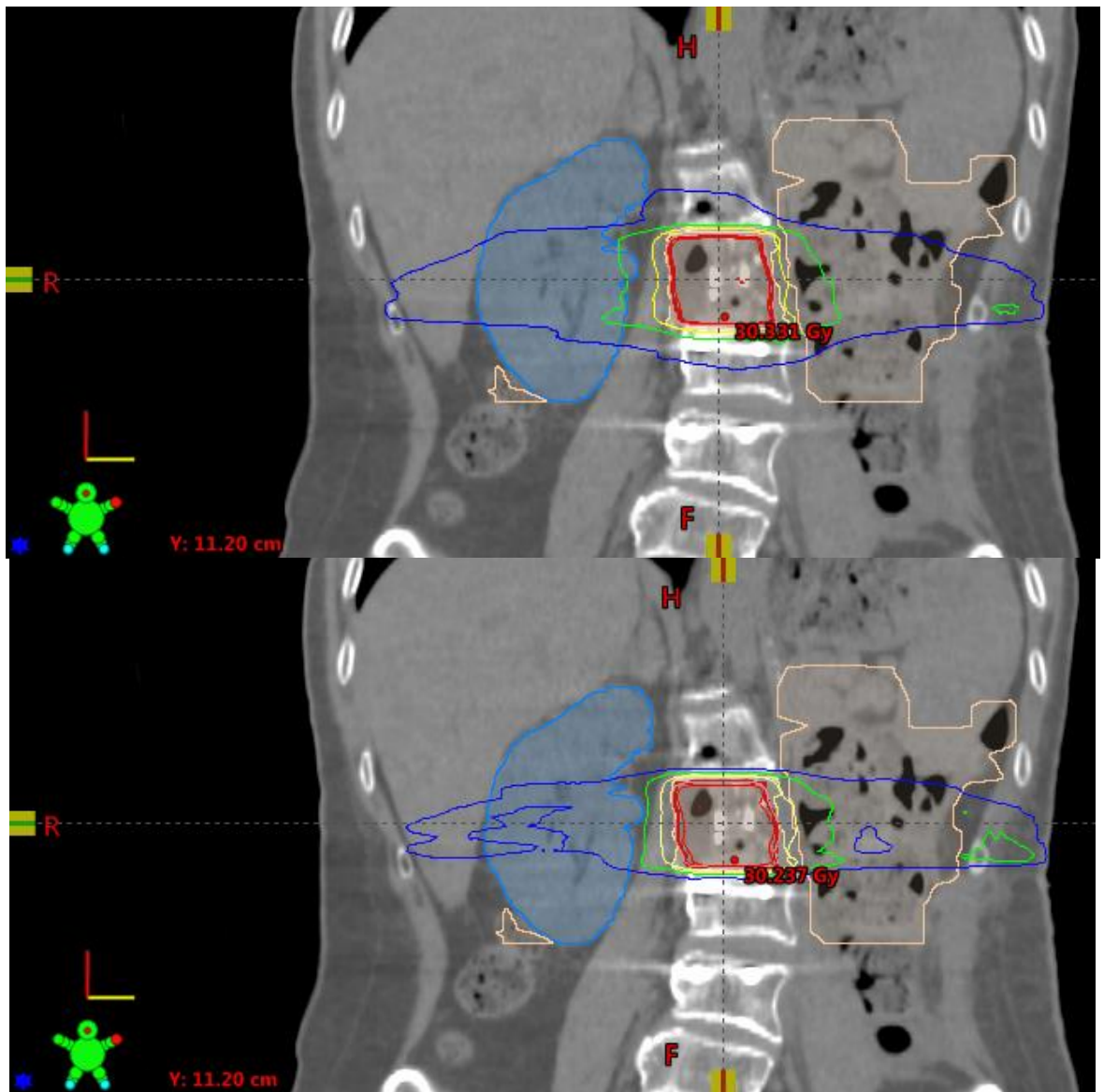


Figure 5-18: Patient 5 coronal isodose images. Top: FF Plan, Bottom: FFF Plan

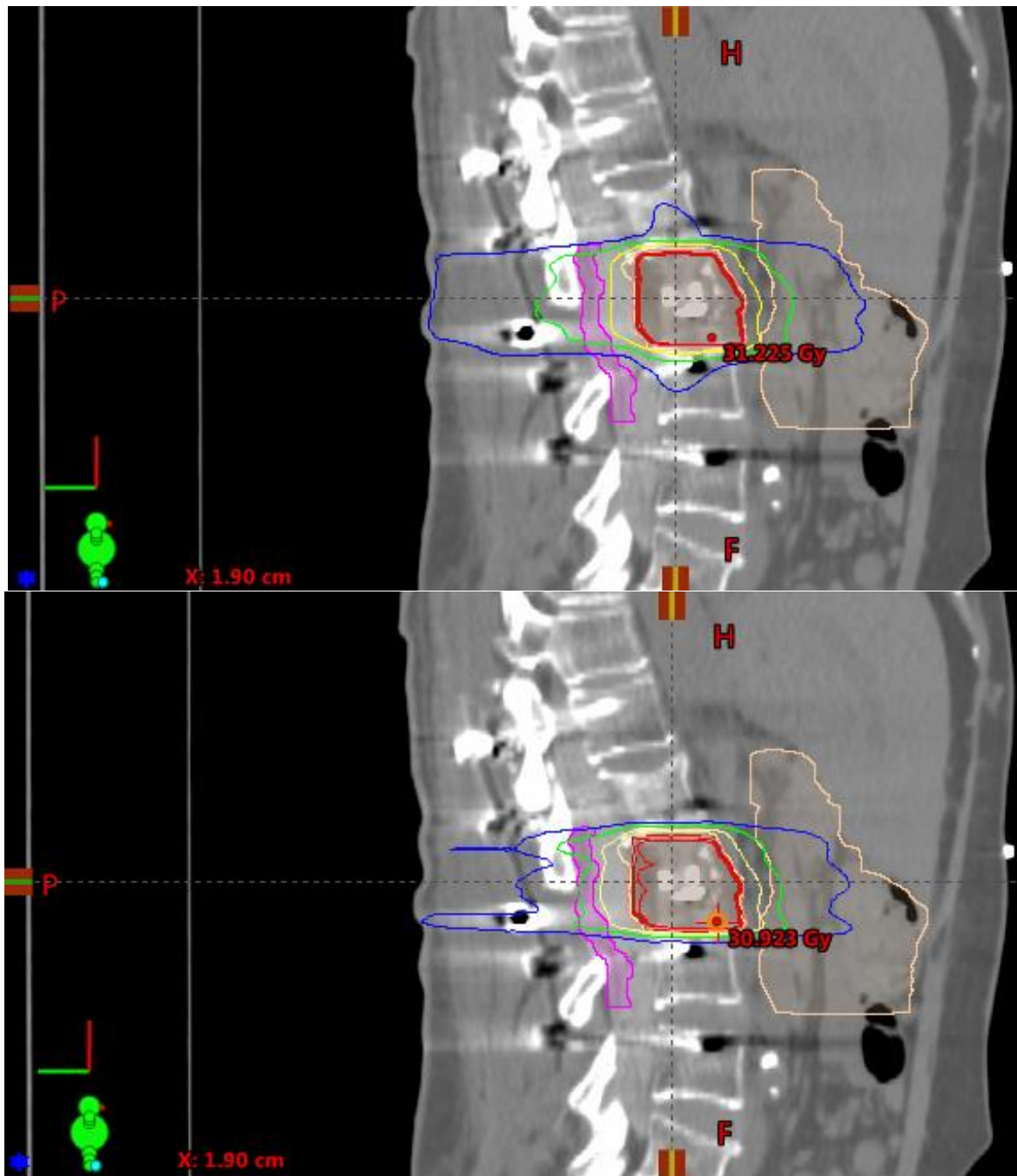


Figure 5-19: Patient 5 sagittal isodose images. Top: FF Plan, Bottom: FFF Plan

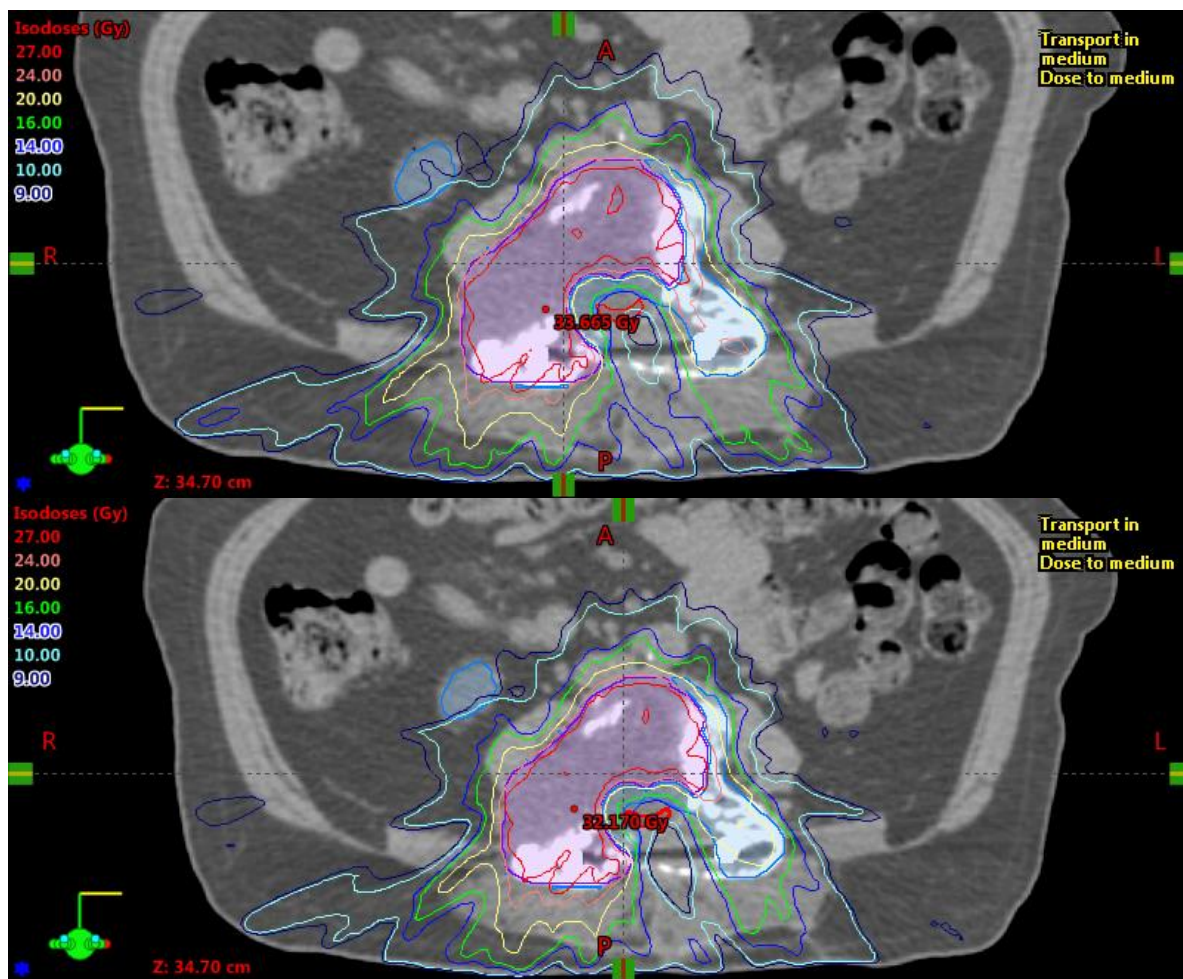


Figure 5-21: Patient 6 axial isodose images. Top: FF Plan, Bottom: FFF Plan

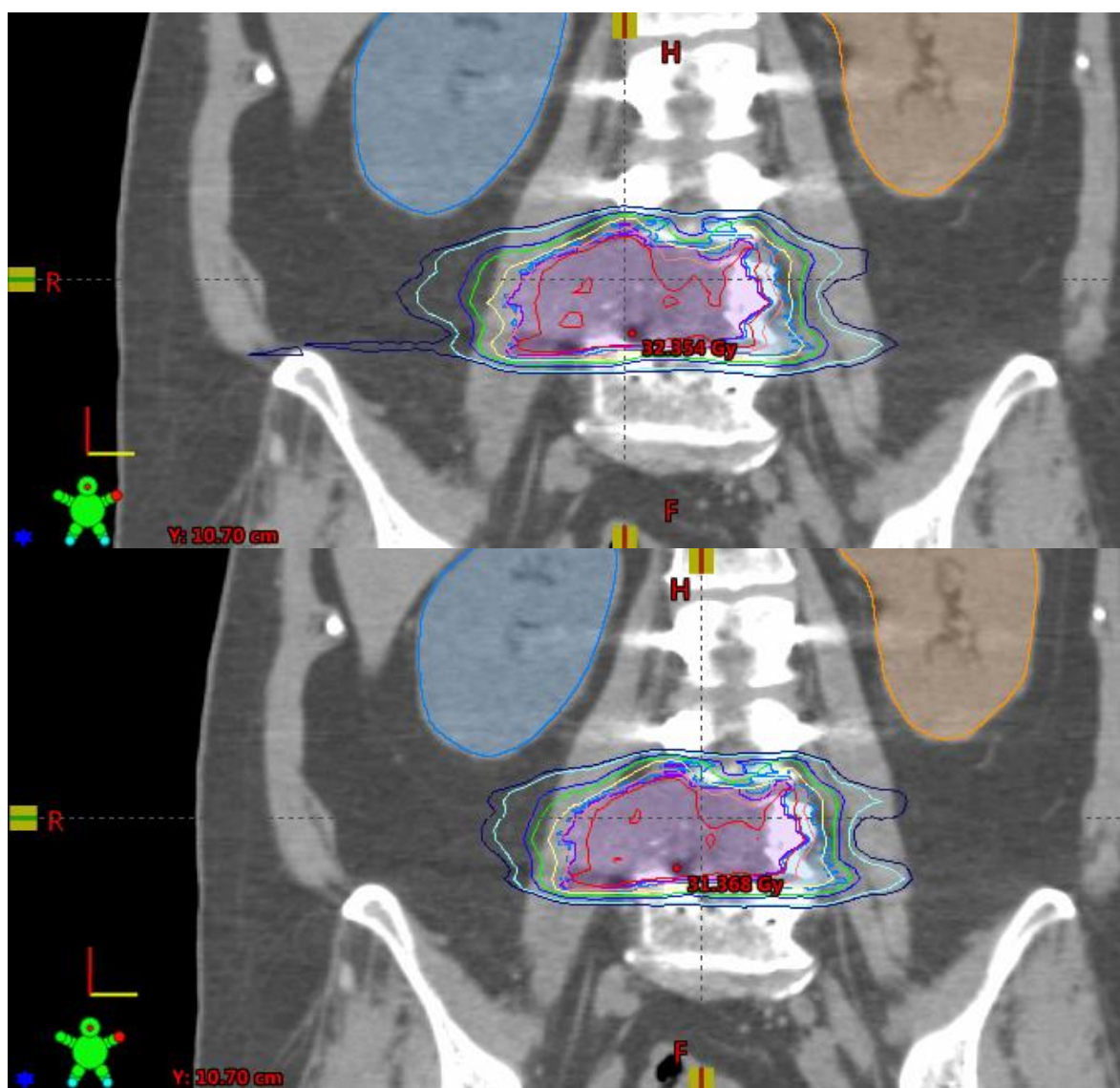


Figure 5-22: Patient 6 coronal isodose images. Top: FF Plan, Bottom: FFF Plan

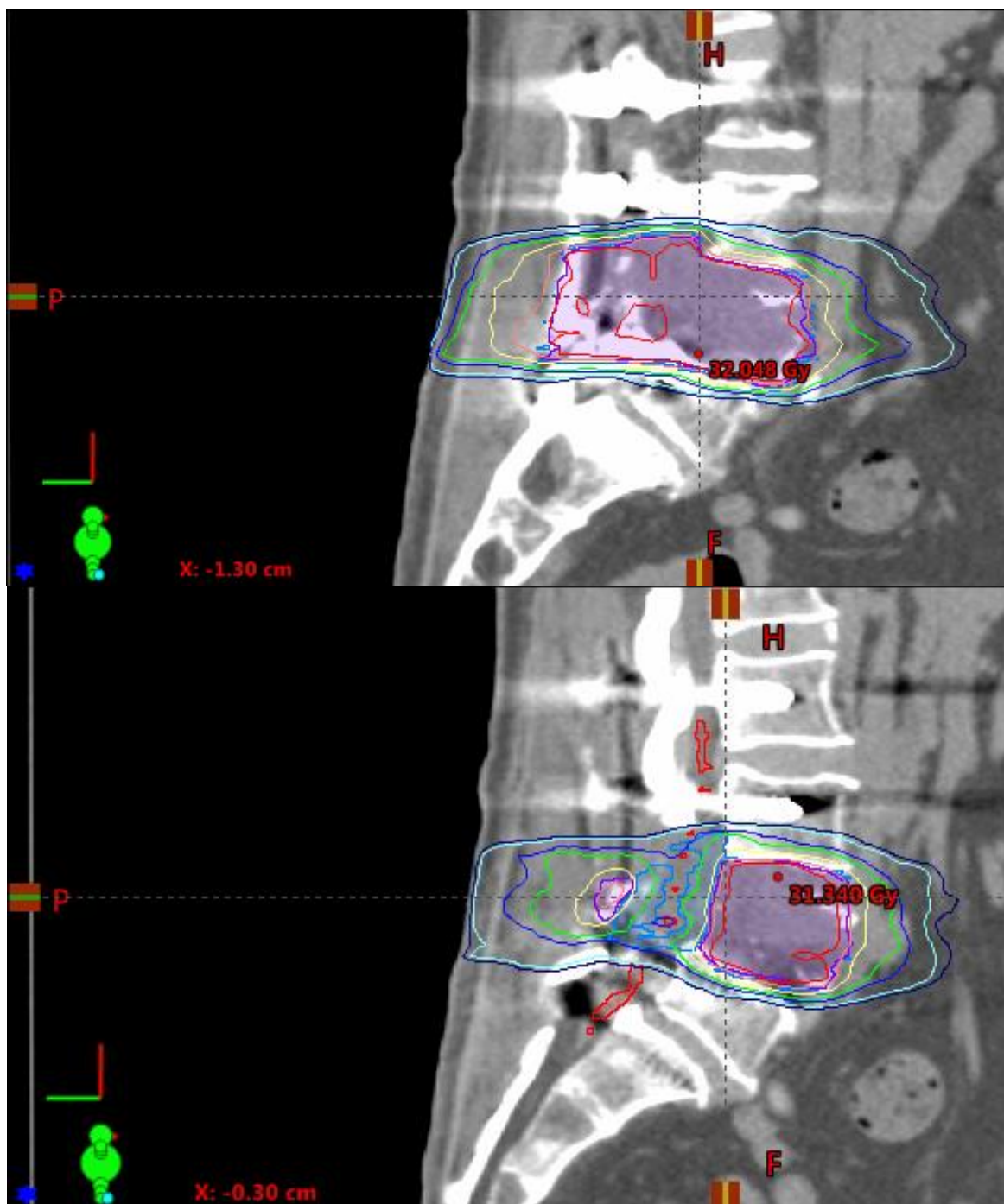


Figure 5-23: Patient 6 sagittal isodose images. Top: FF Plan, Bottom: FFF Plan

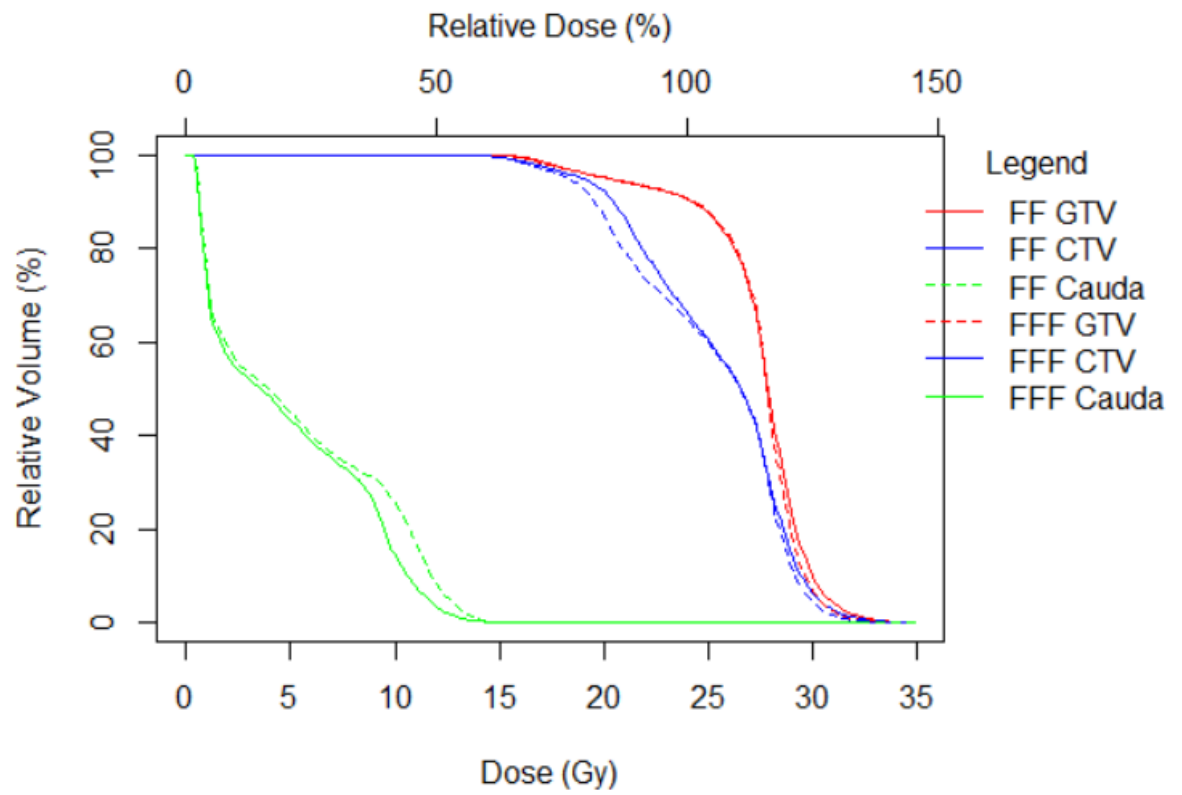


Figure 5-24: Patient 6 DVH

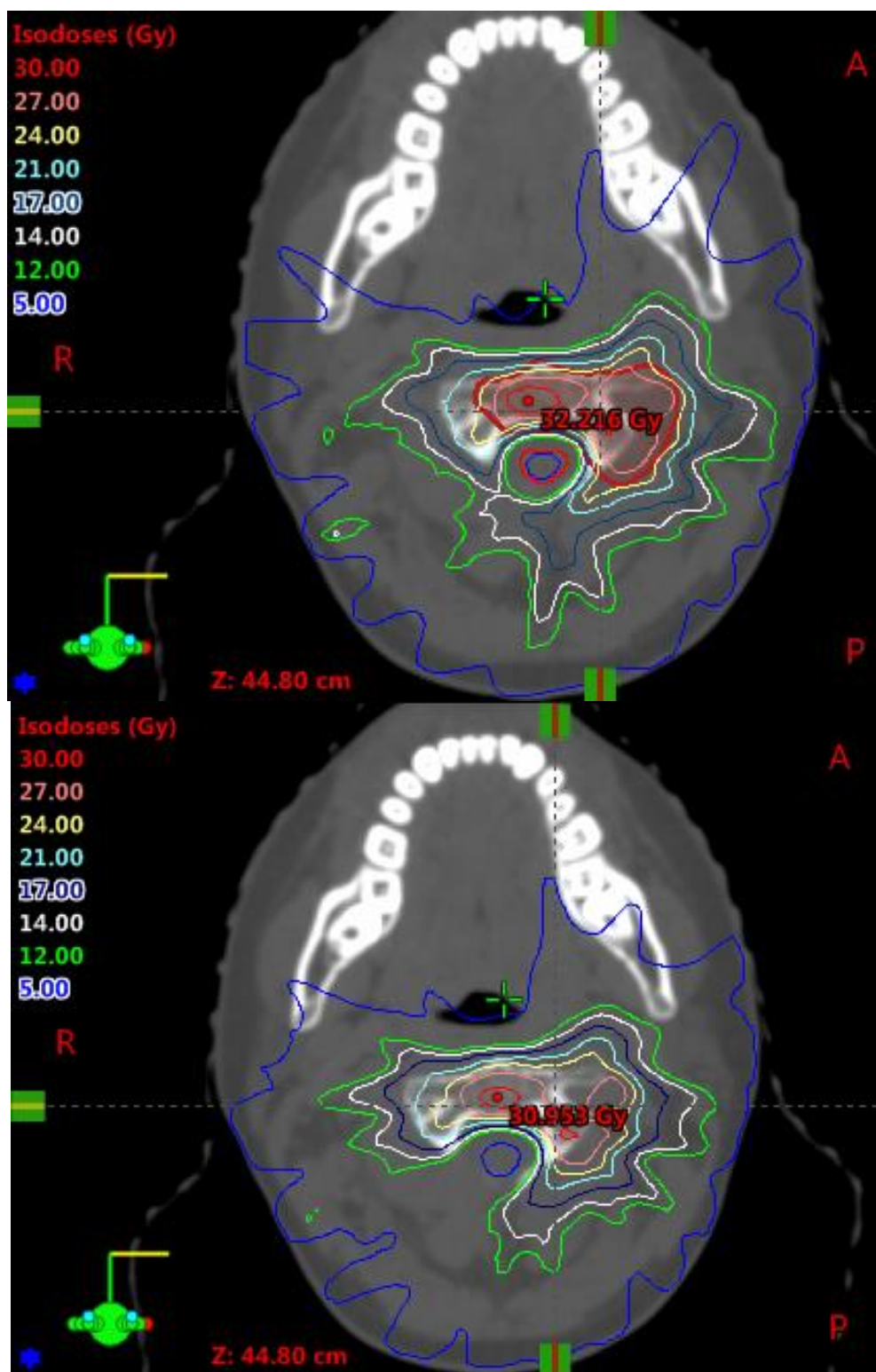
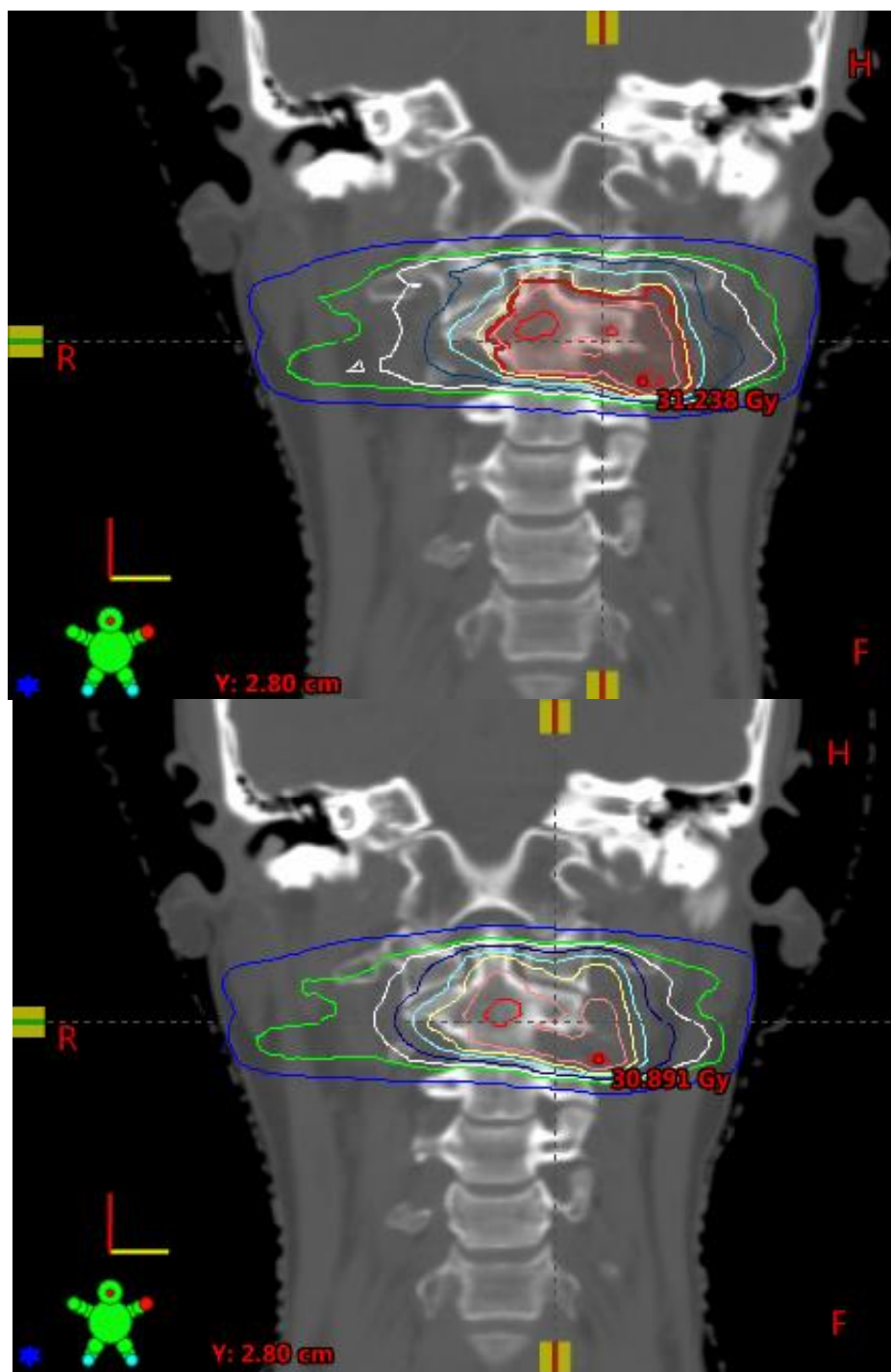


Figure 5-25: Patient 7 axial isodose images. Top: FF Plan, Bottom: FFF Plan



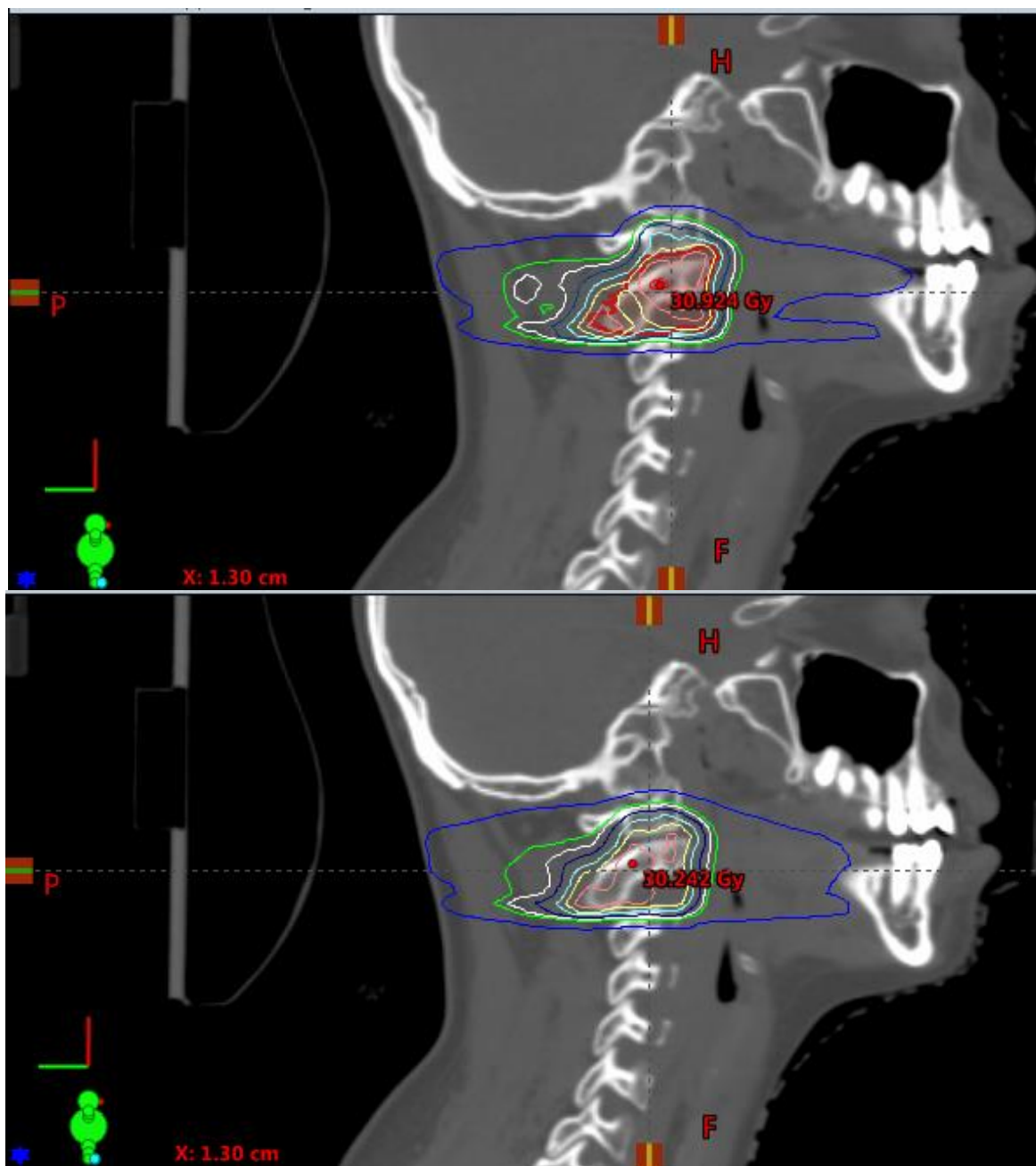


Figure 5-27: Patient 7 sagittal isodose images. Top: FF Plan, Bottom: FFF Plan

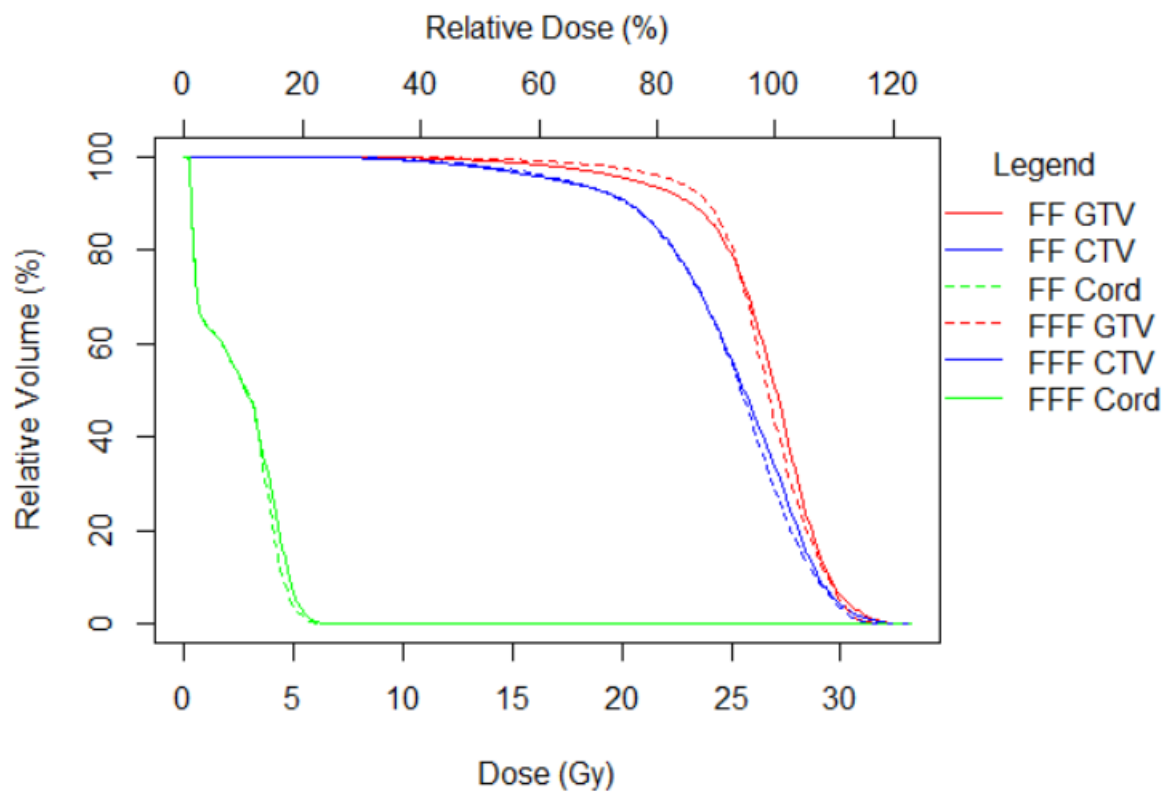


Figure 5-28: Patient 7 DVH

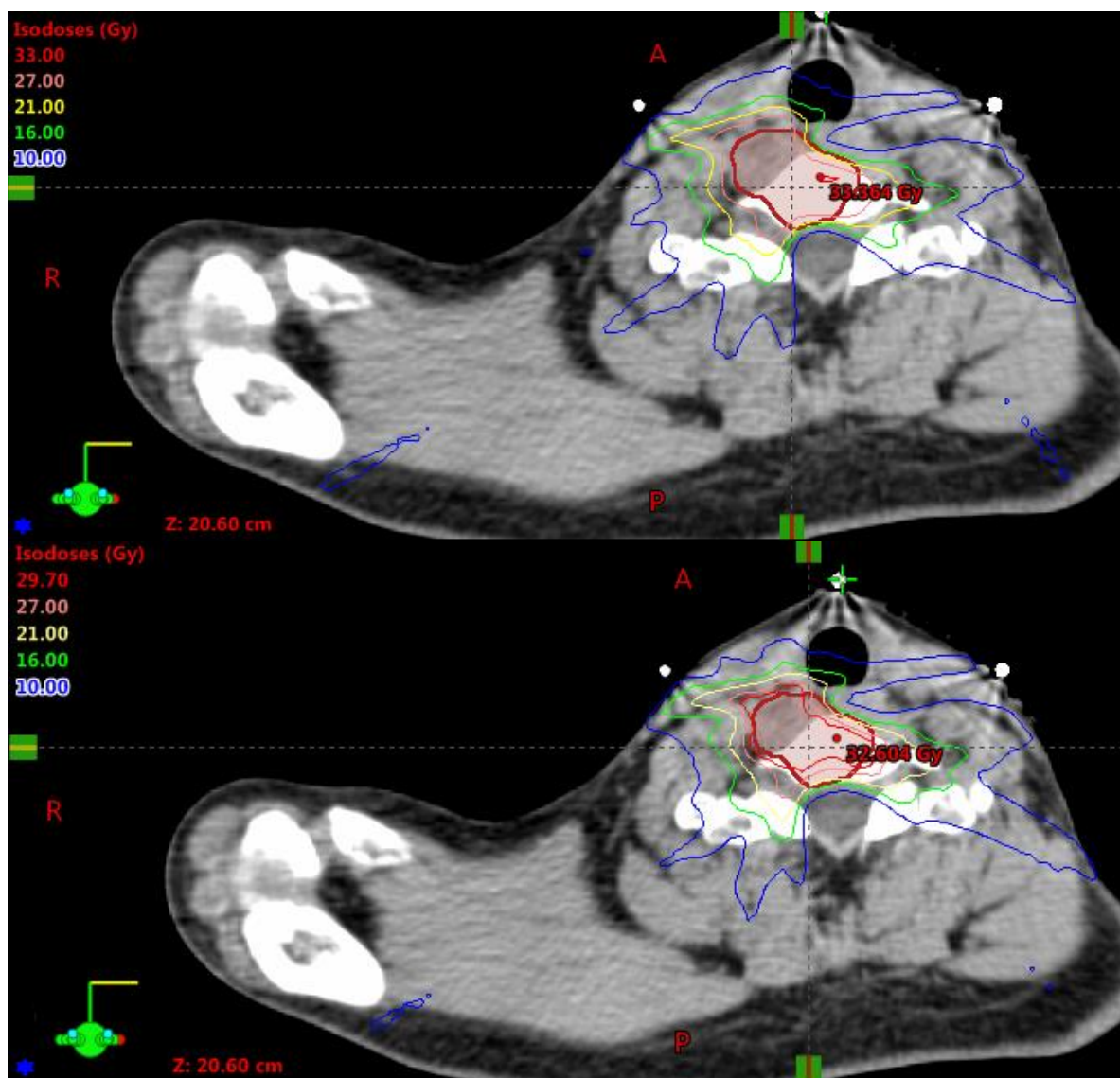


Figure 5-29: Patient 8 axial isodose images. Top: FF Plan, Bottom: FFF Plan

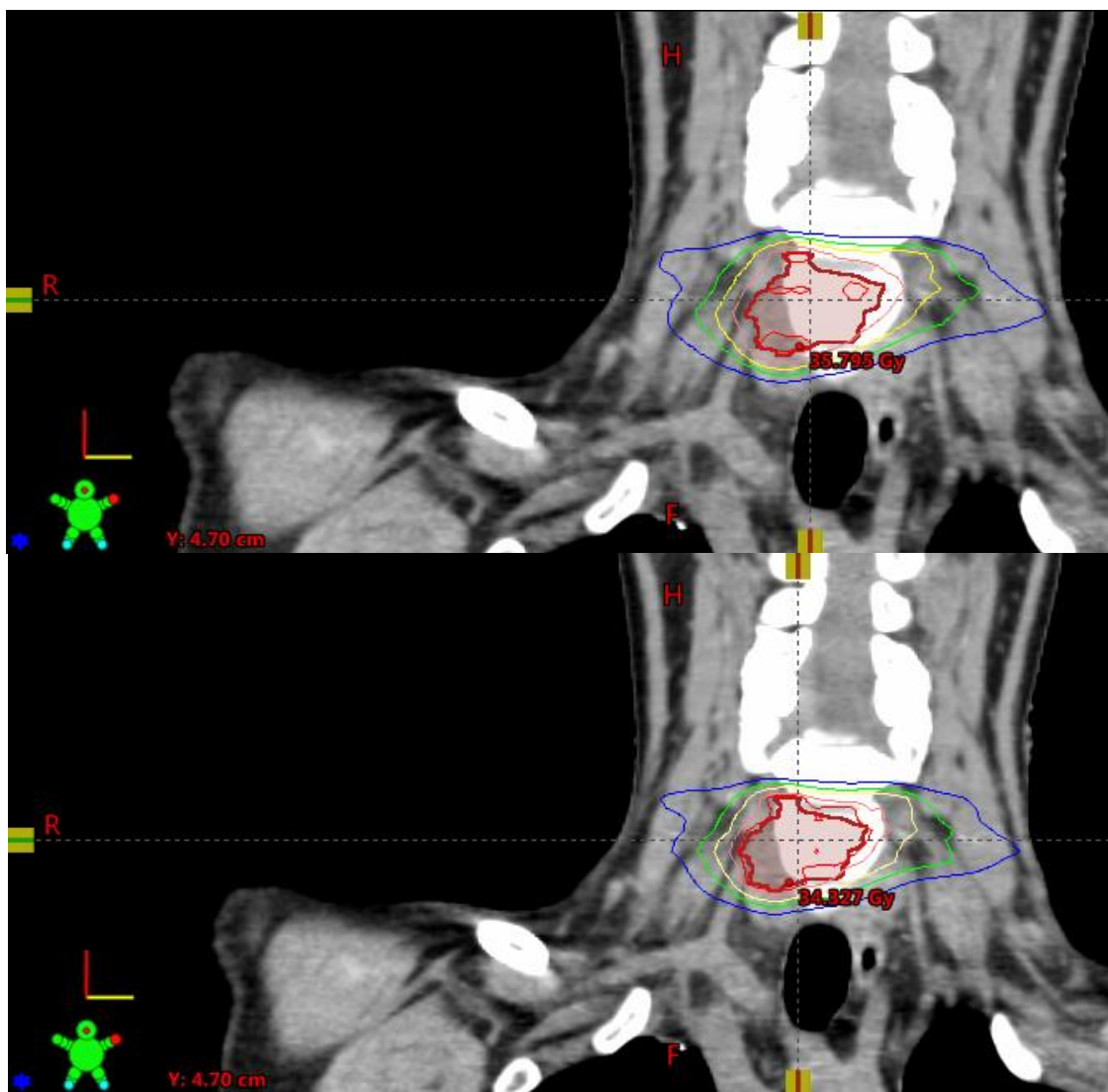


Figure 5-30: Patient 8 coronal isodose images. Top: FF Plan, Bottom: FFF Plan

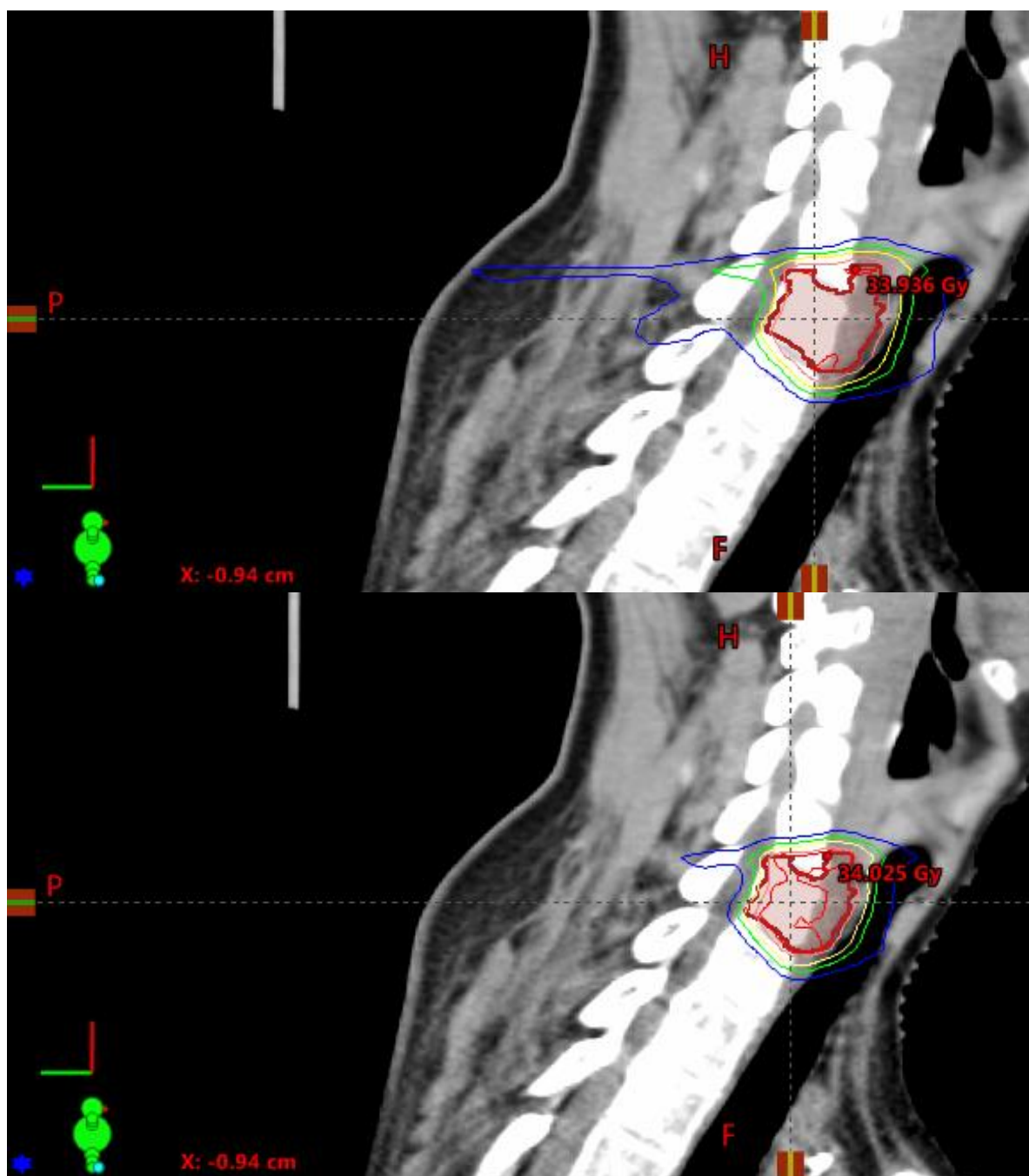


Figure 5-31: Patient 8 sagittal isodose images. Top: FF Plan, Bottom: FFF Plan

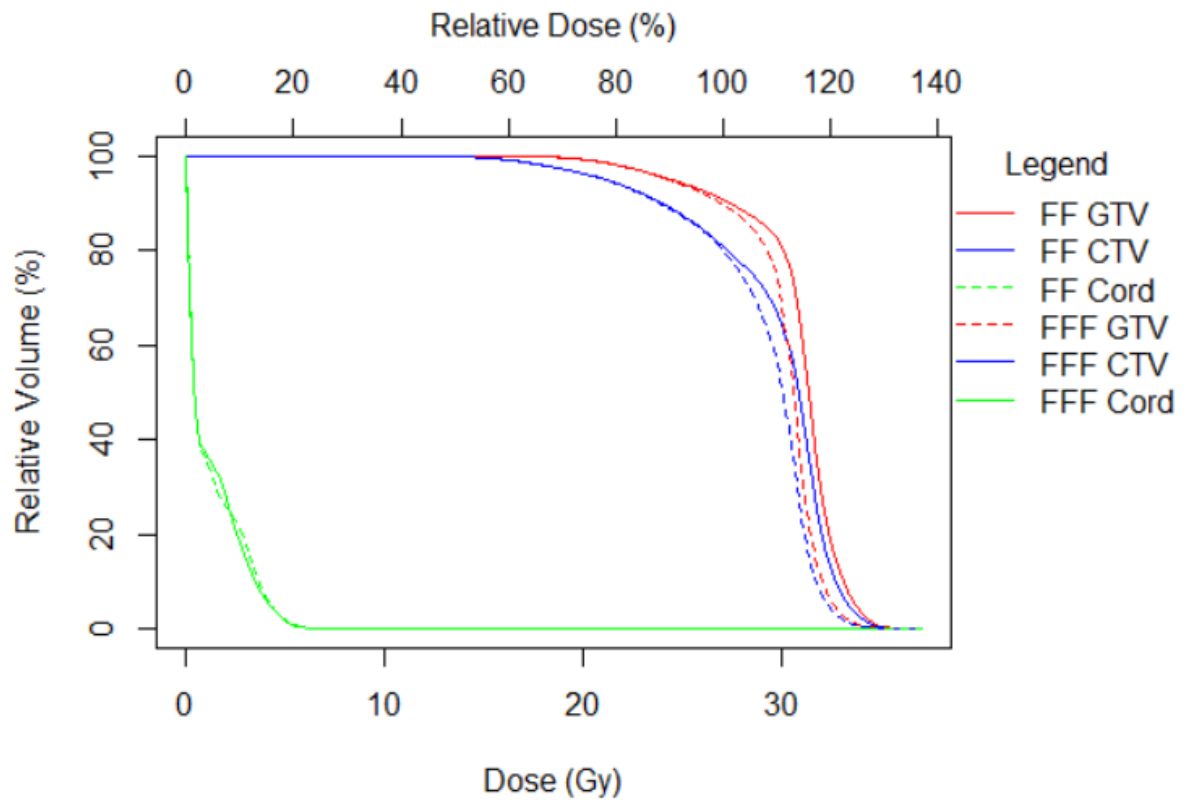


Figure 5-32: Patient 8 DVH

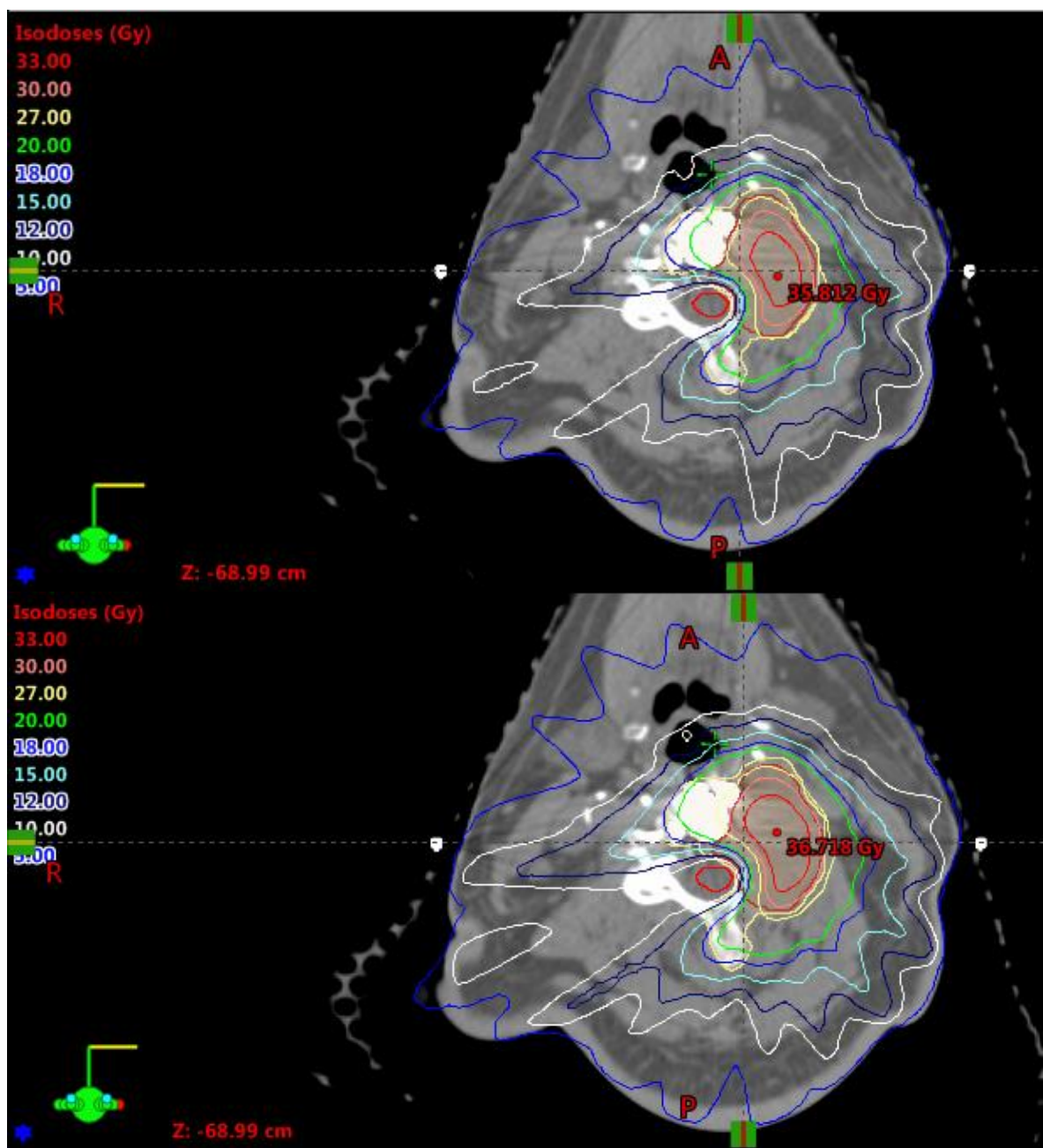


Figure 5-33: Patient 9 axial isodose images. Top: FF Plan, Bottom: FFF Plan, Bottom: Plan

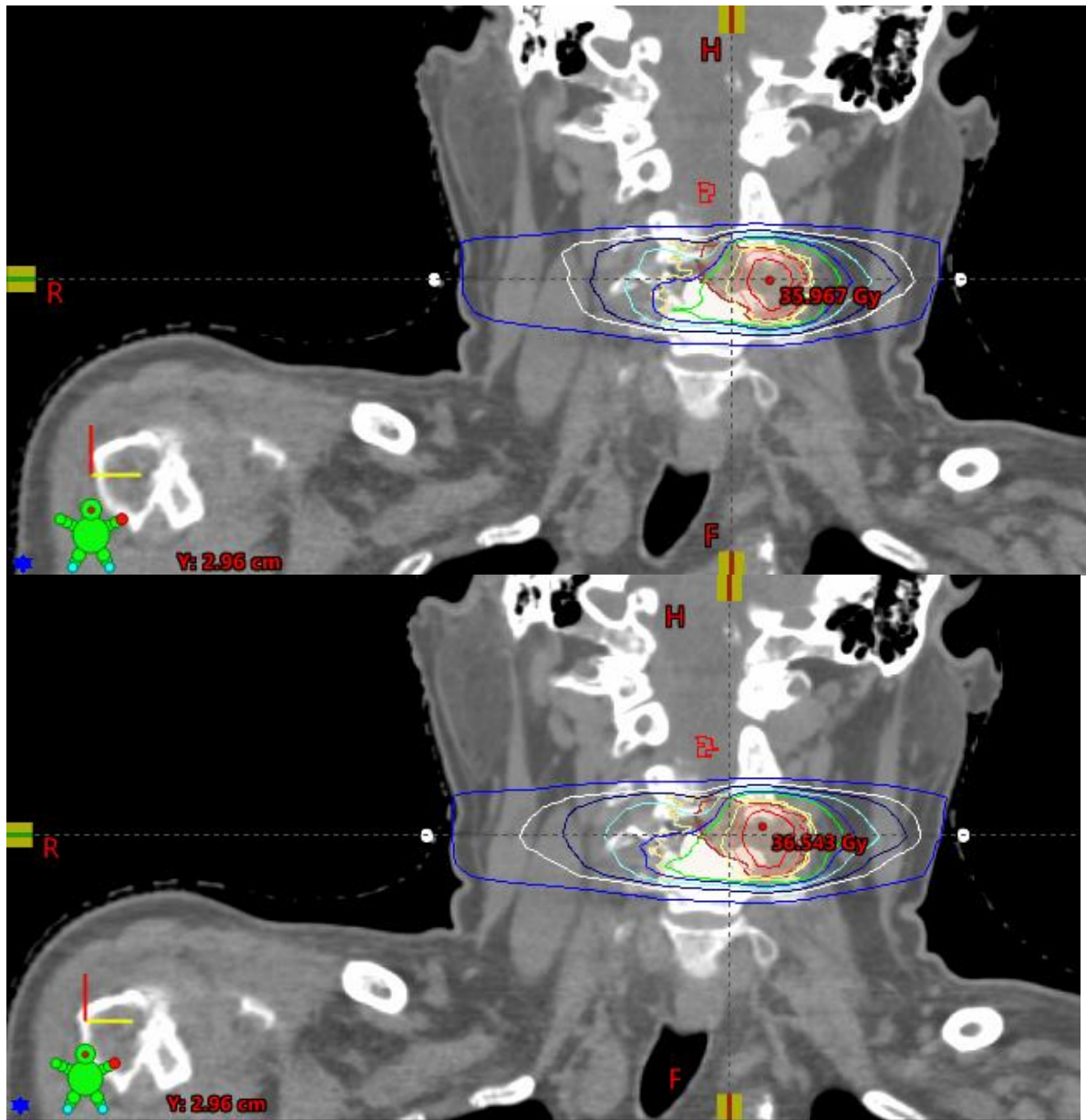


Figure 5-34: Patient 9 coronal isodose images. Top: FF Plan, Bottom: FFF Plan, Bottom: Plan

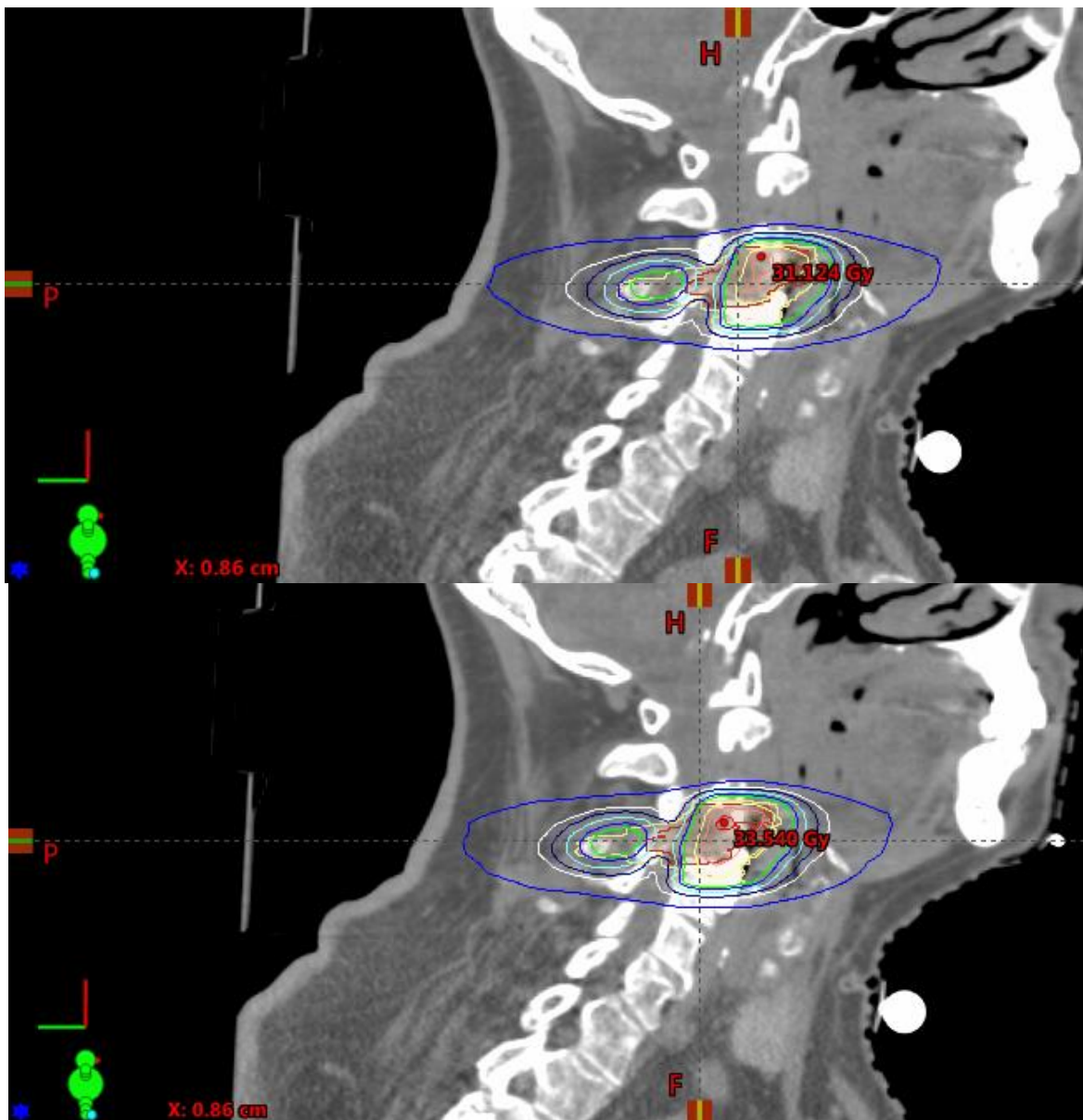


Figure 5-35: Patient 9 sagittal isodose images. Top: FF Plan, Bottom: FFF Plan, Bottom: Plan

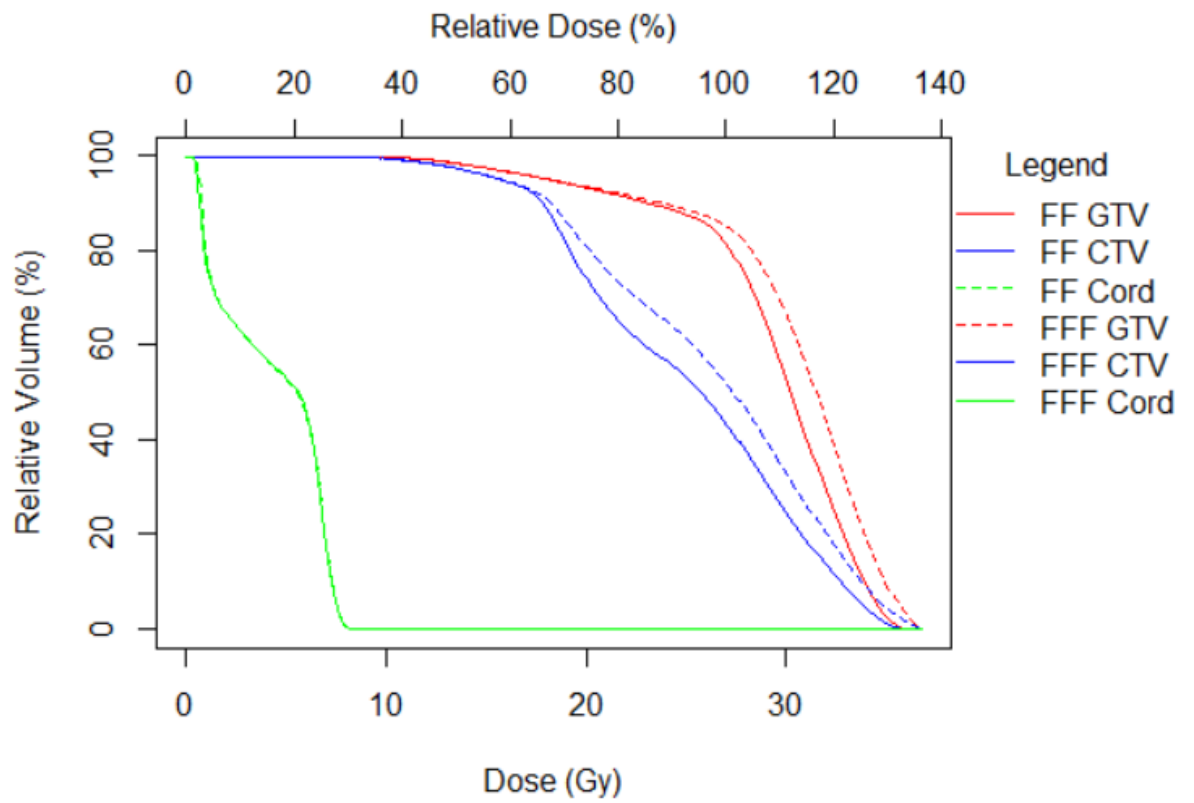


Figure 5-36: Patient 9 DVH

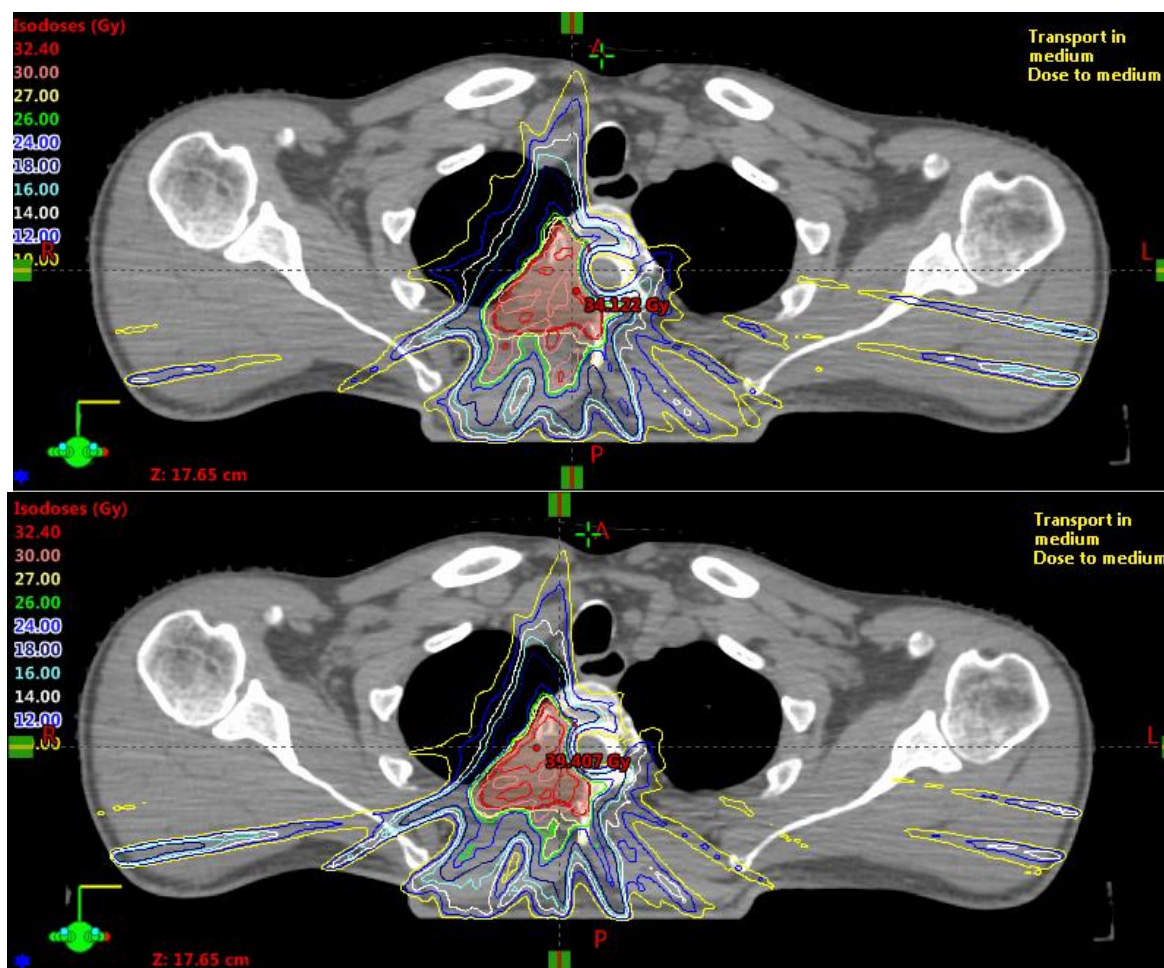


Figure 5-37: Patient 10 axial isodose images. Top: FF Plan, Bottom: FFF Plan

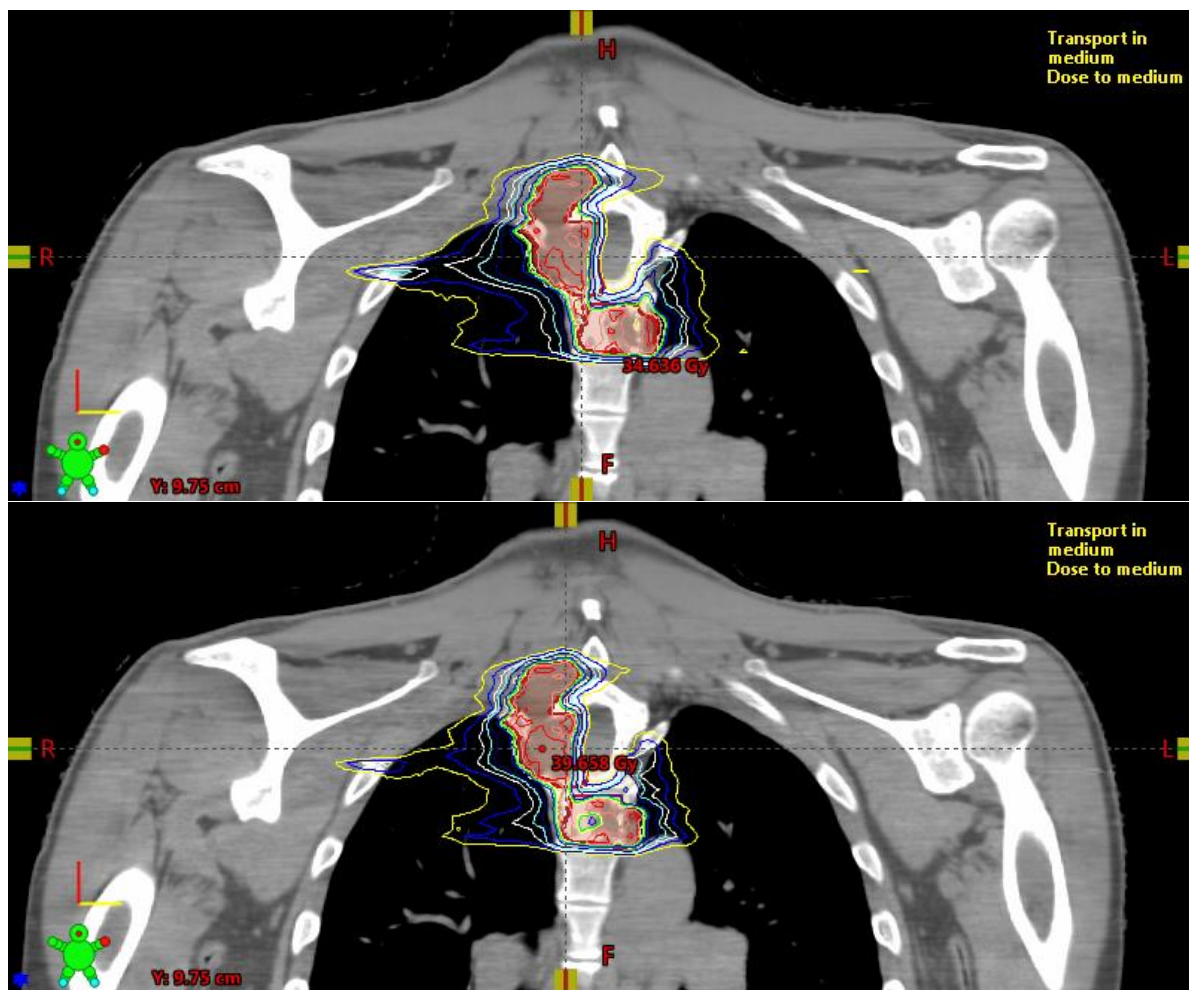


Figure 5-38: Patient 10 coronal isodose images. Top: FF Plan, Bottom: FFF Plan

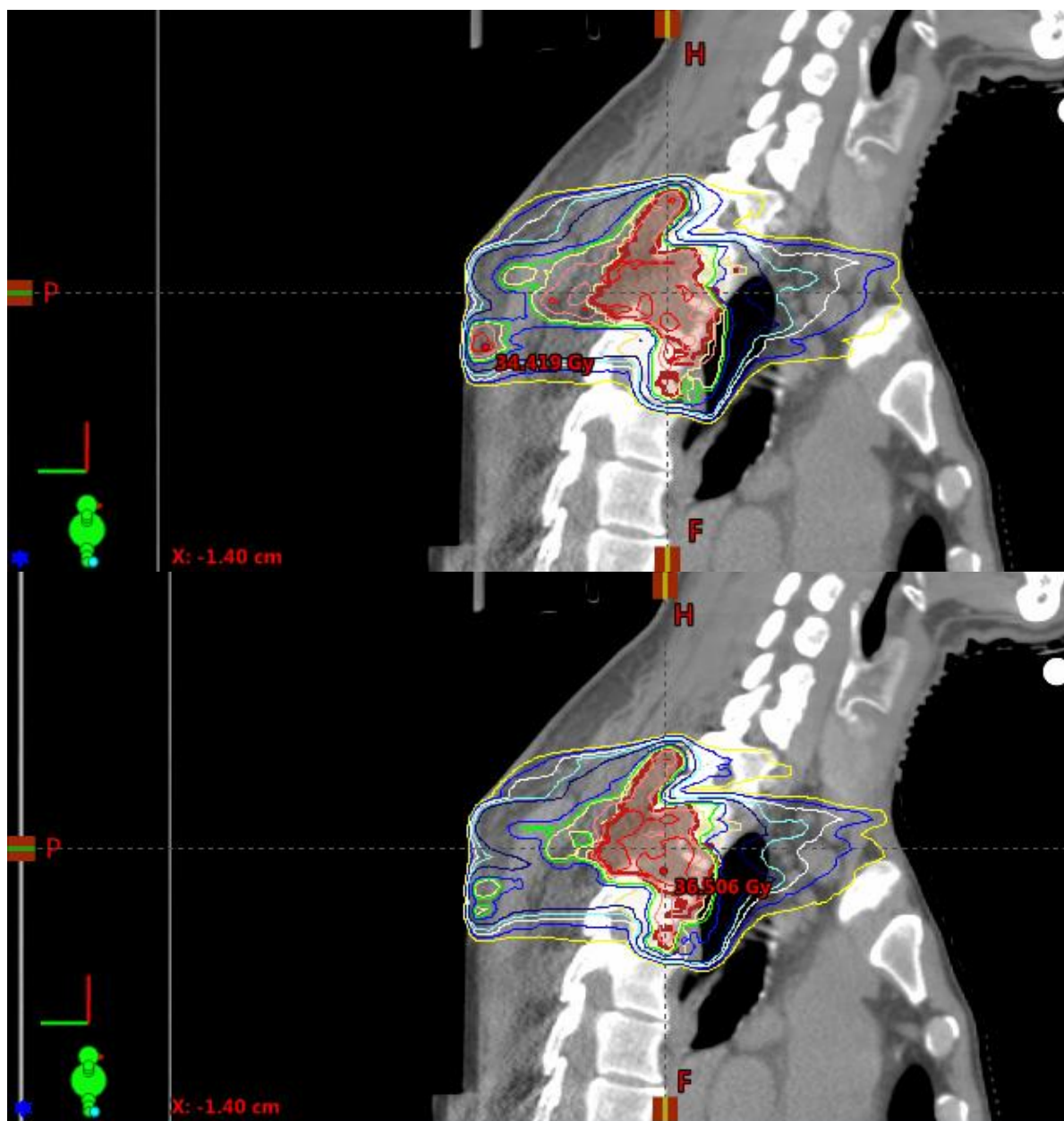


Figure 5-39: Patient 10 sagittal isodose images. Top: FF Plan, Bottom: FFF Plan

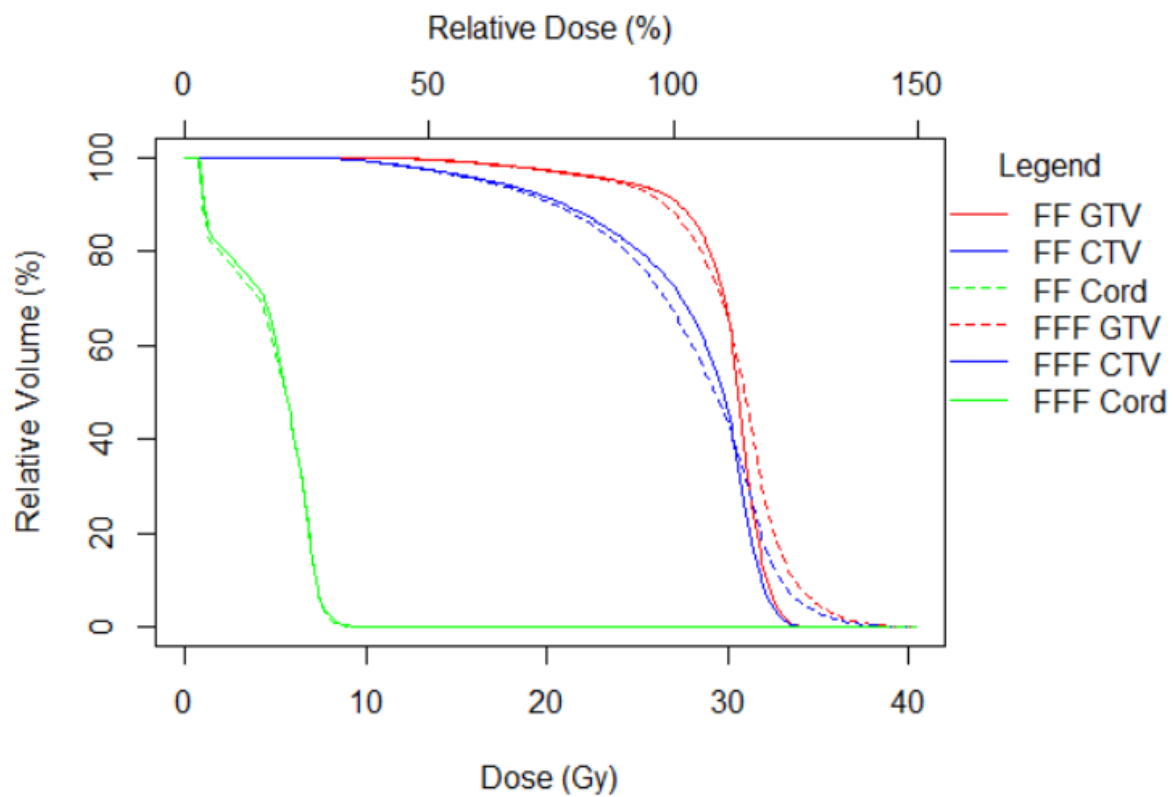


Figure 5-40: Patient 10 DVH

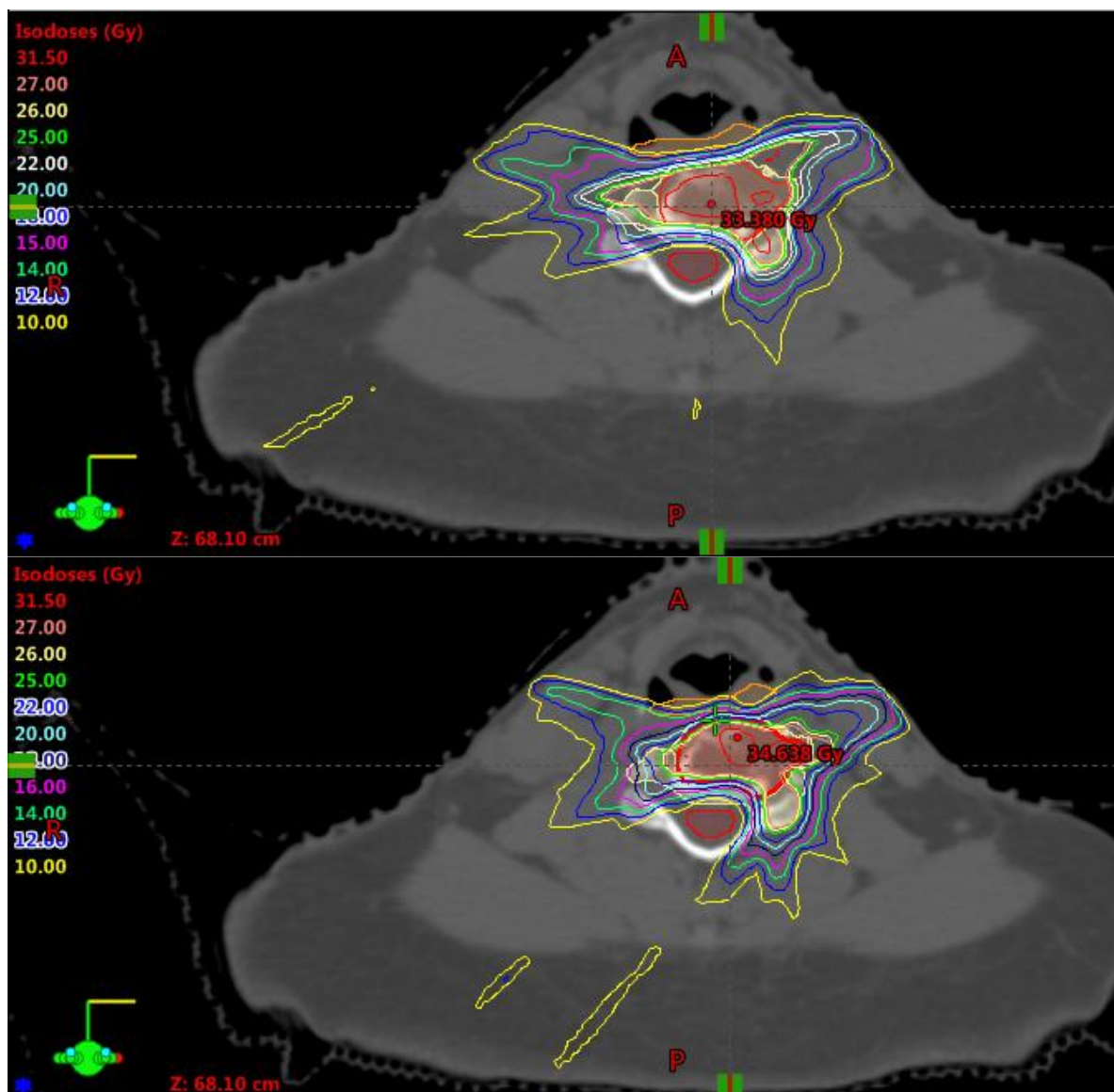


Figure 5-41: Patient 11 axial isodose images. Top: FF Plan, Bottom: FFF Plan

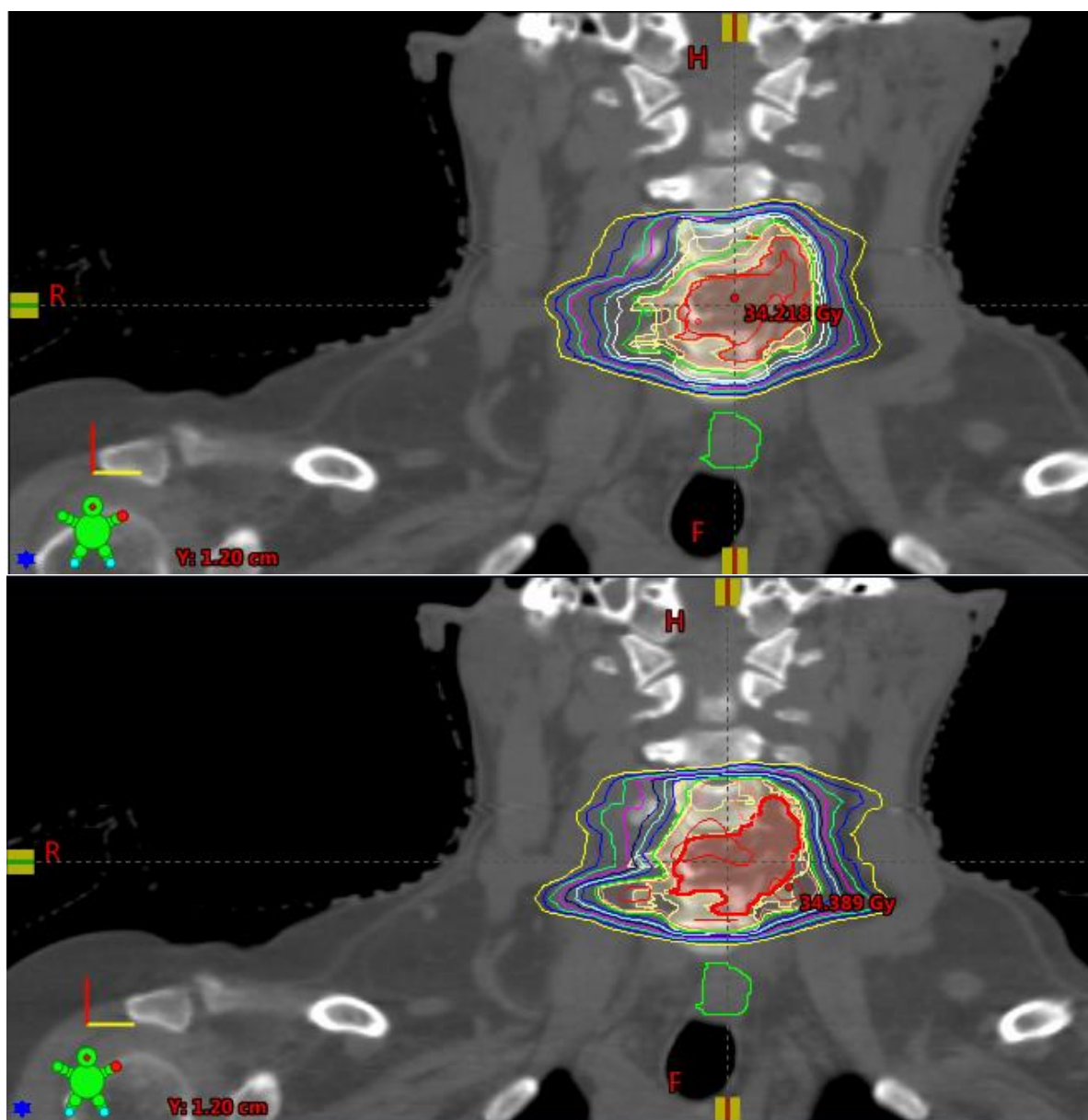


Figure 5-42: Patient 11 coronal isodose images. Top: FF Plan, Bottom: FFF Plan

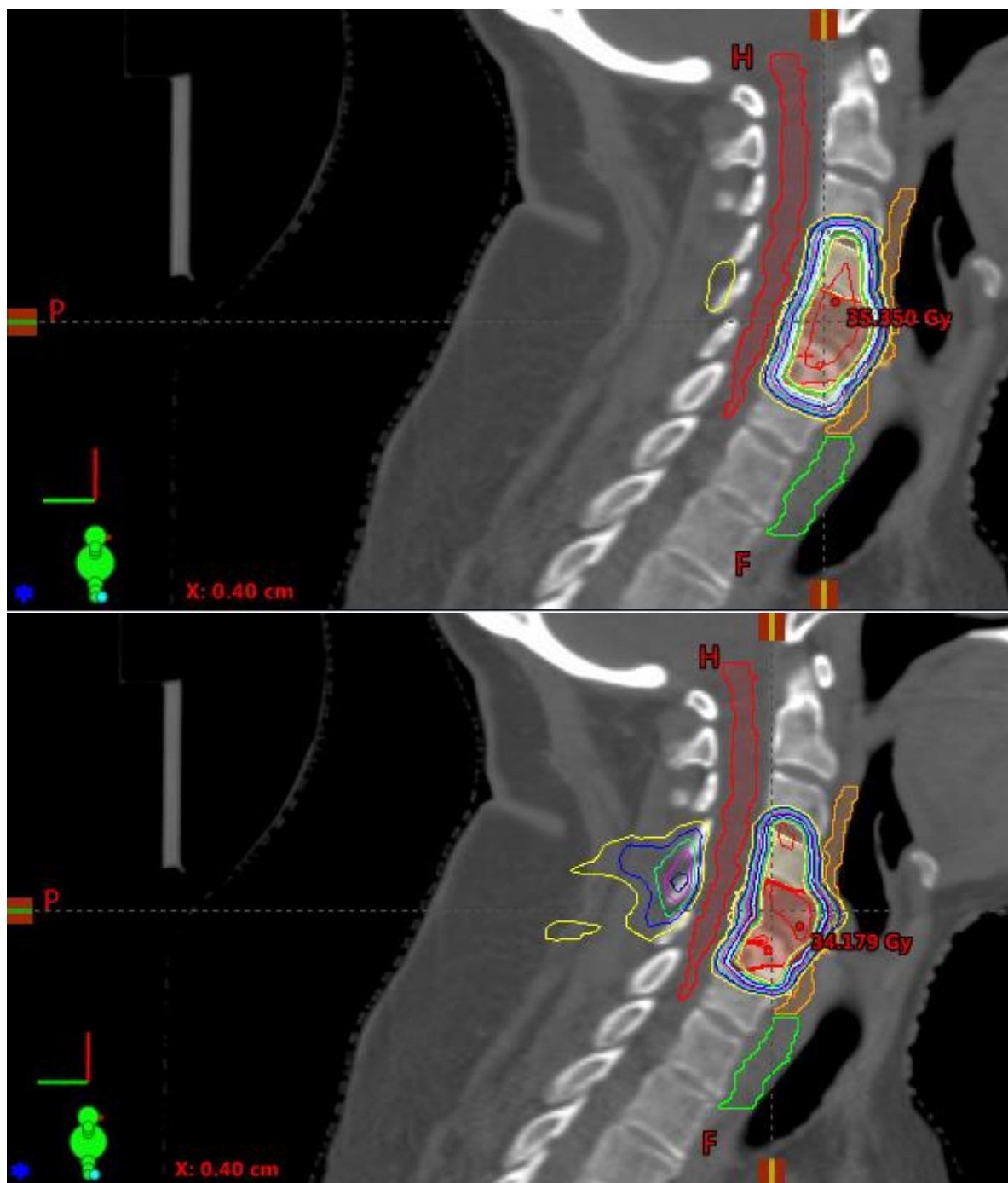


Figure 5-43: Patient 11 sagittal isodose images. Top: FF Plan, Bottom: FFF Plan

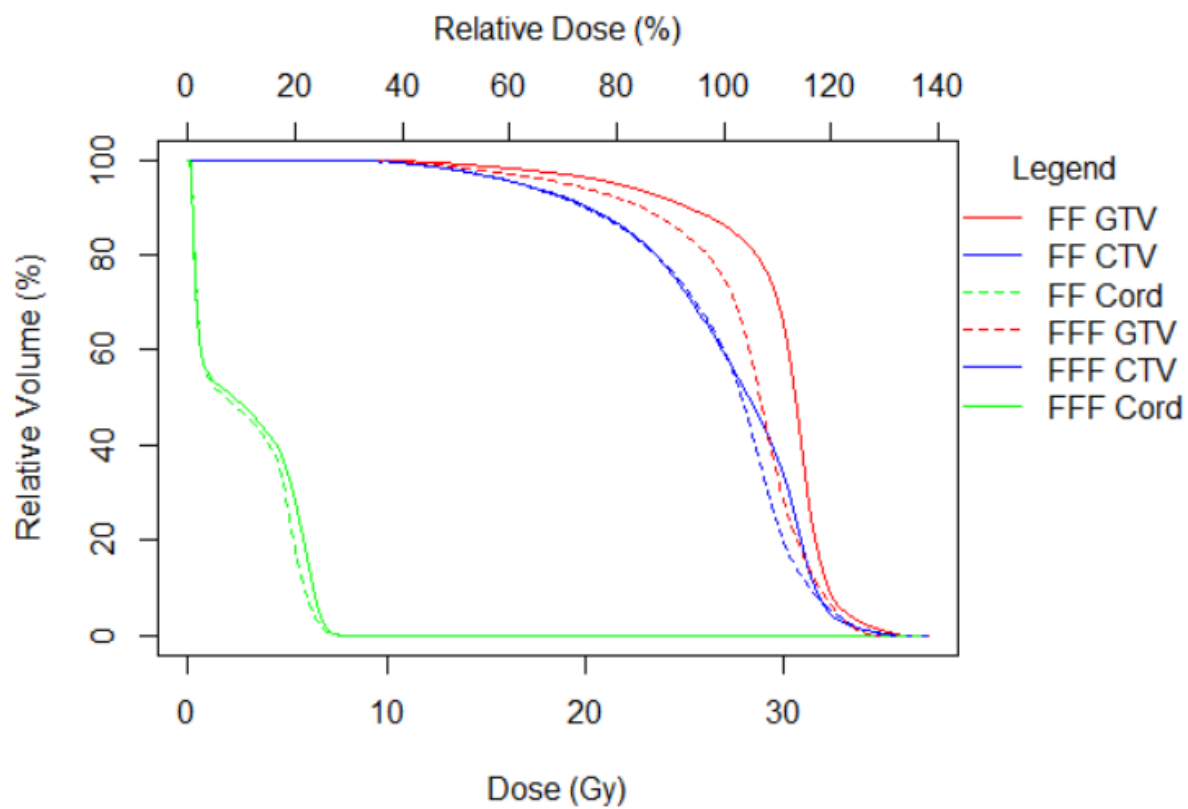


Figure 5-44: Patient 11 DVH

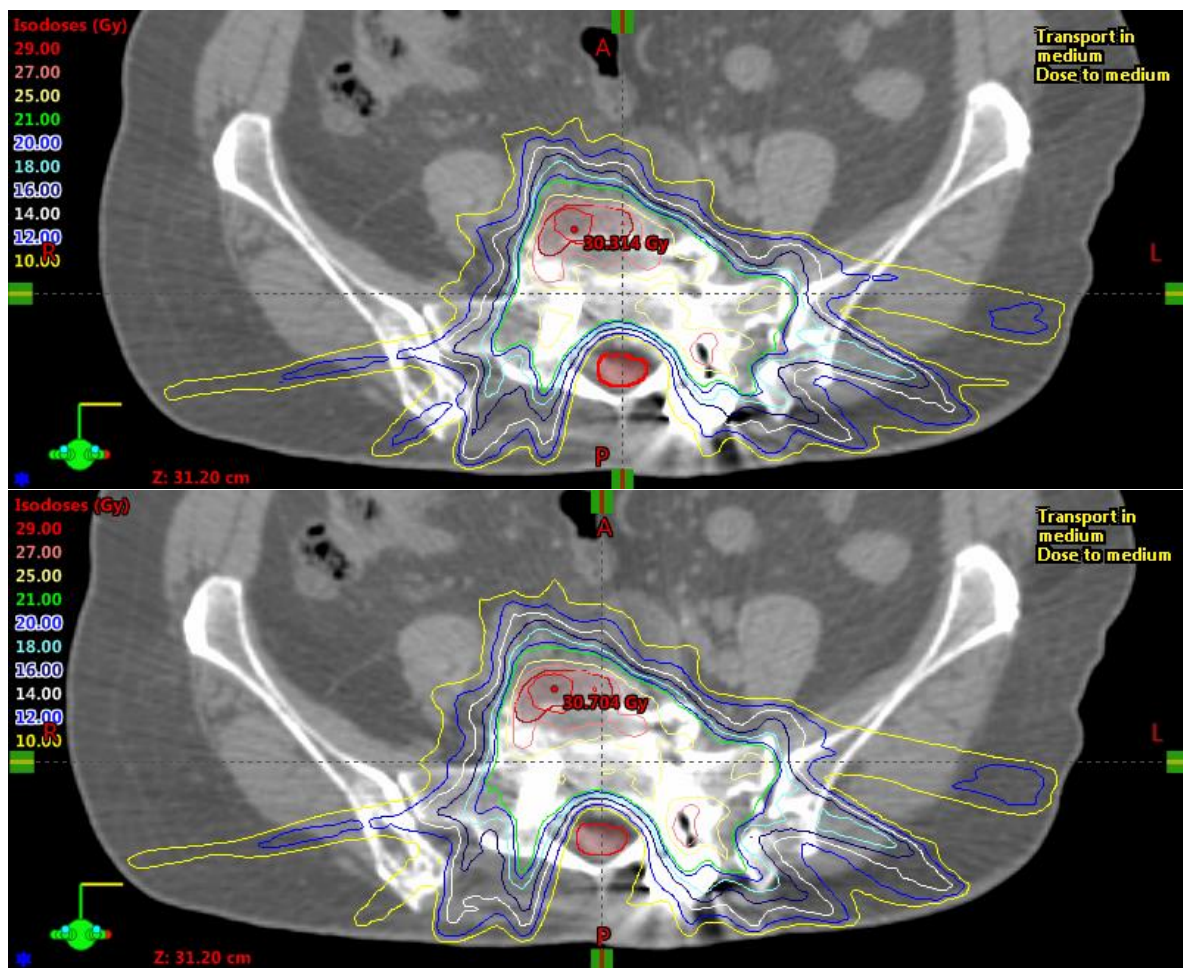


Figure 5-45: Patient 12 axial isodose images. Top: FF Plan, Bottom: FFF Plan, Bottom: Plan

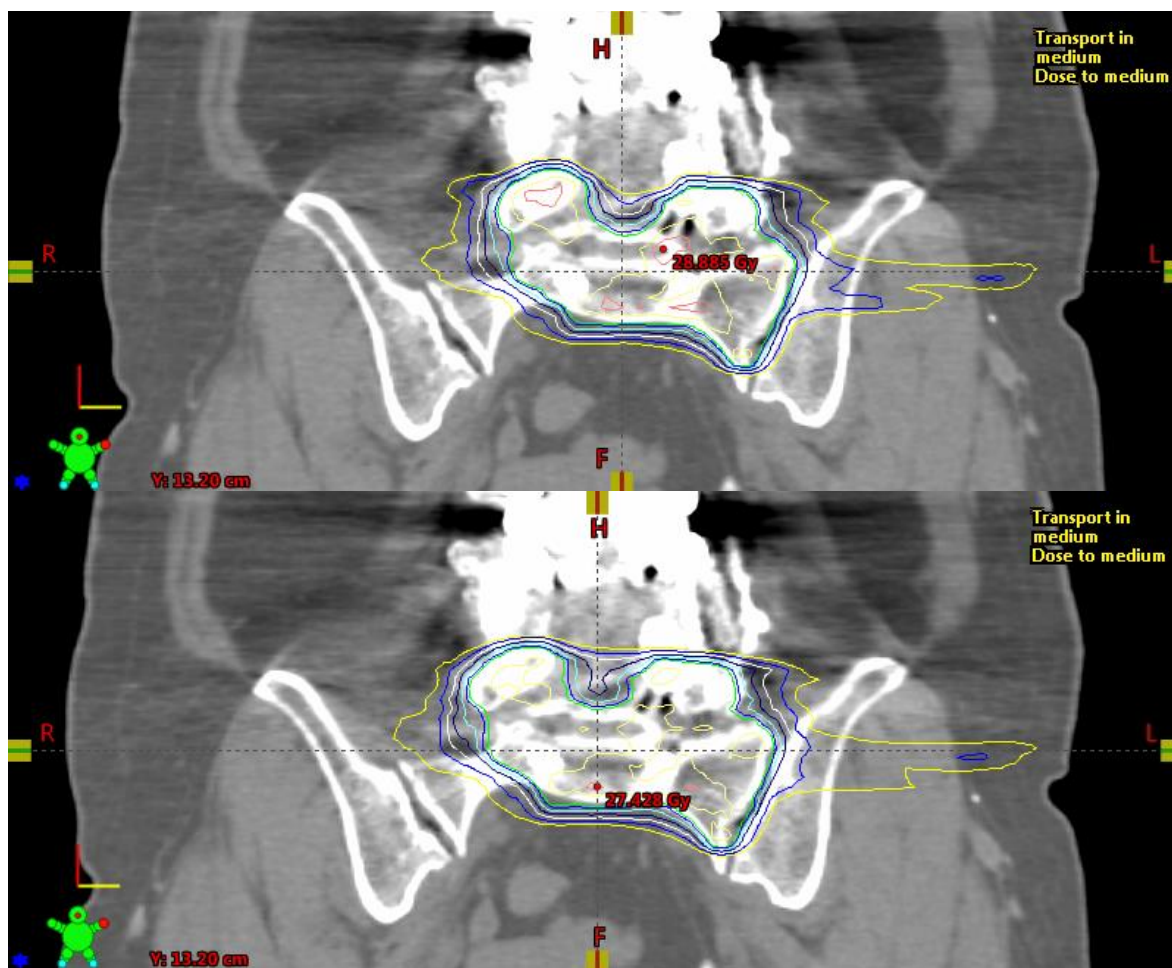


Figure 5-46: Patient 12 coronal isodose images. Top: FF Plan, Bottom: FFF Plan

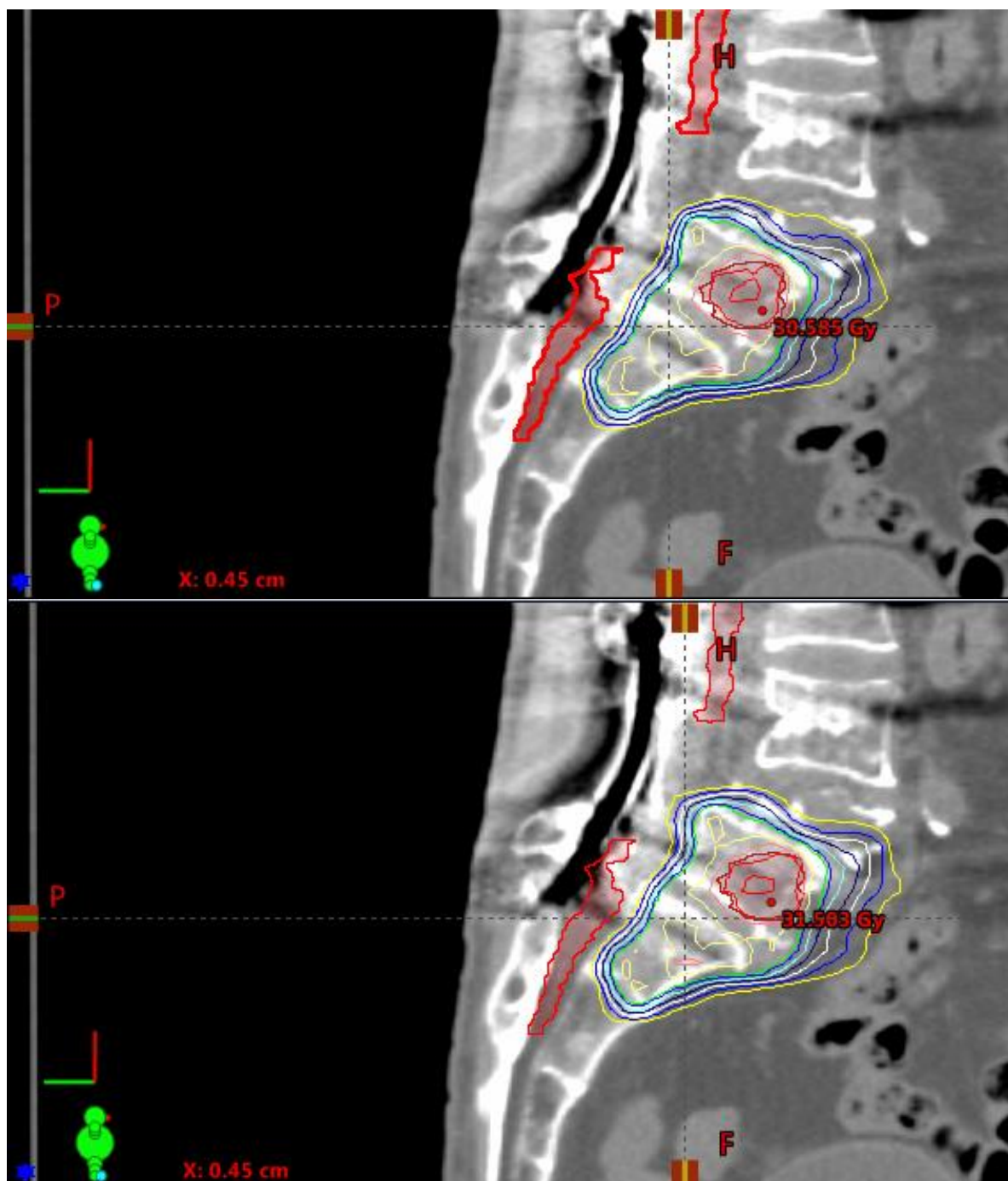


Figure 5-47: Patient 12 sagittal isodose images. Top: FF Plan, Bottom: FFF Plan

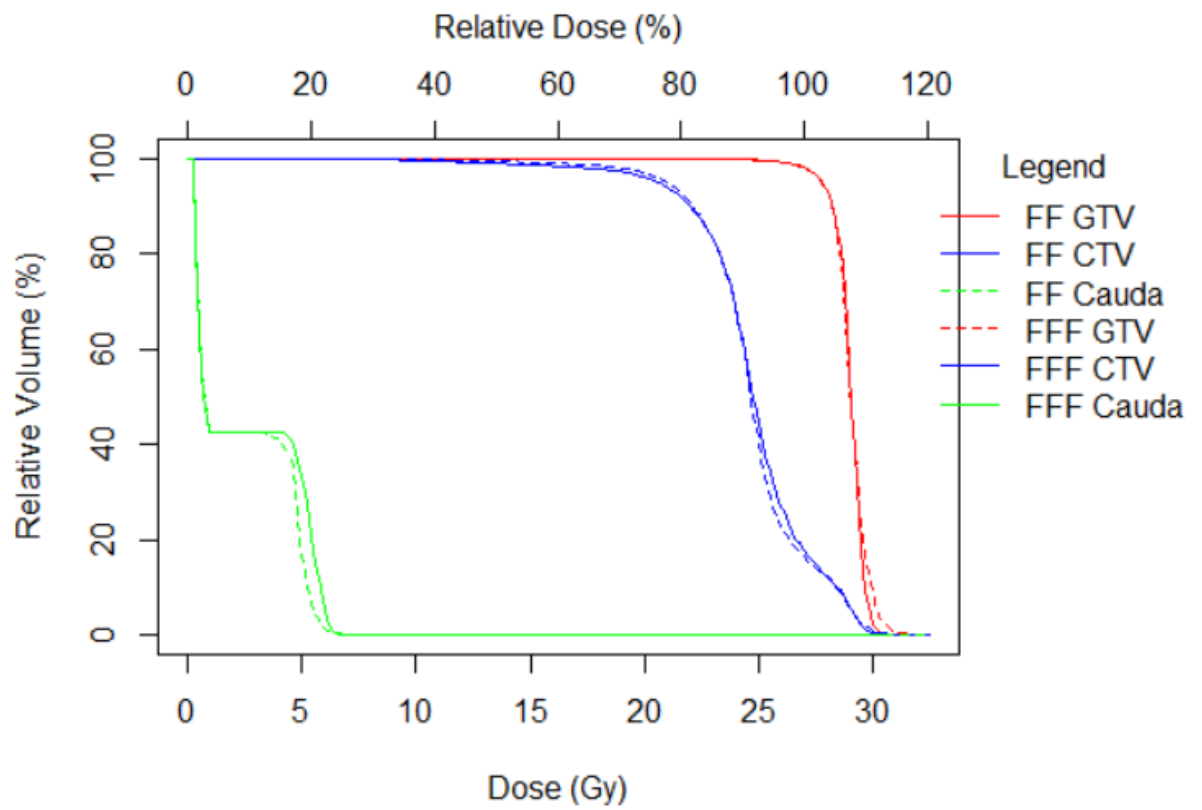


Figure 5-48: Patient 12 DVH

5.2 – Dose to Water vs. Dose to Medium

Dose was calculated as dose to medium rather than dose to water; it should be noted that there exist minor differences between these two calculation methods, as demonstrated below in Figure 2-3. The difference between dose to medium and dose to water has been shown to differ by as little as 1.0% for soft tissue and 10% for cortical bone⁵⁴. Dose to water has been the historical method of dose calculation due to how linacs are typically calibrated; nevertheless, accurate methods of computing absorbed dose to medium offer a more realistic view of how dose is deposited in the patient. Therefore, we chose to forego dose to water calculation and instead used dose to medium for this study.

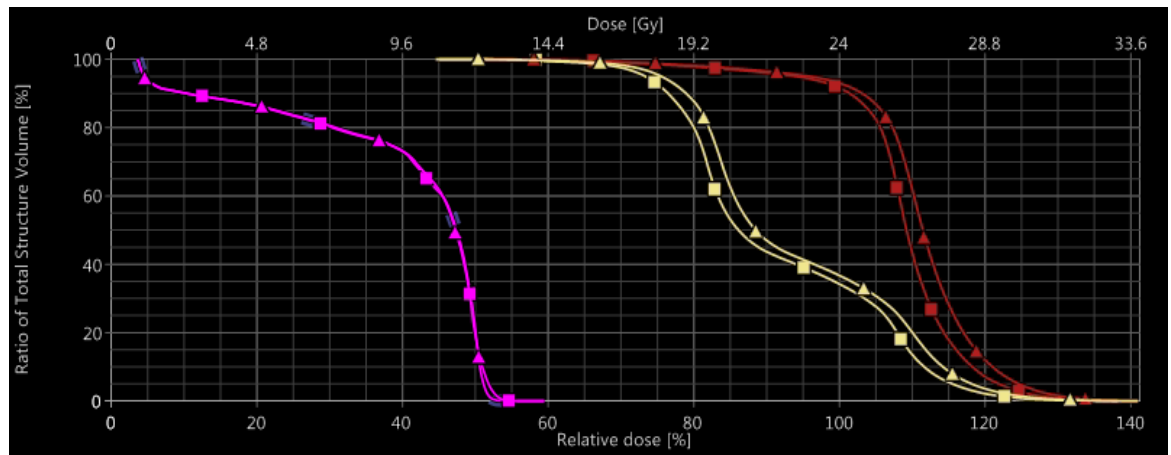


Figure 5-49: DVH for Dose to Medium vs. Dose to Water. Dose to Water is indicated with triangles; dose to medium with squares. Magenta, yellow, and red represent cauda equina, CTV, and GTV, respectively.

References

1. Bishop, A. J. *et al.* Outcomes for Spine Stereotactic Body Radiation Therapy and an Analysis of Predictors of Local Recurrence. *Radiat. Oncol. Biol.* **92**, 1016–1026 (2015).
2. Steinmetz, M. P., Mekhail, A. & Benzel, E. C. Management of metastatic tumors of the spine: strategies and operative indications. *Neurosurg. Focus* **11**, e2 (2001).
3. Gunzburg, R., Szpalski, M. & Aebi, M. *Vertebral Tumors*. (Lippincott Williams and Wilkins, 2008).
4. Taneichi, H., Kaneda, K., Takeda, N., Abumi, K. & Satoh, S. Risk Factors and Probability of Vertebral Body Collapse in Metastases of the Thoracic and Lumbar Spine. *Spine (Phila. Pa. 1976)*. **22**, 239–245 (1997).
5. Rose, P. S. & Buchowski, J. M. Metastatic disease in the thoracic and lumbar spine: evaluation and management. *J. Am. Acad. Orthop. Surg.* **19**, 37–48 (2011).
6. Hirabayashi, H. *et al.* Clinical Outcome and Survival after Palliative Surgery for Spinal Metastases Palliative Surgery in Spinal Metastases. doi:10.1002/cncr.11039
7. Moulding, H. D. *et al.* Local disease control after decompressive surgery and adjuvant high-dose single-fraction radiosurgery for spine metastases. *J Neurosurg Spine J Neurosurg Spine* **13**, 87–93 (2010).
8. Lutz, S. T., Chow, E. L., Hartsell, W. F. & Konski, A. A. A review of hypofractionated palliative radiotherapy. *Cancer* **109**, 1462–1470 (2007).
9. Nguyen, Q.-N. *et al.* Management of Spinal Metastases from Renal Cell Carcinoma Using Stereotactic Body Radiotherapy. *Int. J. Radiat. Oncol. Biol. Phys.* **76**, 1185–1192 (2010).

10. Crownover, R. L. in *Cancer in the Spine: Comprehensive Care* (ed. McLain, R. F.) 205–210 (Humana Press, 2006).
11. Benzil, D., Mogilner, A. & Moorthy, A. Safety and efficacy of stereotactic radiosurgery for tumors of the spine. *J. Neurosurg* **101**, (2004).
12. Ryu, S. *et al.* Image-guided and intensity-modulated radiosurgery for patients with spinal metastasis. *Cancer* **97**, 2013–2018 (2003).
13. Zelefsky, M. J. *et al.* Spinal epidural tumor in patients with prostate cancer. Clinical and radiographic predictors of response to radiation therapy. *Cancer* **70**, 2319–2325 (1992).
14. Yamada, Y. *et al.* High-dose, single-fraction image-guided intensity-modulated radiotherapy for metastatic spinal lesions. *Int. J. Radiat. Oncol. Biol. Phys.* **71**, 484–490 (2008).
15. Ahmed, K. A. *et al.* Stereotactic Body Radiation Therapy in Spinal Metastases. *Int J Radiat. Oncol Biol Phys* **82**, 803–809 (2011).
16. Ma, L. *et al.* Nonrandom Intrafraction Target Motions and General Strategy for Correction of Spine Stereotactic Body Radiotherapy. *Int. J. Radiat. Oncol. Biol. Phys.* **75**, 1261–1265 (2009).
17. Sahgal, A., Larson, D. A. & Chang, E. L. Stereotactic Body Radiosurgery for Spinal Metastases: A Critical Review. *Int. J. Radiat. Oncol. Biol. Phys.* **71**, 652–665 (2008).
18. Sahgal, A. *et al.* Stereotactic body radiotherapy for spinal metastases: current status, with a focus on its application in the postoperative patient A review. *J Neurosurg Spine J Neurosurg Spine* **14**, 151–166 (2011).
19. Titt, U. *et al.* A flattening filter free photon treatment concept evaluation with Monte

- Carlo. *Med. Phys.* **33**, 1595–1602 (2006).
20. Georg, D., Knöös, T. & McClean, B. Current status and future perspective of flattening filter free photon beams. *Med. Phys.* **38**, 1280–93 (2011).
 21. Xiao, Y. *et al.* Flattening filter-free accelerators: a report from the AAPM Therapy Emerging Technology Assessment Work Group. *J. Appl. Clin. Med. Phys.* (2015). doi:10.1120/jacmp.v16i3.5219
 22. Vassiliev, O. N. *et al.* Dosimetric properties of photon beams from a flattening filter free clinical accelerator. *Cancer* **51**, 1907–1917 (2006).
 23. Kry, S. F., Vassiliev, O. N. & Mohan, R. Out-of-field photon dose following removal of the flattening filter from a medical accelerator. *Phys. Med. Biol.* **55**, 2155–2166 (2010).
 24. Paynter, D., Weston, S. J., Cosgrove, V. P., Evans, J. a & Thwaites, D. I. Beam characteristics of energy-matched flattening filter free beams. *Med. Phys.* **41**, 052103 (2014).
 25. Almberg, S. S., Frengen, J. & Lindmo, T. Monte Carlo study of in-field and out-of-field dose distributions from a linear accelerator operating with and without a flattening-filter. *Med. Phys.* **39**, 5194 (2012).
 26. Fu, W., Dai, J., Hu, Y., Han, D. & Song, Y. Delivery time comparison for intensity-modulated radiation therapy with/without flattening filter: a planning study. *Phys. Med. Biol. Weihua Fu al Phys. Med. Biol* **49**, 1525–1547 (2004).
 27. Lang, S., Hrbacek, J., Leong, A. & Klöck, S. Ion-recombination correction for different ionization chambers in high dose rate flattening-filter-free photon beams Ion-recombination correction for different ionization chambers in high dose rate flattening-

- filter-free photon beams. *Phys. Med. Biol. Phys. Med. Biol* **57**, 2819–2827 (2012).
28. Guckenberger, M. *et al.* Precision required for dose-escalated treatment of spinal metastases and implications for image-guided radiation therapy (IGRT). *Radiother. Oncol.* **84**, 56–63 (2007).
 29. Chuang, C. *et al.* Effects of residual target motion for image-tracked spine radiosurgery. *Med. Phys.* **34**, 4484–4490 (2007).
 30. Dubois, L. *et al.* High dose rate and flattening filter free irradiation can be safely implemented in clinical practice. *Int. J. Radiat. Biol.* (2015).
doi:10.3109/09553002.2015.1068457
 31. Kogel, A. van der. in *Basic Clinical Radiobiology* (eds. Joiner, M. & Kogen, A. van der) 158–168 (Hodder Education, 2009).
 32. Johns, H. E. & Cunningham, J. R. *The Physics of Radiology, Fourth Edition*. (Charles C. Thomas, 1983).
 33. Titt, U., Vassiliev, O. N., Pönisch, F., Kry, S. F. & Mohan, R. Monte Carlo study of backscatter in a flattening filter free clinical accelerator. *Med. Phys.* **33**, 3270–3273 (2006).
 34. Pönisch, F., Titt, U., Vassiliev, O. N., Kry, S. F. & Mohan, R. Properties of unflattened photon beams shaped by a multileaf collimator. *Med. Phys.* **33**, 1738–1746 (2006).
 35. Vassiliev, O. N. *et al.* Monte Carlo study of photon fields from a flattening filter-free clinical accelerator. *Med. Phys.* **33**, 820–827 (2006).
 36. Vassiliev, O. N. *et al.* Treatment-Planning Study of Prostate Cancer Intensity-Modulated Radiotherapy With a Varian Clinac Operated Without a Flattening Filter.

- Int. J. Radiat. Oncol. Biol. Phys.* **68**, 1567–1571 (2007).
37. Stathakis, S., Esquivel, C., Gutierrez, A., Buckey, C. & Papanikolaou, N. Treatment Planning and Delivery of IMRT using 6 and 18 MV Photon Beams Without Flattening Filter. *Appl. Radiat. Isot.* **67**, 1629–1637 (2009).
 38. Zwahlen, D. R. *et al.* The Use of Photon Beams of a Flattening Filter-free Linear Accelerator for Hypofractionated Volumetric Modulated Arc Therapy in Localized Prostate Cancer. *Radiat. Oncol. Biol.* **83**, 1655–1660 (2012).
 39. Scorsetti, M. *et al.* Feasibility and early clinical assessment of flattening filter free (FFF) based stereotactic body radiotherapy (SBRT) treatments. doi:10.1186/1748-717X-6-113
 40. Vassiliev, O. N. *et al.* Stereotactic radiotherapy for lung cancer using a flattening filter free clinac. *J. Appl. Clin. Med. Phys.* **10**, 14–21 (2009).
 41. Boda-Heggemann, J. *et al.* Stereotactic ablative RT Flattening-filter-free intensity modulated breath-hold image-guided SABR (Stereotactic ABlative Radiotherapy) can be applied in a 15-min treatment slot. *Radiother. Oncol.* **109**, 505–509 (2013).
 42. Mancosu, P. *et al.* Stereotactic body radiation therapy for liver tumours using flattening filter free beam: dosimetric and technical considerations. *Radiat. Oncol.* **7**, 16–25 (2012).
 43. Reggiori, G. *et al.* Can volumetric modulated arc therapy with flattening filter free beams play a role in stereotactic body radiotherapy for liver lesions? A volume-based analysis. *Med. Phys.* **39**, 1112–1118 (2012).
 44. Stieler, F., Fleckenstein, J., Simeonova, A., Wenz, F. & Lohr, F. Intensity modulated radiosurgery of brain metastases with flattening filter-free beams. *Radiother. Oncol.*

- 109**, 448–451 (2013).
45. Abacioglu, U. *et al.* Critical appraisal of RapidArc radiosurgery with flattening filter free photon beams for benign brain lesions in comparison to GammaKnife: a treatment planning study. doi:10.1186/1748-717X-9-119
 46. Ong, C. L. *et al.* Dosimetric Impact of Intrafraction Motion During RapidArc Stereotactic Vertebral Radiation Therapy Using Flattened and Flattening Filter-Free Beams. *Radiat. Oncol. Biol.* **86**, 420–425 (2013).
 47. Dobler, B. *et al.* Re-irradiating spinal column metastases using IMRT and VMAT with and without flattening filter - a treatment planning study. *Radiat. Oncol.* (2016). doi:10.1186/s13014-016-0603-0
 48. Fogliata, A. *et al.* Definition of parameters for quality assurance of flattening filter free (FFF) photon beams in radiation therapy. *Med. Phys.* **39**, 6455–6464 (2012).
 49. Bilsky, M. H. *et al.* Reliability analysis of the epidural spinal cord compression scale. *J. Neurosurg. Spine* **13**, 324–328 (2010).
 50. Tseng, C.-L. *et al.* Spine Stereotactic Body Radiotherapy: Indications, Outcomes, and Points of Caution. doi:10.1177/2192568217694016
 51. Fogliata, A. *et al.* Dosimetric validation of the Acuros XB Advanced Dose Calculation algorithm: fundamental characterization in water. *Phys. Med. Biol.* **56**, 1879–1904 (2011).
 52. Ojala, J. The accuracy of the Acuros XB algorithm in external beam radiotherapy – a comprehensive review. *Int. J. Cancer Ther. Oncol.* **2**, 020417 (2014).
 53. Benedict, S. H. *et al.* Stereotactic body radiation therapy: The report of AAPM Task Group 101. *Med. Phys.* **37**, (2010).

54. Siebers, J. V, Keall, P. J., Nahum, A. E. & Mohan, R. Converting absorbed dose to medium to absorbed dose to water for Monte Carlo based photon beam dose calculations. *Phys. Med. Biol* **45**, 983–995 (2000).

Laura Christine Bennett was born with sister Rachel Lindsay Bennett in Oklahoma City, Oklahoma on April 14th, 1992 to parents Malia Katherine Bennett and Stephen Craig Bennett. After graduating from Westmoore High School in 2011, she attended the University of Science and Arts of Oklahoma, where she briefly studied history and political science before graduating with a Bachelor of Science in Physics in the spring of 2015. She matriculated to the University of Texas MD Anderson Cancer Center Graduate School of Biomedical Science in fall of 2015.